Shelly fossils from the lower Cambrian White Point Conglomerate, Kangaroo Island, South Australia

MARISSA J. BETTS, THOMAS M. CLAYBOURN, GLENN A. BROCK, JAMES B. JAGO, CHRISTIAN B. SKOVSTED, and JOHN R. PATERSON

Betts, M.J., Claybourn, T.M., Brock, G.A., Jago, J.B., Skovsted, C.B., and Paterson, J.R. 2019. Shelly fossils from the lower Cambrian White Point Conglomerate, Kangaroo Island, South Australia. *Acta Palaeontologica Polonica* 64 (3): 489–522.

The lower Cambrian (Series 2) White Point Conglomerate (WPC) on Kangaroo Island, South Australia contains exotic clasts representing a diverse array of lithologies, including metamorphics, chert, sandstone, and abundant carbonates, notably archaeocyath-rich bioclastic limestone. Acetic acid digestion of the WPC bioclastic limestone clasts reveals a diverse shelly fauna. This assemblage includes abundant organophosphatic brachiopods such as *Cordatia erinae* Brock and Claybourn gen. et sp. nov., *Curdus pararaensis, Eodicellomus elkaniformiis*, *Eohadrotreta* sp. cf. *E. zhenbaensis*, *Eoobolus* sp., *Kyrshabaktella davidii*, and *Schizopholis yorkensis*. Additional shelly taxa include the solenopleurid trilobite *Trachoparia*? sp., the tommotiids *Dailyatia odyssei*, *Dailyatia decobruta* Betts sp. nov., *Kelanella* sp., and *Lapworthella fasciculata*, spines of the bradoriid arthropod *Mongolitubulus squamifer*, and several problematica, such as *Stoibostrombus crenulatus* and a variety of tubular forms. The upper age limit for the WPC is constrained by biostratigraphic data from the overlying Marsden Sandstone and Emu Bay Shale, which are no younger than the *Pararaia janeae* Trilobite Zone (Cambrian Series 2, Stage 4). The shelly fossil assemblage from the WPC limestone clasts indicates an upper *Dailyatia odyssei* Zone (= *Pararaia tatei* to lower *P. janeae* trilobite zones), equivalent to the Atdabanian–early Botoman of the Siberian scheme. This contrasts with the previously suggested late Botoman age for the limestone clasts, based on the diverse archaeocyath assemblage. The minor age difference between the WPC and its fossiliferous limestone clasts suggests relatively rapid reworking of biohermal buildups during tectonically-active phases of deposition in the Stansbury Basin.

Key words: Brachiopoda, Trilobita, Tommotiida, chronostratigraphy, early Cambrian, Australia.

Marissa J. Betts [marissa.betts@une.edu.au], Palaeoscience Research Centre, School of Environmental and Rural Science, University of New England, Armidale, NSW, Australia, 2351; Early Life Institute and Department of Geology, State Key Laboratory for Continental Dynamics, Northwest University, Xi'an 710069, China.
Thomas M. Claybourn [thomas.claybourn@hdr.mq.edu.au], Department of Biological Sciences, Macquarie University, North Ryde, Sydney, NSW, Australia, 2109; Department of Earth Sciences, Palaeobiology, Uppsala University, Villav. 16, SE-75236, Uppsala, Sweden.
Glenn A. Brock [glenn.brock@mq.edu.au], Department of Biological Sciences, Macquarie University, North Ryde, Sydney, NSW, Australia, 2109.
James B. Jago [jim.jago@unisa.edu.au], School of Natural and Built Environments, University of South Australia, Mawson Lakes, Adelaide, SA, Australia, 5005.
Christian B. Skovsted [christian.skovsted@nrm.se], Department of Palaeobiology, Swedish Museum of Natural History, Box 50007, SE 104 05 Stockholm, Sweden.
John R. Paterson [jpater20@une.edu.au], Palaeoscience Research Centre, School of Environmental and Rural Science, University of New England, Armidale, NSW, Australia, 2351.

Received 19 December 2018, accepted 17 April 2019, available online 23 August 2019.

Introduction

The White Point Conglomerate (WPC) is part of the Kangaroo Island Group, a ~2000 m thick package of mostly siliciclastic rocks that crops out on the northern and central parts of Kangaroo Island, South Australia (Fig. 1). The WPC occurs stratigraphically below the famous Emu Bay Shale (EBS; Paterson et al. 2008, 2016) and Marsden Sandstone (Fig. 2) and contains allochthonous limestone clasts that are conspicuous due to the abundant and diverse archaeocyath fauna they contain (Gravestock 1995; Gehling et al. 2011; Kruse and Moreno-Eiris 2013). Dating and correlation of the WPC has been difficult due to uncertainties in tracing

equivalent facies, and lack of in situ biostratigraphic controls. Previous attempts at biostratigraphically constraining and correlating the WPC and the clasts it contains have been made using archaeocyaths (Kruse and Moreno-Eiris 2013). These genus-level assessments correlated the WPC with the late Botoman stage of the Siberian scheme. However, archaeocyaths are subject to strong facies dependence and high levels of endemism, making it difficult to assign accurate ages (Peng et al. 2012; Betts et al. 2016, 2017a, b, 2018). Hence, application of complementary temporal proxies is required.

Early Cambrian shelly fossils are widely applied as biostratigraphic tools for relative dating and correlation (Steiner et al. 2004, 2007; Devaere et al. 2013; Guo et al. 2014; Yang et al. 2015; Betts et al. 2016, 2017b). The new shelly fossil biostratigraphic scheme for the lower Cambrian of South Australia (Betts et al. 2016, 2017b) employs a wide variety of shelly taxa. Stratigraphic ranges of *Dailyatia* species, in addition to other key tommotiid and brachiopod taxa form the backbone of this scheme, supplemented by range data of various ecdysozoans and molluscs. These biozones have recently been integrated with $\delta^{13}C$ chemostratigraphy and CA-TIMS radiometric dates from volcanic ash beds, which has produced a tightly resolved regional chronostratigraphy, enabling robust regional and global correlation of the lower Cambrian successions in South Australia (Betts et al. 2016, 2017a, b, 2018; Jago et al. 2018). In this paper we describe the diverse shelly fauna from the WPC limestone clasts, which includes arthropods (trilobites and bradoriids), organophosphatic brachiopods, tommotiids and problematica (Figs. 3–19). We apply the new shelly fossil biostratigraphic scheme developed by Betts et al. (2016, 2017b) and the new chronostratigraphic scheme for South Australia (Betts et al. 2018) to re-evaluate the ages of the WPC clasts and adjacent units.

Institutional abbreviations.—SAM P, South Australian Museum, Palaeontological collections, Adelaide, Australia.

Other abbreviations.—EBS, Emu Bay Shale; DBS, Donkey Bore Syncline; KLM, Koolywurtie Limestone Member; WPC, White Point Conglomerate.

Nomenclatural acts.—This published work and the nomenclatural acts it contains, have been registered in ZooBank: urn:lsid:zoobank.org:pub:511DB76B-9F74-4068-998A-389CC14ED841

Geological setting

The WPC is part of the Kangaroo Island Group, which crops out on northern Kangaroo Island, southwest of Fleurieu Peninsula on mainland South Australia (Fig. 1). At the time of deposition of the WPC, South Australia was equatorial, positioned in the tropical carbonate development zone (Brock et al. 2000; Gehling et al. 2011). Deposition of the WPC is likely related to tectonic extension throughout the Stansbury Basin (Belperio et al. 1998). Uplift and rapid erosion of Proterozoic–lower Cambrian rocks led to the deposition of the WPC and associated units as fan deltas accumulated against an uplifted fault block (Daily and Forbes 1969; Daily et al. 1980; Gehling et al. 2011). Conglomeratic boulders decrease in size and the unit thins to the south, suggesting the uplifted source area was located to the north of the present-day coastline of Kangaroo Island (Gehling et al. 2011). Imbricate clasts also suggest flow direction was toward the south (Kruse and Moreno-Eiris 2013).

The WPC is up to ~580 m thick, though thickness can vary considerably (Gehling et al. 2011). In the coastal sections where the WPC is thickest, the lower 170 m consists of a fine, red, feldspathic sandstone with minor siltstone and shale (Daily et al. 1980; Gehling et al. 2011; Kruse and Moreno-Eiris 2013). An erosional surface separates this interval from the overlying 410 m of polymictic, very poorly sorted, and mostly clast-supported conglomerate (Gehling et al. 2011). These characteristics, as well as the angular to sub-rounded clasts, indicate minimal transport (Kruse and Moreno-Eiris 2013). The poorly-sorted calcareous lithic sandstone matrix surrounding the clasts has a markedly different composition to the red sandstone at the base of the unit, suggesting some variation in the source of the sediments (Gravestock 1995). Fine-grained sandstone and mudstone units are interspersed throughout the conglomerate, but are rare and feature erosive upper boundaries at contacts with successive conglomerate beds. Trilobite fragments have been found in a mudstone interval in the WPC (Gravestock 1995), and Gehling et al. (2011) note trilobite-like traces in mudstone and sandstone beds.

A wide variety of lithologies are represented by the WPC clasts, such as gneiss, quartzite, chert, granite, red sandstone, and abundant carbonates, including dolostone and archaeocyath-rich limestone (Gravestock 1995; Kruse and Moreno-Eiris 2013). The largest clasts are up to 1.5 m across, and limestone clasts reach approximately 0.3 m across (Daily et al. 1980). Kruse and Moreno-Eiris (2013) produced many thin sections of the archaeocyath-rich limestone clasts. They described both reef fabrics (calcimicrobe-archaeocyath boundstone, framestone and cementstone in which the components were organically bound during deposition; Lokier and Al Junaibi 2016) and inter-reef fabrics (floatstone with transported archaeocyaths in a matrix of bioclasts, intraclasts, and peloids). The only other occurrence of archaeocyaths on Kangaroo Island is in a thin, oolitic bed at the top of the Mt. McDonnell Formation (Gehling et al. 2011, Kruse and Moreno-Eiris 2013). These archaeocyaths are similar to those from the bioherms in the lower part of Fork Tree Limestone on Fleurieu Peninsula (*Kulparina rostrata* Zone) (Kruse and Moreno-Eiris 2013; Betts et al. 2018), and bear little resemblance to the archaeocyaths from the WPC bioclastic limestone clasts (Gravestock 1995).

Immediately above the WPC is the Rouge Mudstone Member of the Marsden Sandstone, which contains the emuellid trilobite *Balcoracania dailyi* (Gehling et al. 2011; Paterson 2014). The facies represented by the Marsden

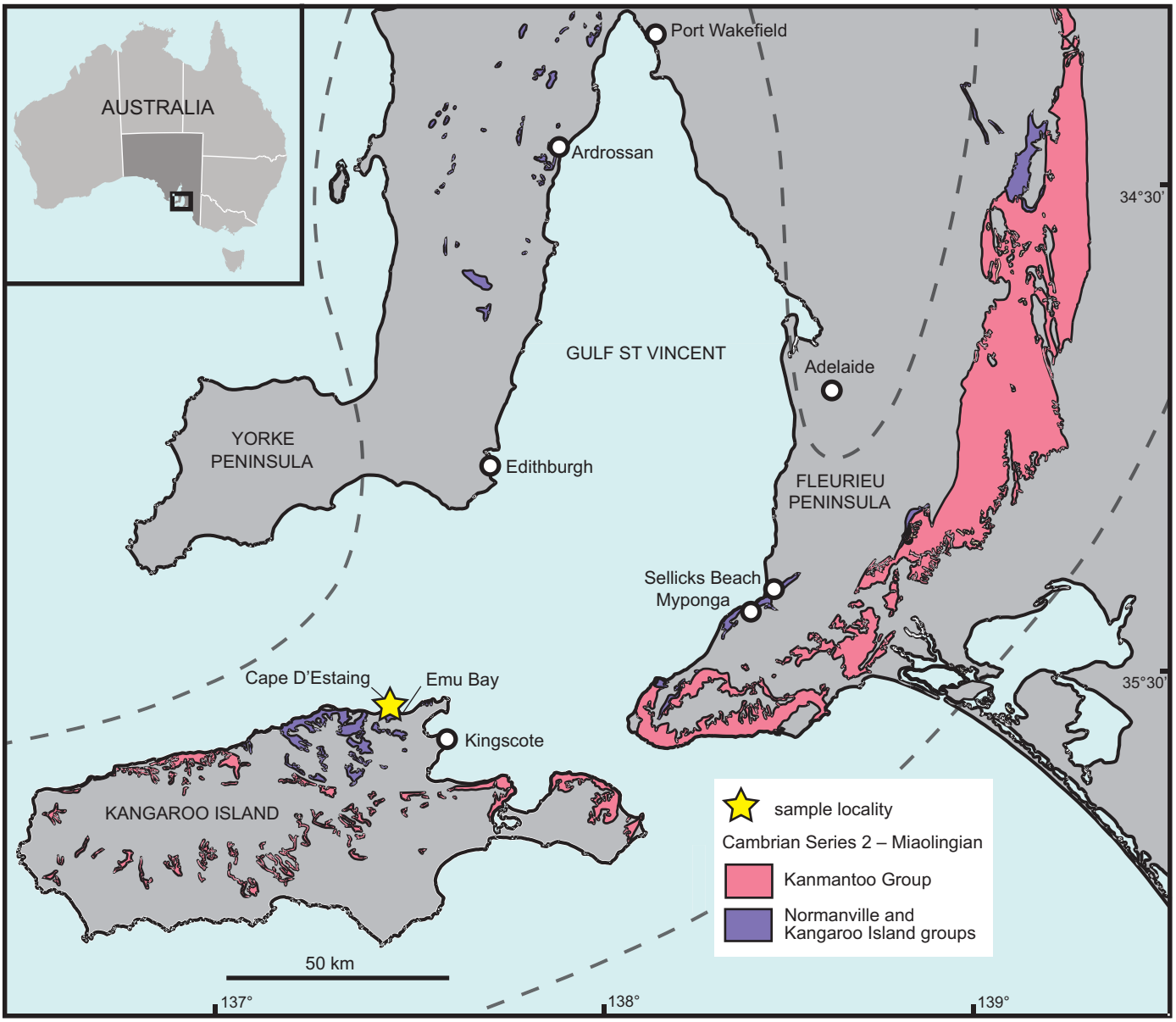

Fig. 1. Map showing study area on northern Kangaroo Island, Australia. Dashed line indicates Stansbury Basin extent.

Sandstone and lower Emu Bay Shale represent a localised deepening event due to subsidence, post deposition of the WPC (Gehling et al. 2011). Minor conglomerate beds in the basal part of the Emu Bay Shale indicate a sequence boundary (Gehling et al. 2011; Kruse and Moreno-Eiris 2013). Gehling et al. (2011) note that the conglomerate in the lower EBS has clast compositions similar to those in the WPC, implying a similar source for these deposits.

White Point Conglomerate.—On sedimentological grounds, the lower Cambrian succession on Kangaroo Island in the southern Stansbury Basin has little in common with the northwestern and eastern successions of the basin on the Yorke and Fleurieu peninsulas, respectively, and likely post-dates the development of Terreneuvian, Stage 2 carbonate facies in these regions (Gehling et al. 2011; Betts et al. 2018). Uncertainties in tracing equivalent facies and lack of in situ biostratigraphic controls have impeded reliable dating and correlation of the WPC. Within the Stansbury Basin, the WPC has previously been correlated with the upper Parara Limestone (containing the KLM) on Yorke Peninsula, and the upper Heatherdale Shale on the Fleurieu Peninsula (Gravestock 1995). In contrast, Gehling et al. (2011) correlated the WPC with the lower Minlaton Formation on Yorke Peninsula and the lower Kanmantoo Group on Fleurieu Peninsula, based on widespread changes in depositional patterns.

Placing an upper age limit of Cambrian Series 2, Stage 4 on the WPC is achievable with trilobites. In particular, the emuellid trilobite *Balcoracania dailyi* not only occurs in the overlying Marsden Sandstone and Emu Bay Shale on Kangaroo Island (Stansbury Basin), but also in the Billy Creek Formation of the Arrowie Basin (Fig. 2) (Pocock

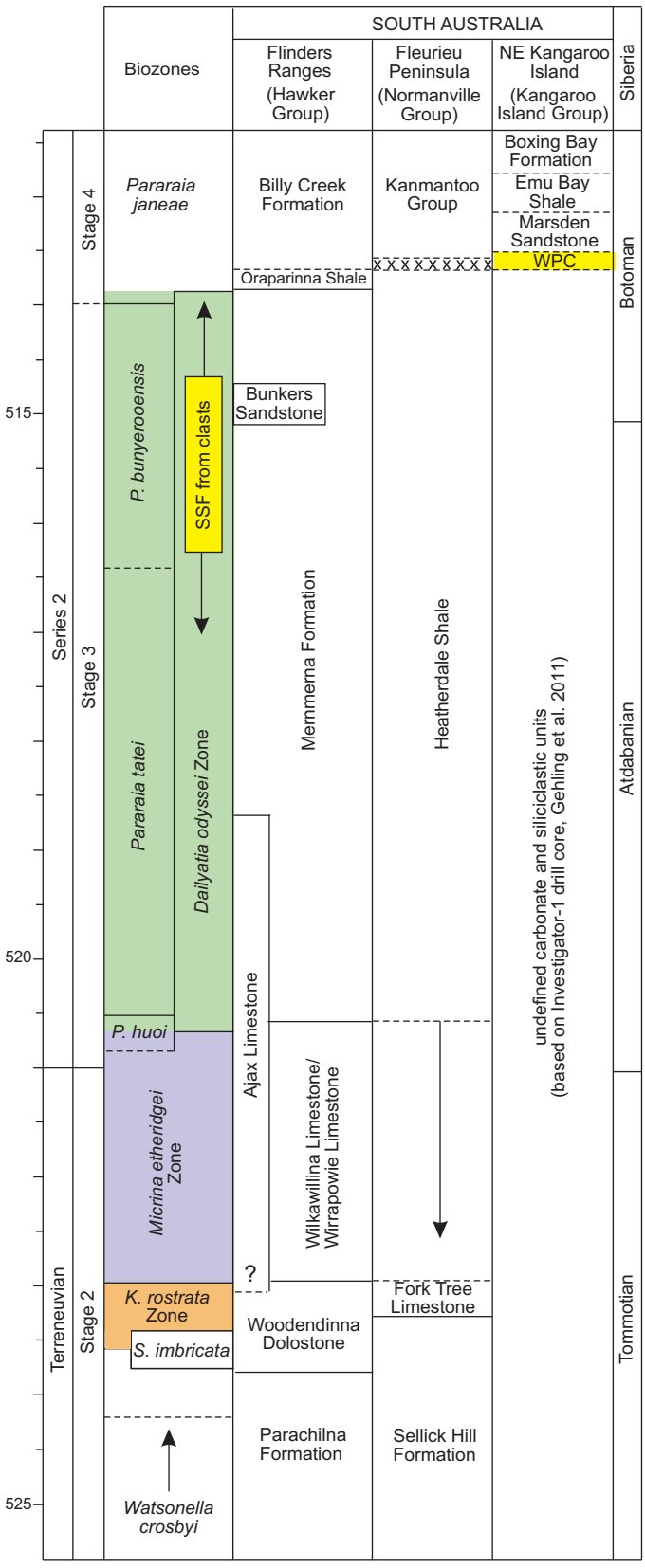

1970; Paterson and Edgecombe 2006; Paterson et al. 2007a; Gehling et al. 2011). The Billy Creek Formation is considered Cambrian Series 2, Stage 4 (*Pararaia janeae* Zone) in age (Jell in Bengtson et al. 1990; Paterson and Brock 2007; Betts et al. 2017b), which is supported by a radiometric (CA-TIMS) date of 511.87 ± 0.14 Ma obtained from a volcanic ash bed in this formation (Betts et al. 2018). A lower age bracket for the WPC can now be determined using the abundant shelly fauna from the bioclastic limestone clasts (see below).

WPC limestone clasts.—Abundant shelly fossils were recovered from WPC bioclastic limestone clasts, including arthropods such as the solenopleurid trilobite *Trachoparia*? sp. (Figs. 3, 4) and spines of the bradoriid *Mongolitubulis squamifer* Missarzhevsky, 1977 (Fig. 5). The clasts yielded an abundant brachiopod fauna including *Eodicellomus elkaniiformis* Holmer and Ushatinskaya in Gravestock et al., 2001 (Fig. 6), *Eoobolus* sp. (Fig. 7A–C), *Kyrshabaktella davidi* Holmer and Ushatinskaya in Gravestock et al., 2001 (Fig. 7D–T), *Curdus pararaensis* Holmer and Ushatinskaya in Gravestock et al., 2001 (Fig. 8), *Schizopholis yorkensis* (Holmer and Ushatinskaya in Gravestock et al., 2001) (Fig. 9), *Eohadrotreta* sp. cf. *E. zhenbaensis* (Fig. 10), and *Cordatia erinae* Brock and Claybourn gen. et sp. nov. (Figs. 11, 12). Other shelly taxa from the WPC clasts include the problematic shelly taxon *Stoibostrombus crenulatus* Conway Morris and Bengtson in Bengtson et al., 1990 (Fig. 13A–F), the tommotiids *Lapworthella fasciculata* Conway Morris and Bengtson in Bengtson et al., 1990 (Fig. 13G–N), *Kelanella* sp. (Fig. 13O), *Dailyatia odyssei* (Fig. 14) and *D. decobruta* Betts sp. nov. (Figs. 15–18), and a variety of tubular forms (Fig. 19).

Species of *Dailyatia* are known only from lower Cambrian carbonate rocks in South and central Australia, as well as Antarctica. Six species of *Dailyatia* have previously been described: *D. ajax* Bischoff, 1976, *D. macroptera* (Tate, 1892), *D. bacata* Skovsted, Betts, Topper, and Brock, 2015a, *D. helica* Skovsted, Betts, Topper, and Brock, 2015a, and *D. odyssei* Evans and Rowell, 1990 from central and South Australia (Laurie 1986; Skovsted et al. 2015a), and *D. odyssei* and *D. braddocki* Evans and Rowell, 1990 from the Transantarctic Mountains (Evans and Rowell 1990). *Dailyatia odyssei* is the only species recovered from both South Australia and Antarctica and is therefore a key faunal link between these two terranes. New, well-preserved shelly fossil material from the clasts in the WPC facilitate description of the new species *Dailyatia decobruta* Betts sp. nov. (= *D.* sp. A in Skovsted et al. 2015a), which has also been recovered from the Mernmerna Formation in the central and eastern Flinders Ranges (Skovsted et al. 2015a; Betts et al. 2017b).

In their comprehensive study of the archaeocyaths from the WPC clasts, Kruse and Moreno-Eiris (2013) suggested

Fig. 2. Correlation chart showing shelly fossil biozones against the stratigraphic succession in the Flinders Ranges, Fleurieu Peninsula, and Kangaroo Island (adapted from Betts et al. 2018: fig. 27). Note: The succession in the NE Kangaroo Island is based on the Investigator-1 drill core in which the Mt. McDonnell Formation is not apparent (Gehling et al. 2011). Lower boundary of White Point Conglomerate (WPC) is likely faulted. Abundant and diverse shelly fauna (SSF) from the bioclastic limestone clasts in the WPC have an upper *Dailyatia odyssei* Zone age. Dashed lines indicate uncertain stratigraphic relationship. Abbreviations: *K.*, *Kulparina*; *P.*, *Parabadiella*; *S.*, *Sunnaginia*.

that material from all sampled clasts was representative of the same fauna, a view supported here based on shelly fossil data, and correlated it with the late Botoman (Series 2, Stage 4) of the Siberian scheme. They also noted strong similarities with post-Flinders Unconformity archaeocyath faunas from the Stansbury and Arrowie basins, particularly the KLM (Parara Limestone) and the Ajax Limestone, respectively.

Kruse and Moreno-Eiris (2013) suggested that the WPC bioclastic limestone was likely sourced from the KLM on Yorke Peninsula. The KLM and Ajax Limestone contain the diverse *Syringocnema favus* archaeocyathan assemblage, which was also considered mid- to late Botoman by Zhuravlev and Gravestock (1994). However, Paterson et al. (2007b) considered the KLM to be of a slightly older (pre-*Pararaia janeae* Zone) age, based on the close shelly faunal similarities between the KLM (Stansbury Basin) and the Ajax Limestone and other units in the Arrowie Basin. Recent biostratigraphic and chemostratigraphic evidence clearly demonstrates that the Ajax Limestone is no younger than the *Pararaia tatei* Trilobite Zone (correlatable with the Atdabanian Stage of Siberia), and straddles the Terreneuvian, Stage 2–Series 2, Stage 3 boundary (approximately equivalent to the Tommotian–Atdabanian in Siberian terminology; Fig. 2) (Betts et al. 2016, 2017b, 2018).

Shelly taxa previously reported from the KLM include the brachiopods *Curdus pararaensis*, *Eoobolus* sp. and Obolidae gen. et sp. indet., the problematic forms *Athelicopalla adnata*, *Anabarites sexalox*, and *Anabarites trymatus*, the halkieriid *Australohalkieria parva*, the hyolith *Cupitheca holocyclata*, the problematic multi-element taxon *Stoibostrombus crenulatus*, the tommotiid *Dailyatia odyssei*, a variety of tubular taxa (e.g., *Hyolithellus filiformis*), and the trilobite *Xela* sp. (Bengtson et al. 1990; Gravestock et al. 2001; Paterson et al. 2007b). Of importance is the occurrence of age-diagnostic taxa *D. odyssei* and *S. crenulatus* in the KLM, which confirms a *D. odyssei* Zone age for this unit (Betts et al. 2017b).

The shelly fauna recovered from the WPC limestone clasts shares some similarities with the faunal assemblage described from the KLM (Paterson et al. 2007b), but also shelly fossil assemblages from the Arrowie Basin. Both the WPC and KLM contain *D. odyssei* and *S. crenulatus* (diagnostic taxa for the *D. odyssei* Zone [Series 2, Stages 3–4]), the brachiopods *Cordatia erinae* Brock and Claybourn gen. et sp. nov. (previously referred to as Obolidae gen. et sp. indet. by Paterson et al. 2007b), *Curdus pararaensis* and *Eoobolus* sp., and similar hyolithelminth forms. However, *D. decobruta* Betts sp. nov., *E. elkaniformiis*, *S. yorkensis*, *K. davidii*, *L. fasciculata*, *Kelanella* sp., and *M. squamifer* have not been recorded from the KLM. In the DBS section in the central Flinders Ranges, *D. decobruta* Betts sp. nov. (= *Dailyatia* sp. A of Betts et al. 2017b: fig. 4) co-occurs in a single horizon with *D. odyssei*, *K. davidi*, *M. squamifer*, *S. crenulatus*, and *S. yorkensis* in the upper Mernmerna Formation (above the Bunkers Sandstone), which falls within the upper range of *L. fasciculata*, as well as trilobite taxa of the lower *P. janeae* Zone (= latest *D. odyssei* Zone) (Topper et al. 2007; Skovsted et al. 2015a; Betts et al. 2017b). In the Mt. Chambers area in the eastern Flinders Ranges (NB section), the only horizon containing *D. decobruta* Betts sp. nov. also falls within the range of *D. odyssei*, *L. fasciculata*, and *E. elkaniformiis* (Skovsted et al. 2015a; Betts et al. 2017b: fig. 10). These shelly fossil co-occurrences suggest an upper *D. odyssei* Zone age (= *P. tatei* to lower *P. janeae* trilobite zones) for the sampled limestone clasts from the WPC, equivalent to the Atdabanian–early Botoman in Siberia (Betts et al. 2018: fig. 27).

This contrasts slightly with the age determination by Kruse and Moreno-Eiris (2013), who suggested that the WPC clasts are late Botoman. This assessment was based on the occurrence of similar archaeocyaths from the KLM (Parara Limestone; Stansbury Basin) and the Ajax Limestone (Arrowie Basin), and a compilation of stratigraphic ranges of archaeocyath genera (Zhuravlev and Gravestock 1994: table 6). New shelly fossil data and revised correlations for these units (Paterson et al. 2007b; Betts et al. 2016, 2017b; herein), supplemented by recent chemostratigraphic and radiometric data (Betts et al. 2018), support the older ages of these strata. It is also important to note that Kruse and Moreno-Eiris (2013) reported some archaeocyath genera from the WPC that only otherwise occur in early Botoman or older strata, suggesting that an older age interpretation for the WPC is indeed possible based on archaeocyaths alone.

Previous studies have noted strong similarities between the bioclastic limestone clasts from the WPC and the KLM, with Daily et al. (1980), Daily (1990) and Kruse and Moreno-Eiris (2013) suggesting that the latter unit is likely the source of the WPC clasts. This is a reasonable proposal, given that there is little other evidence for local sources of bioclastic limestone of this particular age; the archaeocyathan assemblages from the Sellick Hill Formation and Fork Tree Limestone on Fleurieu Peninsula are considerably older (Fig. 2; Debrenne and Gravestock 1990; Zhuravlev and Gravestock 1994; Betts et al. 2018). This suggestion is also supported by the similar shelly faunas from the KLM and WPC.

Material and methods

Shelly fossils were leached from six limestone clasts (each 20–25 cm in diameter) using standard acetic leaching techniques (10% acetic acid solution, washed every 5 days until complete dissolution). Insoluble residues were wet sieved through 60 μm and 125 μm sieves, dried and picked with a stereomicroscope. Selected specimens were mounted on stubs, gold coated and imaged on the JEOL 6480LA scanning electron microscope at Macquarie University, Sydney.

Archaeocyaths were present in all six clasts from the WPC that were acid processed. Four clasts yielded shelly fossils, however only Clasts 1, 4, and 5 produced abundant, well-preserved shelly fossils. Shelly material from the remaining clasts was limited and fragmentary. Clasts 1–3 were sampled by JRP during fieldwork in 2010 from the same locality at Cape D'Estaing as the clasts studied

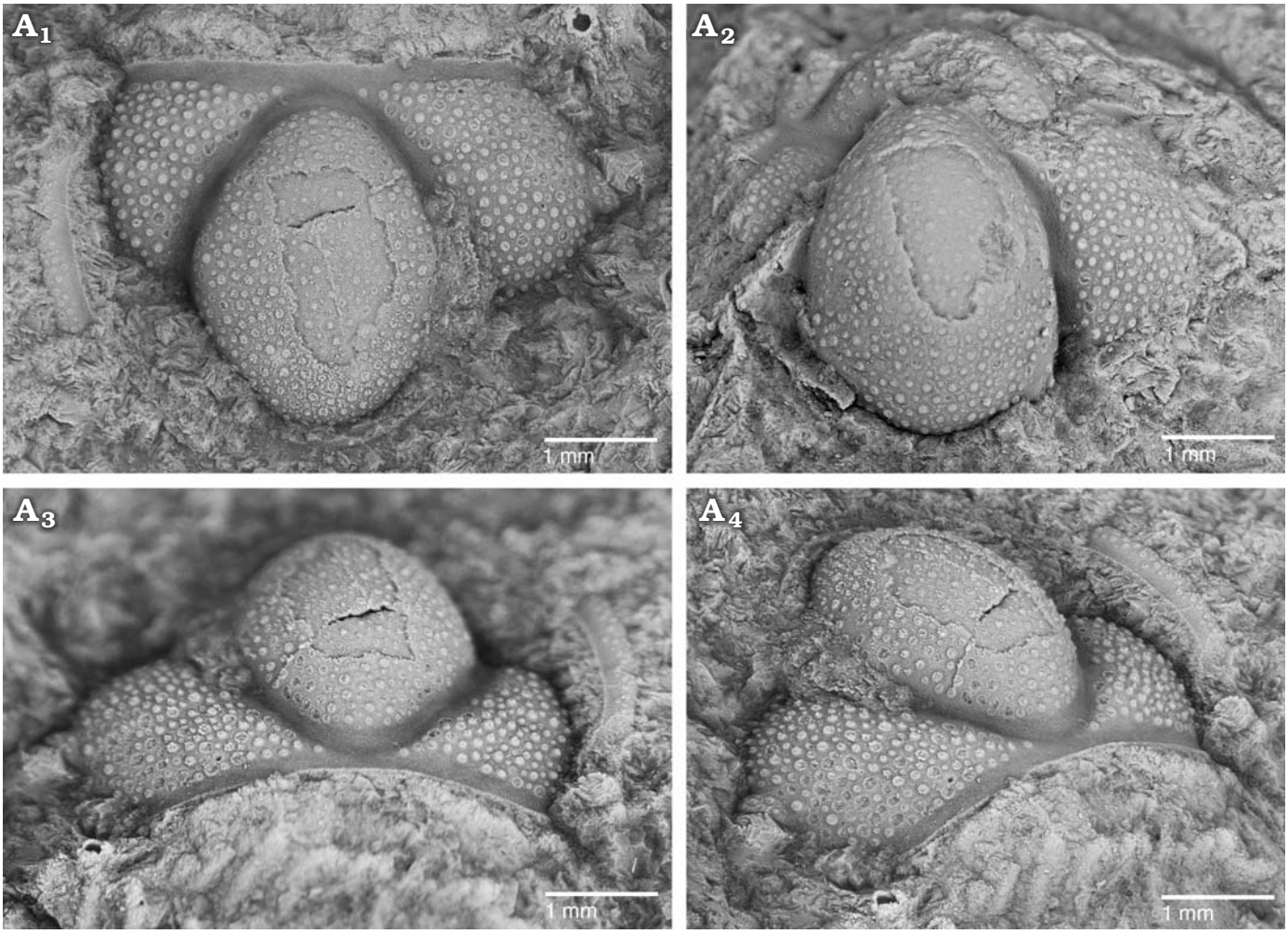

Fig. 3. The solenopleurid trilobite *Trachoparia*? sp. from the lower Cambrian White Point Conglomerate, Kangaroo Island, South Australia. Latex cast of partial cranidium (SAM P57221) showing pustulose ornament and strongly tapered glabella in dorsal (A_1), anterior (A_3), and oblique anterolateral (A_4) views; testate cranidium in dorsal view (A_2).

by Kruse and Moreno-Eiris (2013) for archaeocyath taxa (WGS84 coordinates: 35°34'53" S, 137°29'06" E). Kruse and Moreno-Eiris (2013) noted shelly taxa in thin sections prepared for their study, including trilobite debris, ?brachiopods, chancelloriids and sponge spicules, amongst other indeterminate shelly material. Clasts 4–6 were also sampled by JRP during fieldwork in 2018 from the same locality.

All figured specimens have been assigned SAM P numbers and are stored in the palaeontological collections of the South Australian Museum, Adelaide. Taxonomic authorship is as follows: the trilobite *Trachoparia*? sp. (JRP); brachiopods (GAB and TMC); the tommotiid *Kelanella* sp. (CBS); all other taxa (MJB).

Systematic palaeontology

Phylum Euarthropoda Lankester, 1904 (see Ortega-Hernández 2016)

Class Trilobita Walch, 1771

Family Solenopleuridae Angelin, 1854

Genus *Trachoparia* Chang, 1963

Type species: *Solenoparia bigranosa* Endo, 1937; Changhia Formation (Miaolingian, Drumian), Liaoning, China.

Trachoparia? sp.

Figs. 3, 4.

Material.—Eight partial cranidia, six figured (SAM P57221–57226). All from limestone clasts in the WPC, Kangaroo Island, South Australia; *Dailyatia odyssei* Zone.

Remarks.—The cranidia from the limestone clasts of the WPC, while fragmentary, preserve enough features to confidently assign them to the Solenopleuridae. Of the many genera erected within this family (Jell and Adrain 2003), the WPC taxon is most similar to species of *Trachoparia* from the Miaolingian of North China (Chang 1963; Zhang and Jell 1987; Yuan et al. 2012). Shared cranidial characters include: a prosopon exhibiting pustules of differing sizes; wide axial, anterior border, and posterior border furrows; short (sagittal) anterior border; and the absence of a preglabellar field.

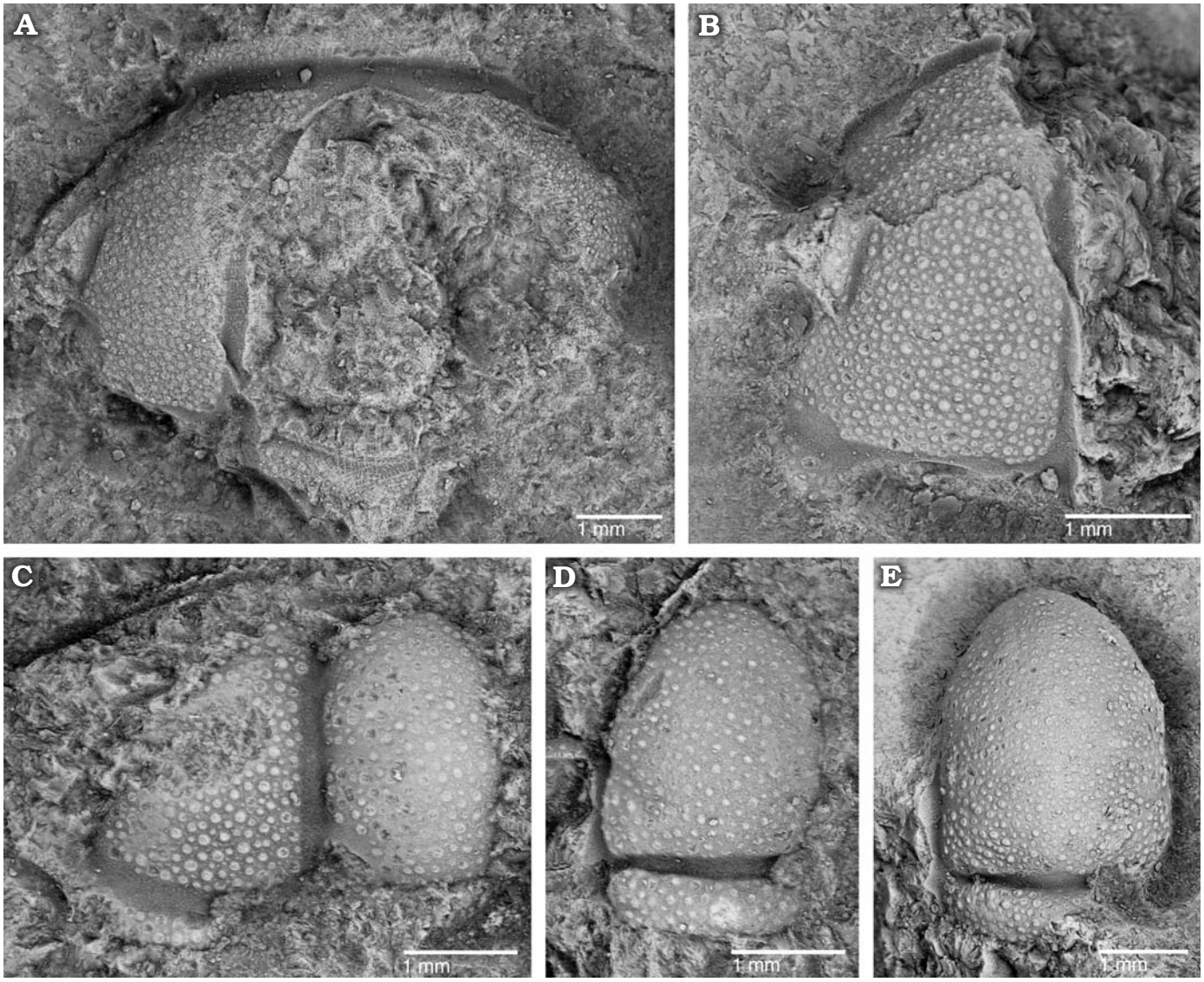

Fig. 4. The solenopleurid trilobite *Trachoparia*? sp. from the lower Cambrian White Point Conglomerate, Kangaroo Island, South Australia. Partial testate cranidia in dorsal views. **A**. SAM P57222 showing short (sag., exsag.) anterior border. **B**. SAM P57223 showing faint eye ridge and palpebral lobe. **C**. SAM P57224 showing wide axial and posterior border furrows. **D**. SAM P57225 showing deep occipital furrow and subquadrate occipital ring. **E**. SAM P57226 showing strongly tapered glabella and subquadrate occipital ring.

Obvious differences in the specimens documented here relate to the shape of the glabella and the occipital ring. The WPC taxon possesses a rather pointed glabellar anterior (Figs. $3A_1$, 4E), compared to the more rounded frontal glabellar lobes of *Trachoparia* species from North China (Chang 1963; Zhang and Jell 1987; Yuan et al. 2012). In this regard, the WPC specimens more closely resemble a fragmentary cranidium from the Changhia Formation in Shandong, North China (Zhang and Jell 1987: pl. 42: 5) that was questionably assigned to the solenopleurid *Eilura*. The WPC taxon also has a subquadrate occipital ring, the lateral extremities of which appear to terminate at the axial furrows (Fig. 4D, E). In contrast, specimens of *Trachoparia* from North China (e.g., Chang 1963: pl. 1: 12; Zhang and Jell 1987: pl. 42: 11; Yuan et al. 2012: pl. 87: 1–3, pl. 88: 4, 7, 10, 12a, pl. 107: 18) show an occipital ring that tapers abaxially and extends onto the proximal posterolateral corners of the fixigenae. Based on cranidial material alone, it is difficult to ascertain if these differences are interspecific within the concept of *Trachoparia* (sensu Yuan et al. 2012), or whether the WPC taxon warrants placement in another (possibly new) genus, hence the tentative assignment here.

Class uncertain

Order Bradoriida Raymond, 1935

Family Mongolitubulidae Topper, Skovsted, Harper, and Ahlberg, 2013

Genus *Mongolitubulus* Missarzhevsky, 1977

Type species: *Mongolitubulus squamifer* Missarzhevsky, 1977; lower Cambrian, Mongolia.

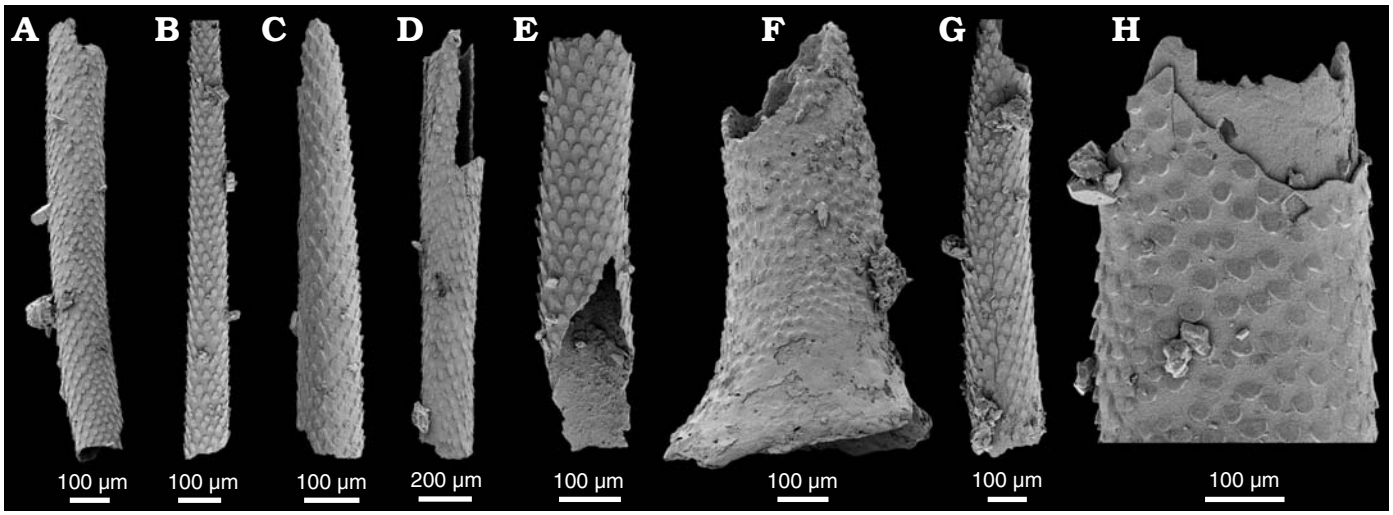

Fig. 5. Spines of the bradoriid arthropod *Mongolitubulus squamifer* Missarzhevsky, 1977 from the lower Cambrian White Point Conglomerate, Kangaroo Island, South Australia. **A**. SAM P57227. **B**. SAM P57228. **C**. SAM P57229. **D**. SAM P57230. **E**. SAM P57231. **F**. SAM P57232, fragment with flared base. **G**. SAM P57233. **H**. SAM P57234, close-up of rhomboid scales.

Mongolitubulus squamifer Missarzhevsky, 1977

Fig. 5.

1977 *Mongolitubulus squamifer*; Missarzhevsky 1977: 13, pl. 1: 1–2.
1981 *Mongolitubulus squamifer*; Missarzhevsky and Mambetov 1981: 79, pl. 14: 1–2.
1985 *Mongolitubulus squamifer*; Meshkova 1985: 127–128, pl. 46: 1–3.
1986 *Mongolitubulus squamifer*; Rozanov 1986: 89, fig. 4.
1986 *Rhombocorniculum* aff. *insolutum*; Brasier 1986: 253, fig. 5j–k.
1988 *Mongolitubulus squamifer*; Peel and Blaker 1988: 56, fig. 2.
1988 *Rhombocorniculum* n. sp.; Landing 1988: 687, fig. 11.6.
1989 *Mongolitubulus squamifer*; Missarzhevsky 1989: 31, figs. 1, 3.
1989 *Mongolitubulus squamifer*; Wrona 1989: 543.
1996 *Mongolitubulus squamifer*; Esakova and Zhegallo 1996: 103, pl. 4: 9–13.
2001 *Mongolitubulus squamifer*; Skovsted and Peel 2001: 137, fig. 2.
2001 *Mongolitubulus* ex gr. *M. squamifer*; Demidenko in Gravestock et al. 2001: 87, pl. 11: 5a, b.
2002 *Mongolitubulus squamifer*?; Landing et al. 2002: 301, fig. 4.19.
2003 *Mongolitubulus squamifer*; Dzik 2003: figs. 2, 3.
2004 *Mongolitubulus squamifer*; Wrona 2004: 43, figs. 23A–H, 24.
2006 *Mongolitubulus squamifer*; Brock and Percival 2006: 86, fig. 5E–J.
2007 *Mongolitubulus squamifer*; Topper et al. 2007: 76, fig. 5A–H.
2009 *Mongolitubulus squamifer*; Wrona 2009: 367, fig. 13A, B.
2011 *Mongolitubulus squamifer*; Topper et al. 2011: fig. 7I–K.

Material.—Five broken spines from Clast 1, and 10 broken spines from Clast 5, eight figured (SAM P57227–57234). All from the *Dailyatia odyssei* Zone, WPC, Kangaroo Island, South Australia.

Description.—Isolated, broken or fragmentary hollow spines. Spines are straight or slightly curved, and bear distinctive, regularly arranged, rhomboid scales along their length (Fig. 5). Individual scales can be up to ~25 µm wide, and inclined at an angle to the spine, oriented toward the tip or narrower end of the spine. Where spines retain a flared base, scales are reduced to low pustules (Fig. 5F).

Remarks.—All material in the WPC is represented by isolated, broken spines. A single, fragmentary specimen retains the flared base (Fig. 5F). While several *Mongolitubulus* species have been recovered with the spine and shield intact, the type species *Mongolitubulus squamifer* is known only from isolated spines, and none have been found attached to a bradoriid shield (Topper et al. 2013). The taxonomic difficulties associated with isolated bradoriid spines are well documented (Skovsted et al. 2006; Topper et al. 2007, 2013; Li et al. 2012; Caron et al. 2013). Li et al. (2012) showed that the ornament on *Mongolitubulus* spines is similar on spines of the trilobite *Hupeidiscus orientalis* (Li et al. 2012). However, as Topper et al. (2013) pointed out, there is a significant size difference between the trilobite spines and those attributed to *Mongolitubulus*, which are generally larger. Caron et al. (2013) also showed a strong similarity between *Mongolitubulus* spines and the dorsal spines of the lobopod *Hallucigenia*. Distinguishing between disarticulated spines of bradoriids and lobopods may be difficult, but Caron et al. (2013) suggested that the spines of *Hallucigenia* lack flaring spine bases, and the presence of such structures in the WPC material support the bradoriid affinity of *M. squamifer*.

Mongolitubulus squamifer spines from the WPC are consistently broken, so their maximum length cannot be ascertained, however the largest specimen is ~300 µm in width, which conforms to the maximum width of *M. squamifer* spines (Topper et al. 2013). The WPC specimens also exhibit the distinctive rhombic scales characteristic of the species (Fig. 5). On the specimen that retains the flared base, the scales are reduced to rounded pustules, and are more widely spaced (Fig. 5F). This is similar to the ornament on spines of other *Mongolitubulus* species which becomes gradually less pronounced on the proximal parts closer to the shield (Betts et al. 2014, 2017b).

Stratigraphic and geographic range.—*Mongolitubulus squamifer* had a global distribution during the early Cambrian,

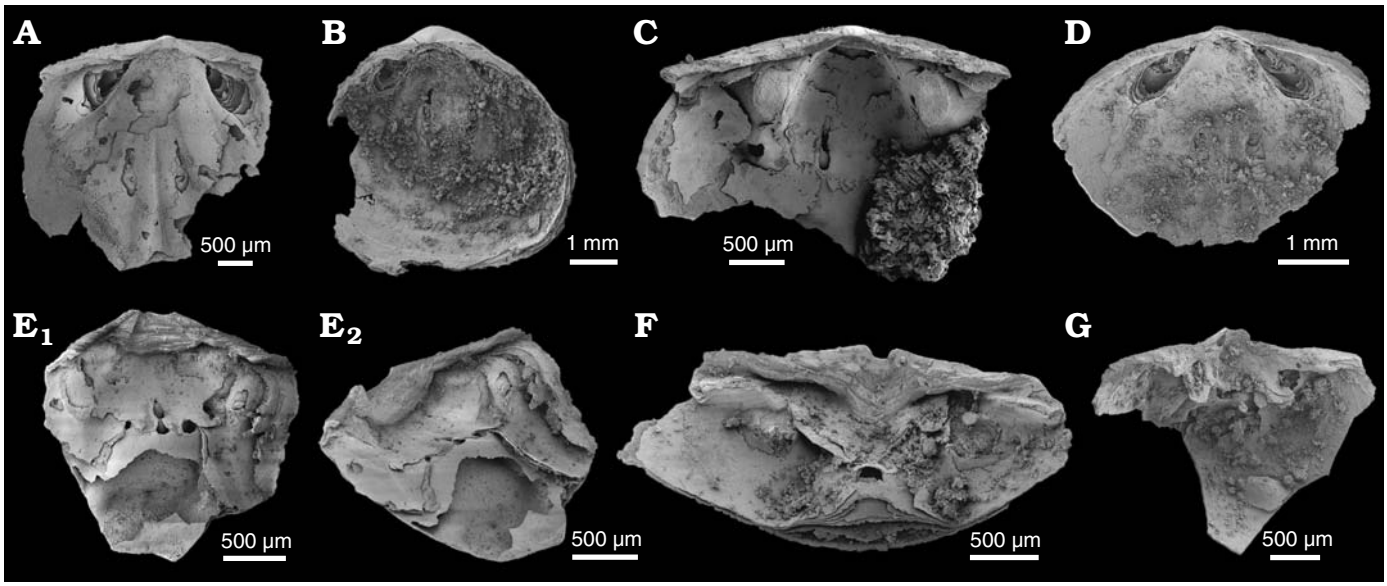

Fig. 6. The lingulid brachiopod *Eodicellomus elkaniiformis* Holmer and Ushatinskaya in Gravestock et al., 2001 from the lower Cambrian White Point Conglomerate, Kangaroo Island, South Australia. Dorsal (A–D) and ventral (E–G) valves. **A**. SAM P57235 in interior view. **B**. SAM P57236 in interior view. **C**. SAM P57237 in interior view. **D**. SAM P57238 in interior view. **E**. SAM P57240 in interior (E_1) and oblique (E_2) views. **F**. SAM P57241 in oblique view. **G**. SAM P57239 in oblique view.

and is known from Mongolia, Maly Karatau (Kazakhstan), east and west Avalonia, Laurentia, and glacial erratics from King George Island, Antarctica (Topper et al. 2007). South Australia, Arrowie Basin: *M. squamifer* ranges from the *Pararaia tatei* Zone (AJX-M section, Mount Scott Range, northern Flinders Ranges) to the *Pararaia janeae* Zone (DBS section, Donkey Bore Syncline, central Flinders Ranges) (Betts et al. 2017b: fig. 13). Stansbury Basin: WPC clasts, Kangaroo Island.

Phylum Brachiopoda Duméril, 1806

Subphylum Linguliformea Williams et al. 1996

Class Lingulata Gorjansky and Popov, 1986

Order Lingulida Waagen, 1885

Superfamily Linguloidea Menke, 1828

Family ?Obolidae King, 1846

Genus *Eodicellomus* Holmer and Ushatinskaya in Gravestock et al., 2001

Type species: *Eodicellomus elkaniiformis* Holmer and Ushatinskaya in Gravestock et al., 2001 from lower Cambrian of South Australia (Horse Gully section, Yorke Peninsula).

Eodicellomus elkaniiformis Holmer and Ushatinskaya in Gravestock et al., 2001

Fig. 6.

1986 *Edreja* aff. *distincta*; Laurie 1986: 451, figs. 5F, 12C–H.
?1988 "Elkaniid-like lingulide"; Rowell et al. 1998: 14, pl. 1: G.
2001 *Eodicellomus elkaniformis*; Holmer and Ushatinskaya in Gravestock et al. 2001: 126, pl. 19: 1–4, 6–11 (non 5a–c).
2006 *Eodicellomus elkaniformis*; Jago et al. 2006: 414, fig. 4K, L.
2016 *Eodicellomus elkaniformis*; Betts et al. 2016: 195, fig. 17I, K–M.

Material.—One dorsal valve from Clast 1, six dorsal valves from Clast 4, 40 dorsal valves and ten ventral valves from Clast 5; eleven figured (SAM P57235–57241). From the *Dailyatia odyssei* Zone, WPC, Kangaroo Island, South Australia.

Description.—Shells are biconvex to weakly ventribiconvex in profile, but variable in outline, ranging from slightly longer than wide (Fig. 6B, C) to equidimensional in juvenile shells to slightly transversely oval in larger shells. Valves of *Eodicellomus elkaniiformis* from the WPC clasts are relatively large (up to ~5 mm width; Fig. 6B, C), biconvex shells with strongly thickened visceral platforms. Mature shells (normally greater than 2 mm width) are on average 92% as long as wide; maximum shell width at, or just posterior of, mid-length.

Ventral valve with a distinctly acuminate beak (Fig. $6E_2$, G). Pseudointerarea apsacline, wide, taking up on average 75% valve width. Propareas are well-developed, narrow and subtriangular with curved anterior edges. Propareas have flattened to gently concave surfaces, are thickened distally and are raised above the valve floor (Fig. 6E–G). Pedicle groove is deeply set below the level of the pseudointerarea and is defined within the umbo by a distinctive concave triangular plate that does not reach, or is only slightly adpressed to the valve floor (Fig. 6F). Flexure lines are well-developed.

Interior of the ventral valve in mature specimens is greatly thickened, developed as a high, raised, visceral platform. Posterior slope of the platform hosts a pair of elongate central muscle scars (Fig. 6E, F). Postero-lateral muscle scars narrowly sub-elliptical to kidney-shaped, occurring on variably elevated muscle pads, that in mature specimens form distinctive platforms, raised high above the valve floor (Fig. 6E, F). *Vascula lateralia* gently curved distally and may be deeply impressed (Fig. 6E).

Dorsal valve with a rounded posterior margin. Pseudointerarea is anacline, flattened with a broad, triangular median plate (Fig. 6B–D). Propareas are long, curved, sometimes enrolled, and very narrow with well-developed flexure lines (Fig. 6A, D). Dorsal visceral area is deeply recessed and concave in the posterior half of the valve, gradually thickening and increasing in elevation to form a platform hosting a pair of central muscle scars (Fig. 6A–D). Median ridge develops just posterior of mid-valve, directly between the raised central muscle scars, and extends and widens anteriorly of central muscle scars (Fig. 6A, D). Postero-lateral muscle scars are elongate, widely divergent and elevated on the postero-lateral slopes of the valve on distinctive muscle pads. In mature and gerontic dorsal valves the postero-lateral muscle pads form into blunt-ended "brachiophore-like" projections that merge posteriorly with the pseudointerarea and are supported anteriorly by distinctive short ridges (Fig. 6C). *Vascula lateralia* are straight, deeply incised, very widely divergent and extend to the anterior margin (Fig. 6A). *Vascula media* arise just anterior of mid valve on either side of the median ridge as deeply incised, relatively broad, straight, weakly divergent grooves (Fig. 6A).

Remarks.—Valves of *Eodicellomus elkaniiformis* from the WPC clasts have biconvex shells with strongly thickened visceral platforms. Recent SEM and microCT work on *E. elkaniiformis* from the Arrowie Basin has resolved details of internal morphology not previously attainable with traditional SEM techniques (Jacquet et al. 2018). Exfoliated shells from the WPC reveal a characteristic, layered microstructure, which is comparable with their findings (Fig. 6E, F). This shows that within the secondary layer, rhythmic compact laminae are separated by either apatite infills or void spaces, once likely filled with organic-rich (chitinous) matrix. This microstructure occurs in both valves, though are more prevalent in dorsal valves which exhibit greatly thickened platforms. Jacquet et al. (2018) showed that these raised platforms tend to exhibit more secondary loss of the organic-rich material, often leaving obvious void spaces in the shells in these areas.

Eodicellomus is comparable to members of the recently reintroduced family Neobolidae Walcott and Schuchert in Walcott, 1908, as they have the diagnostic trilobate thickened visceral platform on the ventral valve, and platforms developed on the dorsal valve interior (Popov et al. 2015: 23). However, *Eodicellomus* has well-developed flexure lines on both the dorsal and ventral propareas and wide pseudointerarea, which are not present in other members of the Neobolidae (Fig. $8C_3$, D, E; Popov et al. 2015).

Holmer and Ushatinskaya in Gravestock et al. (2001: 125–126) recognised a strong similarity between *Eodicellomus* and late Cambrian–Ordovician elkaniids, which have raised muscle platforms on valve interiors (Holmer 1993). However, they did not place *Eodicellomus* in the Elkaniidae because it lacks pitted microornamentation on the adult shell (Holmer and Ushatinskaya in Gravestock et al. 2001). Like the Eoobolidae, the Elkaniidae has broad variability in the pitted post-metamorphic ornamentation, from regularly spaced and shaped rhomboid pits in the Lower Ordovician *Lamanskya splendens* Moberg and Segerberg, 1906 (Holmer 1993: fig. 6a–e) to the irregular, rounded pits of the middle Cambrian *Broeggeria salteri* (Holl 1865; Popov and Holmer 1994: fig. 58c, l). However, a pitted metamorphic shell is often lost to abrasion, and the development of pustulose post-metamorphic ornament is often highly variable. Hence, these are unreliable characters upon which to diagnose family-level classifications (Balthasar 2009: 416).

Stratigraphic and geographic range.—*Eodicellomus elkaniformiis* is an East Gondwanan endemic. It occurs in the Arrowie Basin (*Micrina etheridgei–Dailyatia odyssei* zones): Ajax Limestone, Mt. Scott Range, northern Flinders Ranges; Mernmerna Formation and Wirrapowie Limestone, south and east Arrowie Syncline, northeast Flinders Ranges; Winnitinny Creek Member and Second Plain Creek Member, Wilkawillina Limestone, Bunkers Graben, southern-central Flinders Ranges; Moorowie Formation, Chambers Gorge area, eastern Flinders Ranges. Stansbury Basin (*D. odyssei* Zone): Parara Limestone, Horse Gully, Curramulka Quarry and SYC-101 borehole, Yorke Peninsula; WPC clasts, Kangaroo Island. Amadeus Basin: Todd River Dolomite, Phillipson No. 1 Borehole, Northern Territory.

Family Eoobolidae Holmer, Popov, and Wrona, 1996

Genus *Eoobolus* Matthew, 1902

Type species: *Obolus triparilis* Matthew, 1902; midddle Cambrian (Bourinot Group) of Cape Breton, Canada.

Stratigraphic and geographic range.—*Eoobolus* is a globally distributed genus: See Ushatinskaya and Korovnikov (2014: 31) for a recent synopsis of the distribution of this taxon.

Eoobolus sp.

Fig. 7A–C.

Material.—Fifteen ventral valves from Clast 5, three figured (SAM P57242–57244). From the *Dailyatia odyssei* Zone, WPC, Kangaroo Island, South Australia.

Description.—Material consists of relatively fragmentary ventral valves, making comprehensive description difficult. Valves sharply acuminate, apical angle ca. 80° (Fig. 7A, B). Elongate, apsacline pseudointerarea, propareas narrow, widening slightly anteriorly and separated by adpressed pedicle groove which widens anteriorly (Fig. 7A, B). Flexure lines parallel to posterolateral margins (Fig. 7A, B).

Remarks.—Assignment to the Eoobolidae relies on characters such as a pitted metamorphic shell and a pustulose adult shell that Balthasar (2009) showed was variably expressed, and hence not useful for family-level taxonomic designation. Balthasar (2009) placed *Eoobolus* in the Zhanatellidae, as material from the Mural Formation (Canadian Rocky Mountains) exhibited fine pits on both the metamorphic and adult shells in addition to other characters diagnostic of the Zhanatellidae. The diagnosis of Zhanatellidae Koneva, 1986 in-

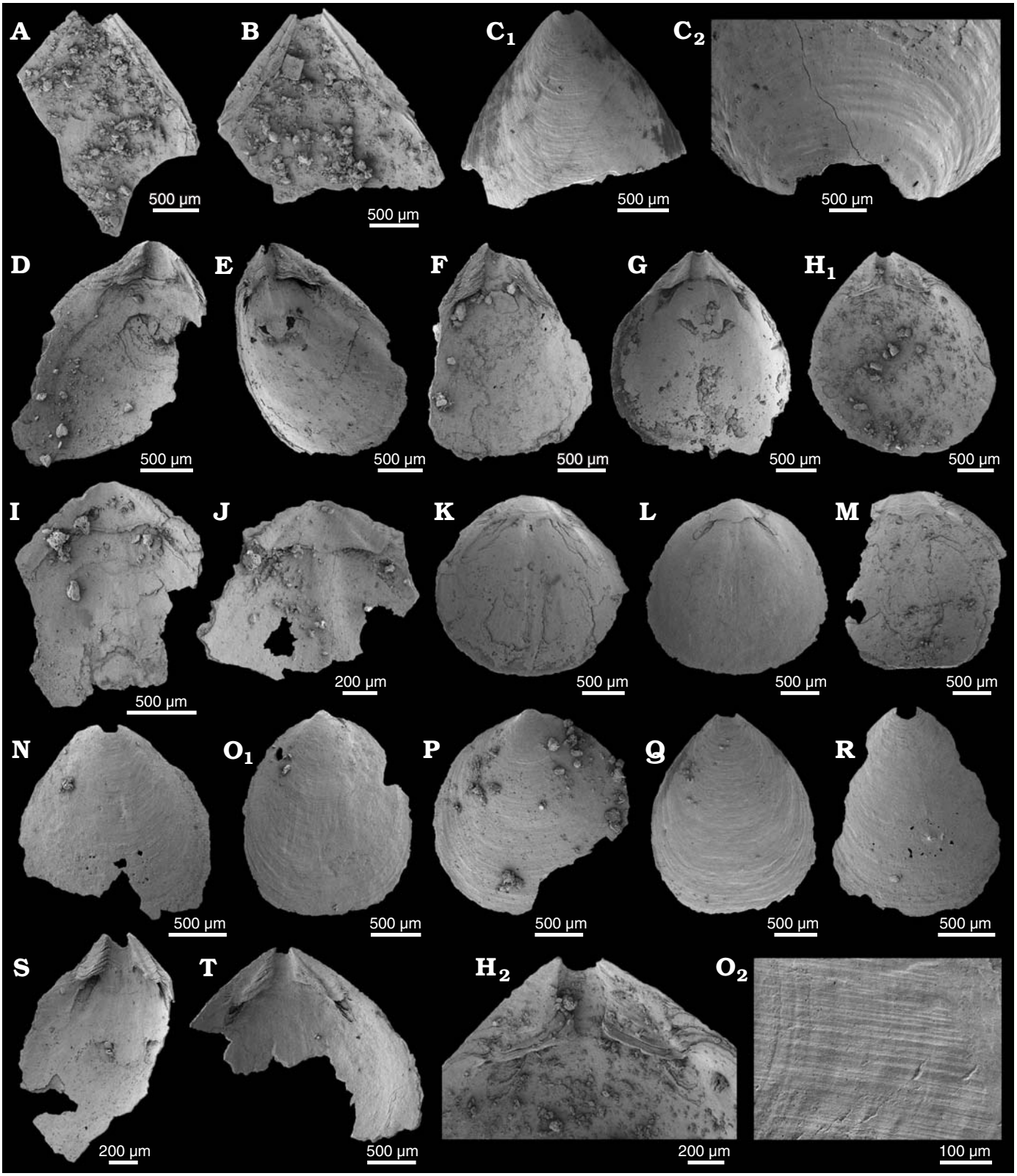

Fig. 7. The lingulid brachiopods *Eoobolus* sp. (A–C) and *Kyrshabaktella davidi* Holmer and Ushatinskaya in Gravestock et al., 2001 (D–T) from the lower Cambrian White Point Conglomerate, Kangaroo Island, South Australia. Ventral (A–H, N, Q–T) and dorsal (I–M, O, P) valves. **A**. SAM P57242 in internal view. **B**. SAM P57243 in internal view. **C**. SAM P57244, in external view (C_1); C_2, detail of post larval shell. **D**. SAM P57245 in internal view. **E**. SAM P57246 in oblique view. **F**. SAM P57247 in internal view. **G**. SAM P57248 in internal view. **H**. SAM P57249 in internal view (H_1); H_2, detail of the interarea. **I**. SAM P57250 in internal view. **J**. SAM P57251 in internal view. **K**. SAM P57252 in internal view. **L**. SAM P57253 in internal view. **M**. SAM P57254 in internal view. **N**. SAM P57255 in external view. **O**. SAM P57256 in external view (O_1); O_2, detail of external radial and concentric ornament. **P**. SAM P57257 in external view. **Q**. SAM P57258 in external view. **R**. SAM P57259 in external view. **S**. SAM P57260 in internal view. **T**. SAM P57261 in internal view.

cludes a flattened ventral valve pseudointerarea with variably developed flexure lines, with no information provided on the elevation of the dorsal pseudointerarea (Popov and Holmer 1994: 70). *Eoobolus* is referred to the Eoobolidae herein, which can be distinguished from the Zhanatellidae in having a ventral pseudointerarea elevated above the valve floor with both a deep pedicle groove and well-developed flexure lines, and with a dorsal pseudointerarea always divided and raised above the valve floor (Holmer et al. 1996: 41).

Distinguishing between species of *Eoobolus* is problematic since most exhibit high intraspecific variability (Balthasar 2009; Ushatinskaya and Korovnikov 2014). The most stable character in *Eoobolus* for determining species appears to be the apical angle in adult ventral valves (Balthasar 2009), along with the relative width and length of the ventral propareas (Ushatinskaya and Korovnikov 2014). The few specimens recovered from the WPC have apical angles of approximately 80°, within the range of *Eoobolus priscus* (Poulsen 1932) from the Bastion Formation of North-East Greenland (Cambrian Series 2) (70–90° according to Skovsted and Holmer 2005: 332) and *E.* aff. *viridis* from the Xihaoping Member of Shaanxi Province, China (Cambrian Series 2, Stage 3) (80–90° according to Li and Holmer 2004: 197). The ventral propareas of *Eoobolus* sp. from the WPC are more slender than the broader triangular propareas of *Eoobolus* aff. *viridis* (compare Fig. 7A, B with Li and Holmer 2004: fig. 6K, 7G). The elongate, slender propareas and triangular pedicle groove of the WPC specimens are also similar to *Eoobolus siniellus* (Pelman, 1983) from the Sinyaya Formation, Siberian Platform (Cambrian Series 2, Botoman Stage) (see Ushatinskaya and Korovnikov 2014: pl. 5: 1–7), although this species has a broader apical angle of 90–105° (Ushatinskaya and Korovnikov 2014: 34).

Family Kyrshabaktellidae Ushatinskaya in Pelman et al., 1992

Genus *Kyrshabaktella* Koneva, 1986

Type species: *Kyrshabaktella certa* Koneva, 1986; the Cambrian Amgan Stage of Kazakhstan.

Kyrshabaktella davidi Holmer and Ushatinskaya in Gravestock et al., 2001

Fig. 7D–T.

2001 *Kyrshabaktella davidi*; Holmer and Ushatinskaya in Gravestock et al. 2001: 127, pl. 20: 1–10.
2006 *Kyrshabaktella davidi*; Jago et al. 2006: 414, fig. 4E, F.
2016 *Kyrshabaktella davidii*; Betts et al. 2016: 195, fig. 17Q–T.

Material.—Fifteen dorsal valves and 24 ventral valves from Clast 1, nine dorsal valves and 21 ventral valves from Clast 4 and 219 dorsal valves and 288 ventral valves from Clast 5; 17 figured (SAM P57345–57261). All from the *Dailyatia odyssei* Zone, WPC, Kangaroo Island, South Australia.

Description.—Valves oval to circular in outline (Fig. 7E, G, K, L, O_1–R); weakly biconvex, slightly longer than wide with maximum width from mid-length to anterior. Ventral valves 1.10–2.85 mm long (mean 2.04 mm, N = 11), 0.95–2.56 mm wide (mean 1.75, N = 9), 110–125% long as they are wide; dorsal valves 1.15–2.30 mm long (mean 1.84, N = 12), 1.00–2.47 mm wide (mean 1.75 mm, N = 12), 95–98% long as they are wide. Ventral valve is gently convex, acuminate posterior and rounded anterior (Fig. 7D–H_1, Q). Dorsal valve gently convex and subcircular in outline (Fig. 7K–M, O_1). Metamorphic shell is almost circular and smooth. Adult shells are covered by thin concentric lines and sometimes by fine radial striae on the lateral slopes (Fig. $7O_2$).

Ventral pseudointerarea is divided by emarginature into two triangular propareas with well-developed flexure lines (Fig. 7D–H, S, T). Ventral interior with thickened visceral area (Fig. 7D, E, H_2), extending to mid-length with umbonal muscle scars barely discernable. Elongate, well-impressed postero-lateral muscle scars located below and distal to the propareas (Fig. 7D, E, G).

Dorsal pseudointerarea is moderately high, subtriangular and orthocline (Fig. 7I–M). Propareas are narrow, curved and elongate with weak flexure lines. Postero-lateral muscles scars elongate (Fig. 7K, L), remaining musculature not preserved. Broad but poorly developed median ridge extending beyond mid-length of valve (Fig. 7K, L).

Remarks.—The recent history of this monogeneric linguloid family has been discussed in detail by Skovsted and Holmer (2006) and Streng et al. (2008) and need not be repeated here. The discovery of a pitted larval shell and columnar shell structure in specimens of *Kyshabaktella* sp. from the lower Cambrian Harkless Formation, Nevada (Skovsted and Holmer 2006: fig. 3) and the recognition of similar shell structure in valves of *K. mudedirri* from the middle Cambrian of the Georgina Basin (see Kruse 1991: fig. 6c) indicates that columnar shell structure is relatively widespread within Lingulida. It should be noted that the presence of columnar shell structure and a pitted metamorphic shell has not yet been documented in the type species of the genus, *K. certa* from the Wuliuan–early Drumian of Kazakhstan. Until these structures are confirmed in the type species, it is possible that the described specimens from Nevada and Australia do not belong to *Kyrshabaktella* (sensu stricto).

Specimens of *Kyrshabaktella davidi* from the WPC reach a much larger maximum size (up to 2.85 mm in length, 2.56 mm in width, Fig. $7H_1$) than those originally described by Holmer and Ushatinskaya in Gravestock et al. (2001), who reported valve lengths of 0.96–1.25 mm and widths of 1.02–1.17 mm for material from the CD-2 drillcore, Parara Limestone on the Yorke Peninsula, South Australia. This is less than half the maximum dimensions of *K. davidi* from the WPC.

On ventral valves of *K. davidi* from the WPC, the pedicle groove is typically more adpressed to the valve floor (Fig. 7D–H, S, T), whereas specimens from the Parara Limestone have a pedicle groove raised above the valve floor (Holmer and Ushatinskaya in Gravestock et al. 2001: pl. 20: 1b, 6). Specimens from the WPC lack the vascula

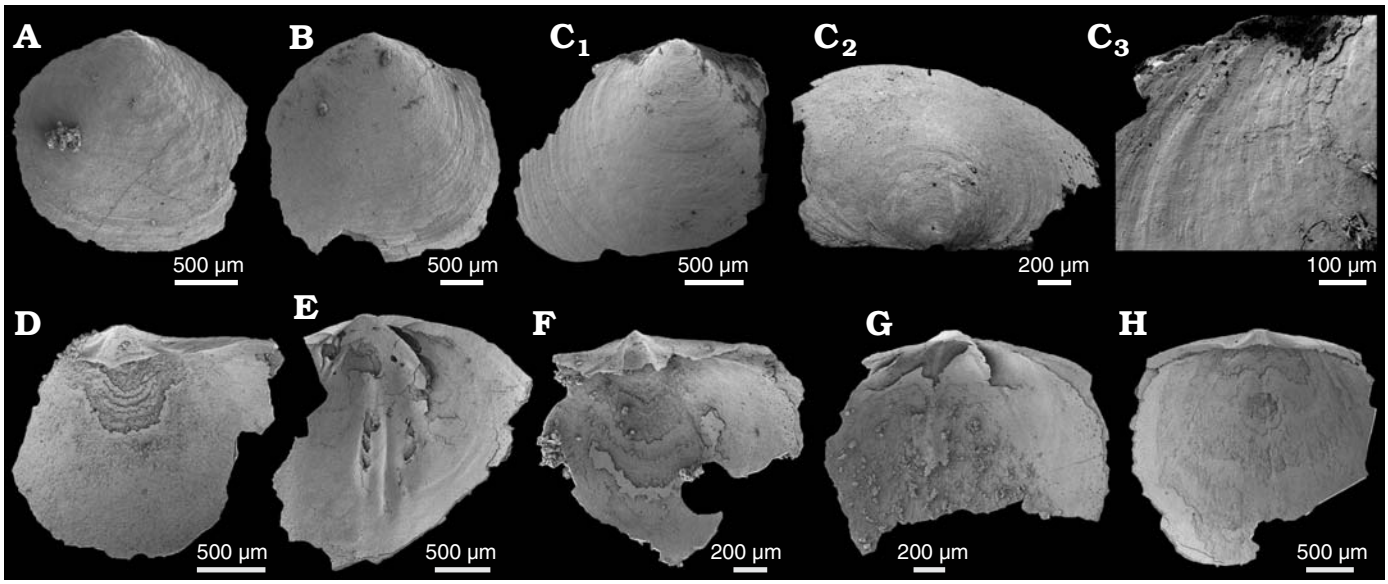

Fig. 8. The lingulid brachiopod *Curdus pararaensis* Holmer and Ushatinskaya in Gravestock et al., 2001 from the lower Cambrian White Point Conglomerate, Kangaroo Island, South Australia. Dorsal (A, B, E, G, H) and ventral (C, D, F) valves. **A**. SAM P57262 in external view. **B**. SAM P57263 in external view. **C**. SAM P57264 in external (C_1) and oblique (posterior) (C_2) views; C_3 shows external ornament of faint concentric growth lines. **D**. SAM P57265 in internal view. **E**. SAM P57266 in internal view. **F**. SAM P57267 in internal view. **G**. SAM P57268 in internal view. **H**. SAM P57269 in internal view.

lateralia and vascula media described figured by Holmer and Ushatinskaya in Gravestock et al. (2001: pl. 20: 1b, 5b), though this may be preservational.

The specimens described here can be readily distinguished from the type species *Kyrshabaktella certa* Koneva, 1986 from the Amgan of Kazahkstan (Wuliuan Stage–earliest Drumian Stage), which has well-developed flexure lines on the much narrower propareas of the ventral valve (Holmer et al. 2001: 34, pl. 5: 7, 10). *Kyrshabaktella mudedirri* from the Tindall Limestone, Northern Territory, Australia (Kruse 1990: pl. 10: D; Terreneuvian, Stage 2–Wuliuan) shares some similarities with *K. davidi* from the WPC. Both have similarly adpressed pedicle grooves and relatively narrow propareas on the ventral valve. However, they can be distinguished, as *K. mudedirri* has a beak at the posterior apex of the dorsal valves (Kruse 1990: pl. 10: H, J), a shorter pedicle groove, and a more rounded delthyrial opening on the ventral valves (Kruse 1990: pl. 10: C, D). The recently described *Kyrshabaktella diabola* Skovsted, Knight, Balthasar, and Boyce, 2017 from the Forteau Formation of Laurentian Newfoundland and southern Labrador (mid-Dyeran; Cambrian Series 2, Stage 4) can be distinguished from *K. davidi* by its narrow pseudointerarea with elongated propareas on the ventral valve (Skovsted et al. 2017: fig. 14.3), and well-developed diamond-shaped dorsal pedicle groove (Skovsted et al. 2017: figs. 14.9, 14.10). *Kyrshabaktella diabola* also lacks flexure lines and has a broader pedicle groove than *K. davidi* (Skovsted et al. 2017: figs. 14.2, 14.3).

Stratigraphic and geographic range.—South Australia, lower Cambrian: Stuart Shelf, Andamooka Limestone. Arrowie Basin (*Micrina etheridgei–Dailyatia odyssei* zones): Ajax Limestone, Mt. Scott Range; Nepabunna Siltstone, north-east Flinders Ranges; Winnitinny Creek Member of the Wilkawillina Limestone; Bunkers Range, Second Plain Creek Member of the Wilkawillina Limestone, Bunkers Graben; Wirrapowie Limestone, south-west Arrowie Syncline; Six Mile Bore, Linns Springs and Third Plain Creek members of the Mernmerna Formation, Bunkers Range and Bunkers Graben; Upper Mernmerna Formation, Donkey Bore Syncline; Mernmerna Formation, Southern Arrowie Syncline, Chambers Gorge region, eastern Flinders Ranges. Stansbury Basin: Curramulka Quarry and CD-2 drillcore on the Yorke Peninsula, WPC clasts, Kangaroo Island.

Family Neobolidae Walcott and Schuchert in Walcott, 1908

Genus *Curdus* Holmer and Ushatinskaya in Gravestock et al., 2001

Type species: *Curdus pararaensis* Holmer and Ushatinskaya in Gravestock et al., 2001; lower Cambrian of South Australia (KLM, Yorke Peninsula).

Curdus pararaensis Holmer and Ushatinskaya in Gravestock et al., 2001

Fig. 8.

2001 *Curdus pararaensis*; Holmer and Ushatinskaya in Gravestock et al. 2001: 130, pl. 22: 1–14.
2007 *Curdus pararaensis*; Paterson et al. 2007b: 139, fig. 3L–N.
2017 *Curdus pararaensis*; Betts et al. 2017b: 257, fig. 15V (non fig. 15P–U).

Material.—One dorsal valve from Clast 1 and 25 dorsal valves and 14 ventral valves from Clast 5; eight figured (SAM P57262–57269). From the *Dailyatia odyssei* Zone, WPC, Kangaroo Island, South Australia.

Description.—Near-complete shells, oval to sub-pentagonal in outline, ventribiconvex. Largest near-complete valve (Fig. 8B) 2.7 mm in length, 2.7 mm in width, all near-complete valves slightly wider than long (mean 93%, N = 3, Fig. 8A, B, H). Ornamentation with irregular filae (Fig. 8A–C) interrupted by drapes and nick-points (Fig. 8A, C_1, C_2). Metamorphic shells poorly preserved, undifferentiated from post-metamorphic shell (Fig. 8C_2, C_3).

Ventral valve pseuodinterarea broad, apsacline, forming shelf and gently curved posterior margin. Propareas are long, with flexure lines, and separated by deep triangular pedicle groove (Fig. 8D, F). Ventral valve interiors poorly preserved, valve floor with single, large, recessed scar, and no information retained of the viscera (Fig. 8D, F). Dorsal valve with more rounded posterior margin; pseudointerarea rudimentary, anacline, and with short propareas separated by a shallow pedicle groove (Fig. 8E, G, H). Well-preserved specimen interior (Fig. 8E) with raised slope immediately anterior of pedicle groove, developing into trilobate platform that extends for most of the valve floor.

Remarks.—This taxon was originally described from subsurface cores CurD1B and SYC-101 through the KLM (of the Parara Limestone) in the Stansbury Basin by Holmer and Ushatinskaya in Gravestock et al. (2001: 130, pl. 22: 1–14). This material was very fragmentary, consisting mostly of broken interareas and metamorphic shells (Gravestock et al. 2001: pl. 22: 1–14). Additional examples of *C. pararaensis* are also fragmentary (Paterson et al. 2007b; Betts et al. 2016, 2017b). Material from the WPC is also often abraded and damaged, though some shells retain outline morphology, revealing that the valves may have been in excess of 3 mm wide (Fig. 8B) and grossly sub-circular to sub-pentagonal in outline (Fig. 8A, B, C_1, D–H). External surfaces of the valves are also abraded, but some retain concentric growth lines, radial "drapes" and striae (Fig. 8C).

Curdus pararaensis bears some similarities to *Minlatonia tuckeri* Holmer and Ushatinskaya in Gravestock et al., 2001. Major differences include ornamentation and the convexity of the valves. However, presentation of external ornament is controlled by preservation, and the shape of the valves in *M. tuckeri* was based on few intact (possibly juvenile) specimens. Hence, it is possible that *C. pararaensis* and *M. tuckeri* may be conspecific, though additional, well-preserved material is required to test this.

Curdus pararaensis was originally assigned to the ?Botsfordiidae based on general similarities witih *Botsfordia asperella* Koneva, 1979, including some internal features (Paterson et al. 2007b). However, *Curdus* does not have tubercles or pits on the metamorphic shell, and lacks a pustulose post-metamorphic shell (Paterson et al. 2007b). Popov et al. (2015) assigned *Curdus* to the Neobolidae which was emended to include genera with a smooth metamorphic and postmetamorphic shell, strong, trilobate platform in the ventral valve, prominent dorsal median ridge and variously developed muscle platforms.

Stratigraphic and geographic range.—Lower Cambrian of South Australia, Arrowie Basin (*D. odyssei* Zone): Linns Springs Member of the Mernmerna Formation, Donkey Bore Syncline. Stansbury Basin (*D. odyssei* Zone): KLM (CurD1B and SYC-101 drillcores) and WPC clasts, Kangaroo Island.

Superfamily Acrotheloidea Walcott and Schuchert in Walcott, 1908

Family Botsfordiidae Schindewolf, 1955

Genus *Schizopholis* Waagen, 1885

Type species: *Karathele coronata* Koneva, 1986; middle Cambrian of Kazakhstan (Maly Karatau).

Schizopholis yorkensis (Holmer and Ushatinskaya in Gravestock et al., 2001)

Fig. 9.

2001 *Karathele yorkensis*; Holmer and Ushatinskaya in Gravestock et al. 2001: 128–129, pl. 21: 1–11.

2016 *Karathele* (= *Schizopholis*) *yorkensis*; Betts et al. 2016: 195, fig. 17A–H.

Material.—Two dorsal valves and a single ventral valve from Clast 4 and seven dorsal valves and six ventral valves from Clast 5; six figured (SAM P57270–57275). From the *Dailyatia odyssei* Zone, WPC, Kangaroo Island, South Australia.

Description.—Fragmentary dorsal and ventral valves lacking information on general morphology (Fig. 9). Ventral valve with procline pseudointerarea (Fig. 9D_1, E, F_1). Broad, open delthyrium in contact with, but not intruding into metamorphic shell, lateral margins widening postiorly (Fig. 9F_2, D_2). Dorsal valve with rounded posterior margin (Fig. 9A, B, C_1) and rudimentary apsacline pseudointarea (Fig. 9E). Interior with proportionally small propareas (0.91 mm wide on a broken dorsal valve which is at least 2.33 mm wide, Fig. 9E) forming narrow shelf overhanging posterior margin of narrow cardinal muscle scars. Short median buttress, in single measured specimen extending 0.35 mm anteriorly along valve floor (Fig. 9E). Valve exteriors covered in irregularly spaced tubercles (Fig. 9C_3) except along the ventral valve pseudointerarea and posterior margin of the dorsal valve, which are smooth (Fig. 9A, B, C_1, D_1, F_1). Dorsal valve metamorphic shell mean length 0.23 mm and width 0.34 mm (N = 3) with two slightly elongate lobes and pitted microornamentation (Fig. 9C_2). Ventral valve metamorphic shell mean length 0.33 mm and width 0.37 mm (N = 2) with single posterior lobe, two low anterior lobes and smooth, lacking microornament (Fig. 9D_2, F_2). Metamorphic shells encircled by halo (Fig. 9C_2, D_2, F_2).

Remarks.—This species was originally assigned to *Karathele* Koneva 1986, which has since been synonymised with *Schizopholis*, a genus known from Cambrian Stage 4 of Australia, Antarctica and the Himalaya (Popov et al. 2015). In their original description of material from the Stansbury Basin, Holmer and Ushatinskaya in Gravestock et al. (2001:

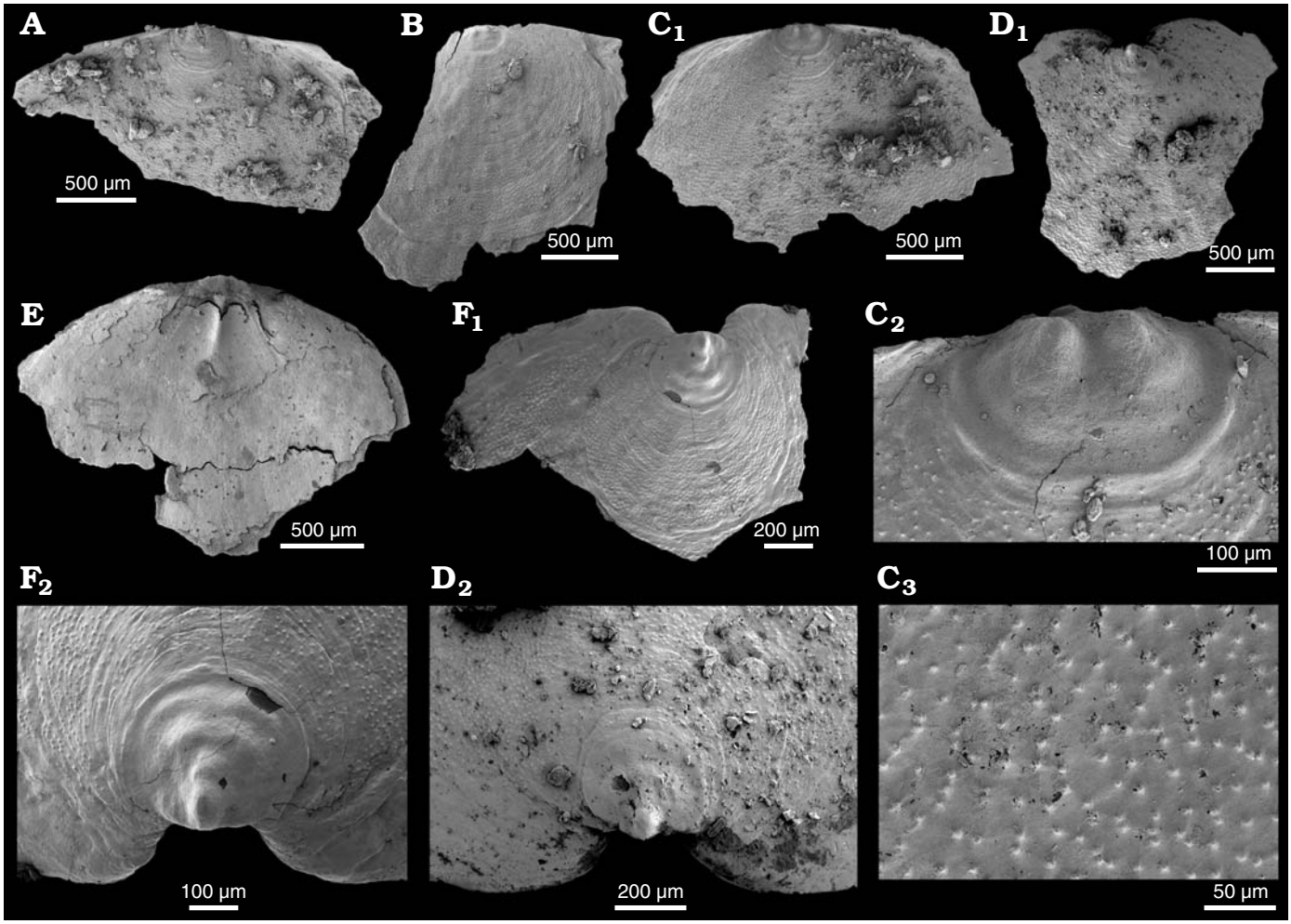

Fig. 9. The lingulid brachiopod *Schizopholis yorkensis* (Holmer and Ushatinskaya in Gravestock et al., 2001) from the lower Cambrian White Point Conglomerate, Kangaroo Island, South Australia. Dorsal (A–C, E) and ventral (D, F) valves. **A**. SAM P57270 in external view. **B**. SAM P57271 in external view. **C**. SAM P57272 in external view (C_1); C_2, detail of the larval shell; C_3, external pustulose ornament. **D**. SAM P57273 in external view (D_1); D_2, detail of the larval shell. **E**. SAM P57274 in internal view. **F**. SAM P57275 in external view (F_1); F_2, detail of the larval shell.

129) reported a maximum shell length of 1 mm and maximum width of 1.1 mm. The new material from the WPC includes shell fragments over 2 mm wide (Fig. 9A, C_1). In addition, the width of the metamorphic shell was described as "150–160 mm across" in the original description Holmer and Ushatinskaya in Gravestock et al. (2001: 129), and despite the fact that the "mm" should have actually been in microns, the average size of the metamorphic shell is actually 360 µm in width (Fig. $9C_2$).

Schizopholis yorkensis from the WPC has a delthyrium that is broad and divergent throughout ontogeny (Fig. 9D, F), distinguishing it from *Schizopholis napuru* Kruse, 1990, in which the delthryium converges later in ontogeny (Kruse 1990: pl. 12: A, B, F). *Schizopholis yorkensis* can also be distinguished from other members of *Schizopholis* in having only two dorsal tubercles on the metamorphic shell (Fig. 9B, C), distinguishing it from *Schizopholis quadrituberculum* Percival and Kruse, 2014 and the type species *Schizopholis coronata* Koneva, 1986, which have four (see Holmer et al. 2001: pl. 17; Percival and Kruse 2014: fig. 8).

Stratigraphic and geographic range.—Lower Cambrian of South Australia, *D. odyssei* Zone. Arrowie Basin (*Micrina etheridgei–D. odyssei* zones): Ajax Limestone, Mt. Scott Range; Winnitinny Creek Member of the Wilkawillina Limestone, Wirrapowie Limestone, Mernmerna Formation and Nepabunna Siltstone, Arrowie Syncline, northcentral-eastern Flinders Ranges; Winnitinny Creek Member of the Wilkawillina Limestone and Third Plain Creek Member of the Mernmerna Formation, Bunkers Range, central Flinders Ranges; Winnitinny Creek Member and Second Plain Creek Member of the Wilkawillina Limestone, Six Mile Bore, Linns Springs and Third Plain Creek members of the Mernmerna Formation, Upper Mernmerna Formation, Bunkers Graben; Wirrapowie Limestone and Mernmerna Formation, Elder Range, southern Flinders Ranges; Linns Springs and Third Plain Creek members of the Mernmerna Formation and Upper Mernmerna Formation, Donkey Bore Syncline, central Flinders Ranges; Mernmerna Formation, North Boundary Creek, Chambers Gorge area, eastern Flinders Ranges.

Stansbury Basin (*D. odyssei* Zone): Parara Limestone, Yorke Penninsula; Curramulka and Minlaton-1 drillcore; WPC clasts, Kangaroo Island.

Order Acrotretida Kuhn, 1949

Superfamily Acrotretoidea Schuchert, 1893

Family Acrotretidae Schuchert, 1893

Genus *Eohadrotreta* Li and Holmer, 2004

Type species: *Eohadrotreta zhenbaensis* Li and Holmer, 2004; lower Cambrian Shuijingtuo Formation, Xiaoyang section, Zhenba, South Shaanxi Province, China.

Eohadrotreta sp. cf. *E. zhenbaensis* Li and Holmer, 2004

Fig. 10.

2017 *Eohadrotreta* sp. cf. *E. zhenbaensis*; Betts et al. 2017b: 269, fig. 15A–O.

Material.—Twelve dorsal and four ventral valves from Clast 4; approximately 1675 dorsal and 1060 ventral valves from Clast 5, 14 figured (SAM P57276–57289). From the *Dailyatia odyssei* Zone, WPC, Kangaroo Island, South Australia.

Description.—See Holmer and Popov (2007: 2560–2562).

Remarks.—Specimens illustrated here are similar to those figured by Betts et al. (2017b: fig. 15A–O) from the upper Mernmerna Formation (10MS section) in the Bunkers Graben, southern-central Flinders Ranges. Brock in Betts et al. (2017b) outlined taxonomic difficulties associated with *Eohadrotreta zhenbaensis* from the Shuijingtuo Formation in South Shaanxi, China. Key issues are the variable development of characters such as the dorsal medium septum and the apical process and apical pits on the interior of the ventral valves (Li and Holmer 2004: 207). Like the specimens from the Flinders Ranges, the material from the WPC clasts do not have the well developed apical pits manifest in the Chinese specimens, hence are referred to *Eohadrotreta* sp. cf. *E. zhenbaensis.*

Zhang et al. (2018) defined three distinct ontogenetic stages for *Eohadrotreta zhenbaensis* in specimens from the Shuijingtuo Formation (Cambrian Series 2, Stage 3, Ajiahe and Wangjiaping sections, Three Gorges area, western Hubei Province, China), some of which are relevant to the identification of *Eohadrotreta*. Firstly, in valves <450 μm in length, the foramen is developed from a pedicle notch ("pedicle foramen forming stage", T1). Secondly, when the valve is 450–750 μm in length, a shallow intertrough and apical process develops in the ventral valve ("pedicle foramen enclosing stage", T2) (Zhang et al. 2018: figs. 4L, 5A). Thirdly, when the ventral valve interior has a valve length of >750 μm, the vascula lateralia is developed (Zhang et al. 2018: fig. 5G), and on dorsal valves <900 μm in length, the bifurcating median septum is developed ("intertrough increasing stage", T3) (Zhang et al. 2018: fig. 5K, L). These growth patterns are observed in *Eohadrotreta* sp. cf. *E. zhenbaensis* from the WPC, as well as *Eohadrotreta* sp. cf. *E. zhenbaensis* from the upper Mernmerna Formation (10MS section of the Bunkers Graben, South Australia, Cambrian Series 2, *D. odyssei* Zone; Brock in Betts et al. 2017b). In the Australian material, an impressed vascula lateralia is not developed in smaller ventral valves (Fig. 10C, D; Betts et al. 2017b: fig. 15B), but is present in larger specimens (cf. Fig. 10K). In contrast, the median septum of *Eohadrotreta* sp. cf. *E. zhenbaensis* from the WPC is not as well developed as in specimens from western Hubei, even in individuals >900 μm in length (Fig. 10H, N).

Eohadrotreta sp. cf. *E. zhenbaensis* from the WPC can be distinguished from *Eohadrotreta zhujiahensis* Li and Holmer, 2004 from Cambrian Series 2 Shuijingtuo Formation, South China by its pedicle foramen becoming enclosed early in ontogeny (Li and Holmer 2004: fig. 14C, J; Zhang et al. 2018: fig. 7). The ventral valve intertrough of *E. zhujiahensis* remains vestigial throughout ontogeny, but becomes better developed in *Eohadrotreta* sp. cf. *E. zhenbaensis* (Fig. 10G_2; Zhang et al. 2018: fig. 7). *Eohadrotreta* sp. cf. *E. zhenbaensis* can be distinguished from *E. haydeni* Popov et al. 2015 from the *Kaotaia parvatya* Trilobite Zone of the Parahio Formation (late Cambrian Stage 4 to Wuliuan Stage of the Parahio Valley, Indian Himalaya), by its better developed ventral valve intertrough and dorsal cardinal muscle scars (Fig. 10H, I, J, G_2; Popov et al. 2015: fig. 22F, H–J, M).

Stratigraphic and geographic range.—Lower Cambrian, South Australia, Arrowie Basin (*D. odyssei* Zone): Upper Mernmerna Formation and limestone beds near the base of the Oraparinna Shale (section 10MS), Bunkers Graben, southern-central Flinders Ranges. Stansbury Basin (*D. odyssei* Zone): WPC clasts, Kangaroo Island.

Class Paterinata Williams, Carlson, Brunton, Holmer, and Popov, 1996

Order Paterinida Rowell, 1965

Superfamily Paterinoidea Schuchert, 1893

Family ?Paterinidae Schuchert, 1893

Genus *Cordatia* Brock and Claybourn nov.

ZooBank LSID: urn:lsid:zoobank.org:act:A3E82895-1D1D-4B3B-8B5C-F2D8A01C0841

Etymology: From Latin, *cordatus*, meaning heart-shaped; in reference to the large, heart-shaped muscle field in both valves.

Type species: *Cordatia erinae* Brock and Claybourn gen. et sp. nov., monotypic, see below.

Diagnosis.—The same as for the type species.

Remarks.—The weakly developed obtuse (Fig. 11A_1, D) to linear (Fig. 11B, C_2) cardinal platform (lateral extremities broken away in some specimens, Fig. 11J–M), orthocline ventral delthyrium and interarea, presence of a pair of very large muscle scars in both valves, and a smooth adult shell with drapes, wrinkling and concentric filae, suggest an affinity with the Order Paterinida. In addition, the stratiform organophosphatic ultrastructure in *Cordatia* Brock and Claybourn gen. nov. is closely comparable with the

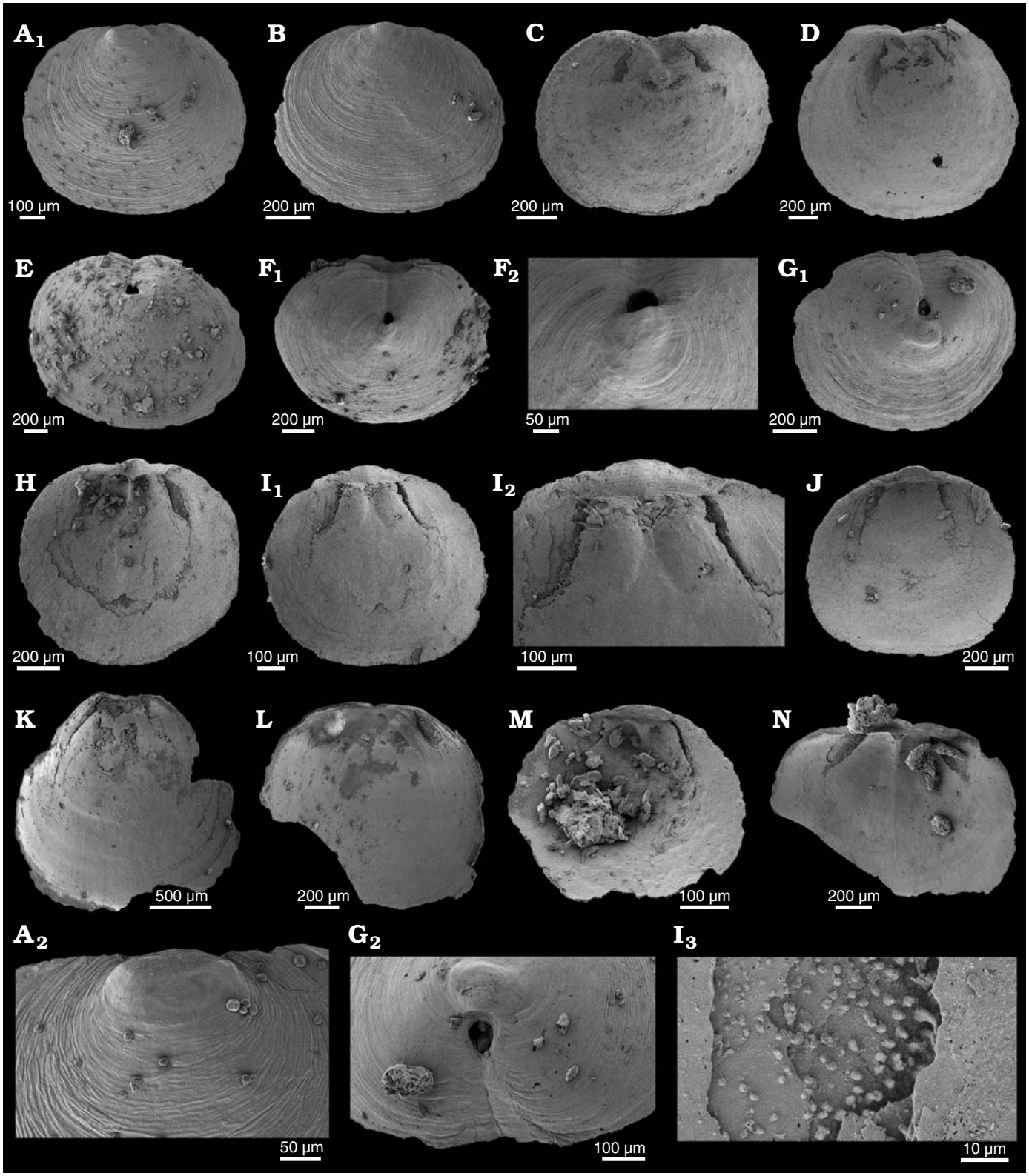

Fig. 10. The lingulid brachiopod *Eohadrotreta* sp. cf. *E. zhenbaensis* Li and Holmer, 2004 from the lower Cambrian White Point Conglomerate, Kangaroo Island, South Australia. Dorsal (A, B, H–J, M, N) and ventral (C–G, K, L) valves. **A**. SAM P57276 in external view (A_1); A_2, detail of the larval shell. **B**. SAM P57277 in external view. **C**. SAM P57278 in internal view. **D**. SAM P57279 in internal view. **E**. SAM P57280 in external view. **F**. SAM P57281 in external view, tilted to show intertrough (F_1); F_2, detail of the foramen. **G**. SAM P57282 in external view, tilted to show intertrough (G_1); detail of the foramen (G_2) showing the intertrough. **H**. SAM P57283 in internal view. **I**. SAM P57284 in internal view; I_2, close up of interarea; I_3, detail of shell microstructre. **J**. SAM P57285 in internal view. **K**. SAM P57286 in internal view. **L**. SAM P57287 in internal view. **M**. SAM P57288 in internal view. **N**. SAM P57289 in internal view.

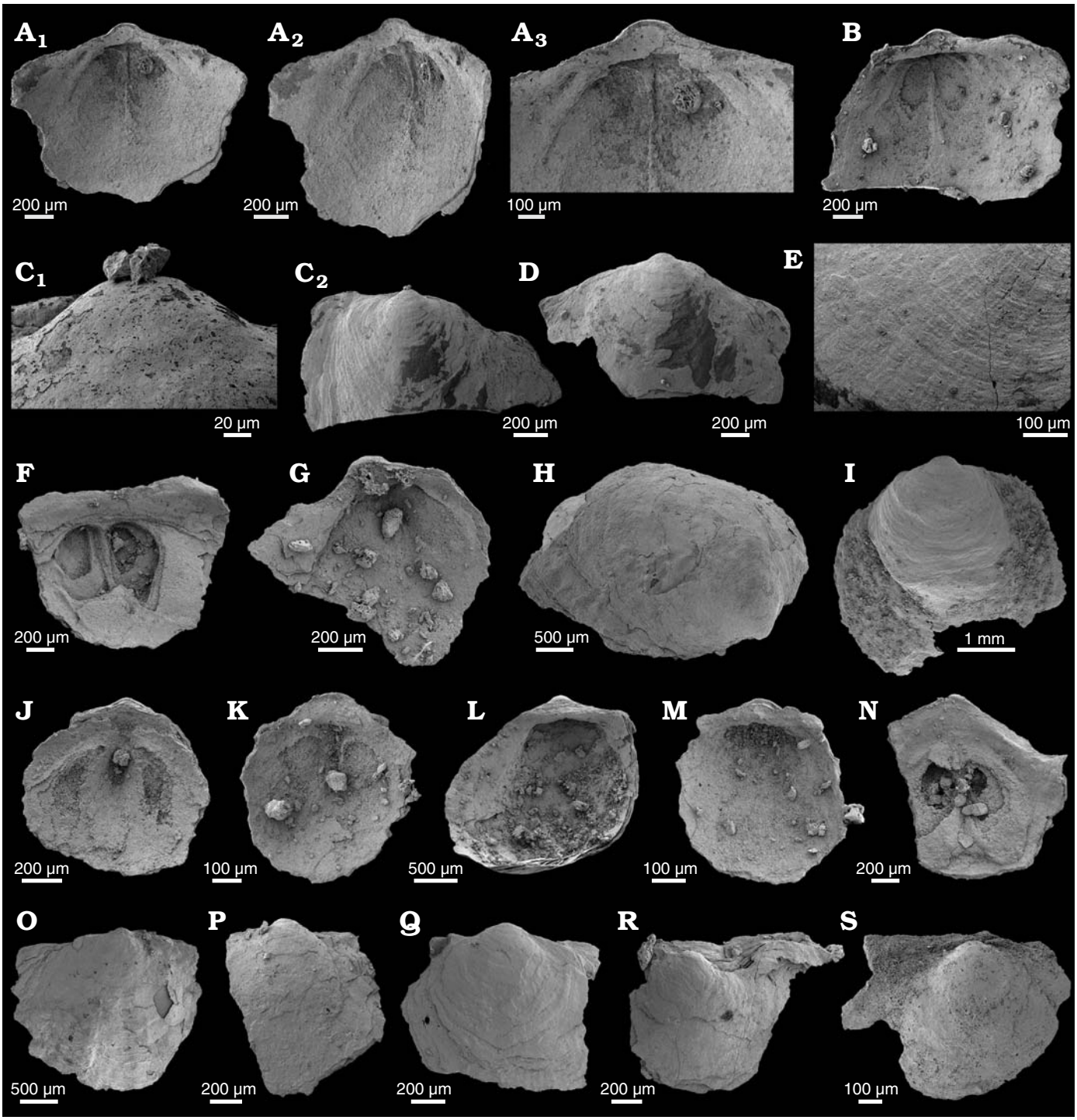

Fig. 11. The lingulid brachiopod *Cordatia erinae* Brock and Claybourn gen. et sp. nov. from the lower Cambrian of South Australia, Ajax Limestone, Flinders Ranges (AJX-M/415) (A–E) and White Point Conglomerate, Kangaroo Island (F–S). Ventral (A, D, G) and dorsal (B, C, E, F, H–S) valves. **A**. SAM P53644, holotype in internal (A_1) and oblique (A_2) views; A_3, detail of the delthyrium, propareas, and muscle field. **B**. SAM P57290 in internal view. **C**. SAM P57291 in external view (C_1); C_1, detail of the metamorphic shell. **D**. SAM P57292 in external view. **E**. SAM P57293, detail of external ornament. **F**. SAM P57294 in oblique internal view. **G**. SAM P57295 in internal view. **H**. SAM P57296 in external oblique view. **I**. SAM P57297 in external view. **J**. SAM P57298 in internal view. **K**. SAM P57299 in internal view. **L**. SAM P57300 in internal view. **M**. SAM P57301 in internal view. **N**. SAM P57302 in internal view. **O**. SAM P57303 in external view. **P**. SAM P57304 in external view. **Q**. SAM P57305 in external view. **R**. SAM P57306 in external view. **S**. SAM P57307 in external view.

shell ultrastructure in cryptotretids, such as *Cryptotreta undosa* from the lower Cambrian of Sweden (e.g., Williams et al. 1998: pl. 5: 2). Better preserved shells of *Cordatia* Brock and Claybourn gen. nov., especially from the Ajax Limestone (Fig. 11A–E), are similar to *Paterina* Beecher, 1891 in general shape and outline, and both taxa lack a

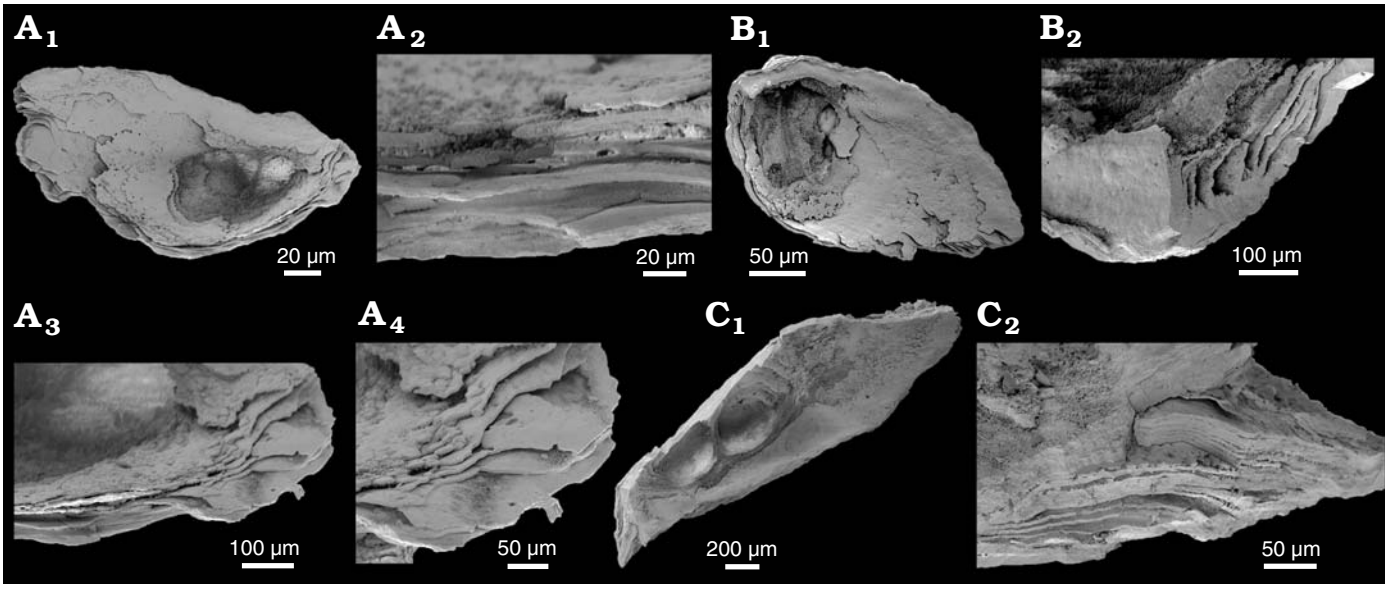

Fig. 12. Shell microstructures of *Cordatia erinae* Brock and Claybourn gen. et sp. nov. from the lower Cambrian White Point Conglomerate, Kangaroo Island, South Australia. **A**. SAM P57308, ventral valve in oblique internal view (A_1); A_2–A_4, details of laminar shell microstructure. **B**. SAM P57309, dorsal valve in oblique internal view (B_1); B_2, detail of laminar shell microstructure. **C**. SAM P57310, shell fragment in oblique internal view (C_1); C_2, detail of laminar shell microstructure.

homeodeltidium and homeochilidium. Both taxa also have a smooth adult shell, ornamented by undulose concentric laminae/filae interrupted by nick points forming sets of drapes. However, the concentric filae/laminae of *Cordatia* Brock and Claybourn gen. nov. are relatively widespread and irregular in growth, whilst those in *Paterina* tend to be much more closely packed, often forming distinct wrinkles (compare Fig. 11E with Laurie 2000: 183, fig. 1a–d; Holmer et al. 2001: pl. 1: 8, 10–12). Internally, the ventral valve of *Paterina* has a well-developed delthyrium supported internally (and laterally) by a pair of strong delthyrial ridges (see Williams et al. 1998: pl. 11: 4, 5; Holmer et al. 2001: pl. 11: 9). *Cordatia* Brock and Claybourn gen. nov., on the other hand, lacks a distinct delthyrium (and the strong delthyrial ridges seen in *Paterina*), instead having a variably developed, generally very shallow and orthocline cardinal platform in front of the beak. The interior of the dorsal valves of *Paterina* are generally poorly known, but none have the large, centrally-located cordate muscle field that characterises *Cordatia* Brock and Claybourn gen. nov.

The lack of a homeodeltidium and/or homeochilidium in *Cordatia* Brock and Claybourn gen. nov. distinguishes it from paterinate genera such as *Pelmanotreta* Skovsted, Ushatinskaya, Holmer, Popov, and Kouchinsky, 2015b (replacement name for the pre-occupied *Cryptotreta* Pelman, 1977), *Tumulduria* Missarzhevsky in Rozanov et al., 1969, *Salanygolina* Ushatinskaya, 1987, *Dzunarzina* Ushatinskaya, 1993, and *Tallatella* Topper and Skovsted, 2014. The characteristic external undulose and irregular concentric ornament interrupted by surface wrinkling and nick points forming repeated sets of drapes, along with an obtuse to linear cardinal platform with orthocline ventral interarea in *Cordatia* Brock and Claybourn gen. nov. is more in keeping with *Aldanotreta* Pelman, 1977 and *Askepasma* Laurie, 1986. However, *Aldanotreta* and *Askepasma* have much more clearly defined and strongly developed cardinalia. In addition, *Askepasma* has a distinctive reticulate shell surface ornament (Topper et al. 2013: fig. $2C_2$) that is also reflected in the ultrastructure of the shell (Topper et al. 2013: fig. 7D), which is absent in *Cordatia* Brock and Claybourn gen. nov.

Stratigraphic and geographic range.—As for the type species, see below.

Cordatia erinae Brock and Claybourn sp. nov.

Figs. 11, 12.

2007 Obolidae gen. et sp. indet.; Paterson et al. 2007b: 138–139, fig. 3F–J.

2017 *Curdus pararaensis*; Betts et al. 2017a: 257, fig. 15P–U.

ZooBank LSID: urn:lsid:zoobank.org:act:9E817F9D-1967-40BE-93F7-1424571E3CB9

Etymology: In honour of Erin Fletcher (née Casey), who discovered the first specimens of this taxon in the Andamooka Limestone in 2005 during her Honours year.

Holotype: Ventral valve SAM P53644 (Fig. 11A).

Type locality: Ajax Limestone, Mt. Scott Range, NW Flinders Ranges, South Australia.

Type horizon: Stratigraphic section AJX-M/415 in the Mt Scott Range, northern Flinders Ranges, located 232.07 m above the base of the section (Betts et al. 2016: fig. 2); early Cambrian, *Dailyatia odyssei* Zone (*Pararaia tatei* Trilobite Zone).

Material.—Thirty-two dorsal valves and two ventral valves from Clast 1, one dorsal valve and three ventral valves from Clast 4 and 28 dorsal valves and eight ventral valves from Clast 5; 22 figured including five specimens from the type locality AJX-M/415 in the Mt Scott Range (SAM P 53644, 57290–57310).

Diagnosis.—Small, uniformly convex ventral valve with transversely obtuse cardinal platform. Delthyrium incipient, little more than a weak, very shallow depression, set on a variably developed platform in front of a relatively small, flat orthocline beak. Ventral muscle field large, transverse with median ridge bounded postero-laterally by divergent low, but well-defined ridges. Interior of dorsal valve paratypes with distinctive rounded cardinal ridge forming the pseudointerea immediately in front of a small recurved beak. A low, narrow well-developed median ridge originates in umbonal chamber and widens and flattens anteriorly to approximately mid valve. A pair of large, elongately ovoid, weakly divergent, centrally located muscle scars straddle the median ridge forming a distinctly cordate muscle field.

Description.—Shell of variable size (length 0.53–3.82 mm, mean 1.6 mm; width 0.48–3.95 mm, mean 1.76 mm, N = 6), biconvex to ventribiconvex, outline ranging from transversely subrectangular to semi-circular in outline; fragmentary specimens often loose cardinal extremities and can appear subovoid in outline (Fig. 11J, K). Metamorphic shell relatively large, circular, seemingly smooth (though poorly preserved in most specimens) with diameter between 0.18–0.25 mm; metamorphic shell margin poorly delineated from adult shell (Fig. 11C_1). Adult shell smooth, with relatively widely spaced, undulose and irregular imbricating lamellae (Fig. 11E), better developed towards shell margin; concentric laminae/filae interrupted by nick points and drapes, occasional wrinkles in well preserved specimens (Fig. 11E). Reticulate micro-ornament absent. Shell structure composed of densely packed stratiform apatitic laminae (Fig. 12) occasionally with crustose or spherulitic interlaminae (Fig. 12B_2, C_2). Columnar features lacking.

Ventral valve with transversely obtuse cardinal platform (Fig. 11A_1, D, G); propareas very narrow, tapering and becoming indistinct laterally (Fig. 11A_1). Delthyrium is little more than a flattened or weakly concave platform (Fig. 11A) distinguished from propareas by presence of a slightly depressed platform located directly anterior of the weakly incurved beak (Fig. 11A). Homeodeltidium absent. Ventral valve interior with few morphological features. Ventral valve with large, indistinct visceral transverse muscle field bisected by very low, narrow short, incipient median ridge in umbo; postero-lateral margins of muscle field with well developed, narrow, gently curved bounding ridges (Fig. 11A_3).

Dorsal valve weakly, but evenly convex, with straight posterior margin. Propareas anacline, narrow, forming a relatively flat continuous platform extending laterally across entire cardinal area (Fig. 11B); beak short, recurved. Homeochilidium absent. Interior of dorsal valve with well-developed, low narrow median ridge originating in umbo, extending, widening and flattening beyond anterior margin of muscle field. A pair of large, elongately ovoid, weakly divergent, centrally located muscle scars occur either side of the median ridge (Fig. 11B, F); muscle scars distinctly cordate in outline. Postero-lateral muscle bounding ridges of the central muscle scars poorly defined (Fig. 11B, F, L). Postero-lateral muscles present but weakly impressed and indistinct. Mantle canal system not preserved.

Remarks.—Paterson et al. (2007b: fig. 3F–K) originally had difficulty in providing a higher-level classification of this taxon, because the relatively few specimens from the KLM of the Parara Limestone tended to be small and the size and shape of the shells were affected by breakage of cardinal extremities, making the outline appear subcircular. The perceived subrounded outline, along with a smooth metamorphic and adult shell, suggested a relationship with the Obolidae. Fragmentary specimens of *Cordatia erinae* Brock and Claybourn gen. et sp. nov. were also incorrectly identified as *Curdus pararaensis* by Betts et al. (2017b: fig. 15P–U). Abundant new material from the WPC, along with well-preserved shells from the Ajax Limestone in the Mt Scott Range, preserves the full morphological details of the species, including the characteristic obtuse to linear cardinal platform (Fig. 11l), densely stratiform organophosphatic ultrastructure (Fig. 12), weakly defined, orthocline delthyrium in the ventral valve, median ridge in the dorsal valve, and external, undulose, irregular, concentric laminae with nick points, drapes and wrinkling, and the large muscle field in both valves. These well-preserved features enable formal description of *C. erinae* gen. et sp. nov. as a new taxon within Paterinata (Laurie 2000).

Stratigraphic and geographic range.—Lower Cambrian of South Australia: Stuart Shelf: SCYW-791A drill core, Andamooka Limestone (*D. odyssei* Zone); Arrowie Basin: AJX-M section, Ajax Limestone, Mt. Scott Range (*D. odyssei* Zone/*P. tatei* Trilobite Zone); MMF section, Third Plain Creek Member, Mernmerna Formation, Bunkers Range (*D. odyssei* Zone/*Pararaia bunyerooensis* Trilobite Zone); 10MS section, Linns Springs and Third Plain Creek members of the Mernmerna Formation, Bunkers Graben (*D. odyssei* Zone). Stansbury Basin: WPC clasts, Kangaroo Island (*D. odyssei* Zone).

Phylum incertae sedis

Family Stoibostrombidae Conway Morris and Bengtson in Bengtson et al., 1990

Genus *Stoibostrombus* Conway Morris and Bengtson in Bengtson et al., 1990

Type species: *Stoibostrombus crenulatus* Conway Morris and Bengtson in Bengtson et al., 1990; lower Cambrian of South Australia (Horse Gully section, Yorke Peninsula).

Stoibostrombus crenulatus Conway Morris and Bengtson in Bengtson et al., 1990

Fig. 13A–F.

1990 *Stoibostrombus crenulatus*; Conway Morris and Bengtson in Bengtson et al. 1990: 145, figs. 93–97.

1990 *Stoibostrombus* cf. *crenulatus*; Conway Morris and Bengtson in Bengtson et al. 1990: 147, fig. 98.

1993 *Stoibostrombus crenulatus*; Brock and Cooper 1993: 768, 770, figs. 8.4–8.6.

2001 *Stoibostrombus crenulatus*; Ushatinskaya and Holmer in Gravestock et al. 2001: 90, pl. 12: 1a–c, 2.
2001 *Stoibostrombus mirus*; Demidenko in Gravestock et al. 2001: 91, pl. 12: 3.
2007b *Stoibostrombus crenulatus*; Skovsted and Brock in Paterson et al. 2007b: 141, fig. 5J–L.
2009 *Stoibostrombus crenulatus*; Topper et al. 2009: 215, fig. 5I–O.
2011 *Stoibostrombus crenulatus*; Skovsted et al. 2011: 653–658, figs. 2, 3.
2016 *Stoibostrombus crenulatus*; Betts et al. 2016: fig. 21H–J, L.

Material.—One specimen from Clast 1 and 14 specimens from Clast 5; 6 figured (SAM P57311–57316). From the *Dailyatia odyssei* Zone, WPC, Kangaroo Island, South Australia.

Description.—See Topper et al. (2009: 215).

Remarks.—*Stoibostrombus crenulatus* is represented by curved, conical sclerites known only from the lower Cambrian of South Australia (Arrowie and Stansbury basins), and are commonly found as disarticulated components in shelly fossil residues. They have a distinctive external ornament that is often abraded, especially toward the apex. Skovsted et al. (2011) demonstrated that the external ornament is variable and can range from nodose plates to pustules, synonymising *Stoibostrombus mirus* (Demidenko in Gravestock et al., 2001), *S.* cf. *crenulatus* (Conway Morris and Bengtson in Bengtson et al., 1990) and *S. crenulatus*. The WPC specimens appear highly abraded and are often smooth or with very weak external texture (Fig. 13A, B, C_1, E, F). Ornament is often best developed around the base or abapical edge (Fig. 13D).

Original composition is likely to have been phosphatic, and *S. crenulatus* does not show evidence of growth by marginal accretion (Skovsted et al. 2011). The abapical edge of sclerites is irregular, and composite (fused) specimens are rare (Skovsted et al. 2011). Despite recovery of articulated sclerites, the gross scleritome morphology remains elusive, and phylogenetic affinity continues to be problematic. Skovsted et al. (2011) suggest that the sclerites of *S. crenulatus* may have been the dermal armour of an ecdysozoan, possibly a palaeoscolecid worm (Skovsted et al. 2011: 656).

Stoibostrombus crenulatus is a key taxon in the new shelly fossil biostratigraphic scheme of Betts et al. (2016, 2017b), as its stratigraphic range is used to define the *D. odyssei* Zone (Cambrian Series 2, Stage 3) in the absence of the eponym (Betts et al. 2016, 2017b). However, occurrence in Toyonian-equivalent strata (late Stage 4) in the Stansbury Basin (Brock and Cooper 1993) suggest that *S. crenulatus* may have a relatively long stratigraphic range.

Stratigraphic and geographic range.—Lower Cambrian of South Australia: Arrowie Basin (*D. odyssei* Zone): Andamooka Limestone, Stuart Shelf; Ajax Limestone, Mt. Scott Range, northern Flinders Ranges; Mernmerna Formation, Arrowie Syncline, northeastern Flinders Ranges, Bunkers Range, central Flinders Ranges; Second Plain Creek Member of the Wilkawillina Limestone, Bunkers Graben, southern-central Flinders Ranges; Six Mile Bore, Linns Springs and Third Plain Creek members of the Mernmerna Formation, central Flinders Ranges. Stansbury Basin (*D. odyssei* Zone): Parara Limestone and KLM, in addition to the Ramsay, Stansbury and Coobowie limestones, Yorke Peninsula; WPC clasts, Kangaroo Island.

Order Tommotiida Missarzhevsky, 1970

Family Lapworthellidae Missarzhevsky in Rozanov and Missarzhevsky, 1966 (emend. Landing 1984)

Genus *Lapworthella* Cobbold, 1921

Type species: *Lapworthella nigra* Cobbold, 1921; lower Cambrian Comley Limestones, Shropshire, UK.

Lapworthella fasciculata Conway Morris and Bengtson in Bengtson et al., 1990

Fig. 13G–N.

1990 *Lapworthella fasciculata*; Conway Morris and Bengtson in Bengtson et al. 1990: 122, figs. 74–76.
1990 *Lapworthella* cf. *fasciculata*; Conway Morris and Bengtson in Bengtson et al. 1990: 124, figs. 77, 78.
2001 *Lapworthella fasciculata*; Demidenko in Gravestock et al. 2001: 116, pl. 8: 1–3.
2004 *Lapworthella fasciculata*; Demidenko 2004: pl. 1: 1–9, pl. 2: 1–7.
2009 *Lapworthella fasciculata*; Topper et al. 2009: 214, fig. 5A–H.
2016 *Lapworthella fasciculata*; Betts et al. 2016: fig. 21A–G, K.

Material.—One specimen from Clast 1, and 17 from Clast 5; eight figured (SAM P57317–57324). From the *Dailyatia odyssei* Zone, WPC, Kangaroo Island, South Australia.

Description.—See Topper et al. (2009: 214).

Remarks.—*Lapworthella fasciculata* is a common component in early Cambrian shelly fossil assemblages from South Australia. It can be extremely abundant in some horizons, e.g., probable lag deposit accumulations in the Second Plain Creek Member of the Wilkawillina Limestone, Bunkers Graben, Flinders Ranges (Smith 2006; Betts et al. 2016: app. 8). *Lapworthella fasciculata* in the WPC is represented by isolated sclerites that are either curved, conical shells with a sub-quadrate cross-section (Fig. 13H, I, M, N), spine-like forms (Fig. 13J, K) or are broad and flattened (Fig. 13L). Growth sets are separated by slightly raised ridges (Fig. 13H, J, M), usually ornamented by small (5–10 μm across) pustules (Fig. 13G). *Lapworthella fasciculata* is often septate (though septae are not visible in the WPC material).

Lapworthella sclerites occur as either sinistrally and dextrally twisted forms, and conjoined elements are rare (Demidenko 2004: pl. 1: 1–9; Gravestock et al. 2001: pl. 8: 3). Fused sclerites demonstrate that the skeletal elements were closely spaced on the body, merging during growth to form an external skeleton (Demidenko 2004). The broad, flattened sclerite from the WPC appears to have had multiple apices (Fig. 13L), though none of the sclerites from the WPC exhibit the elaborate spinose morphology of the conjoined sclerites described by Demidenko (2004).

Lapworthella fasciculata from the WPC are similar to *L. fasciculata* described and figured by Topper et al. (2009: fig. 5A–H) from the Mernmerna Formation in the Flinders

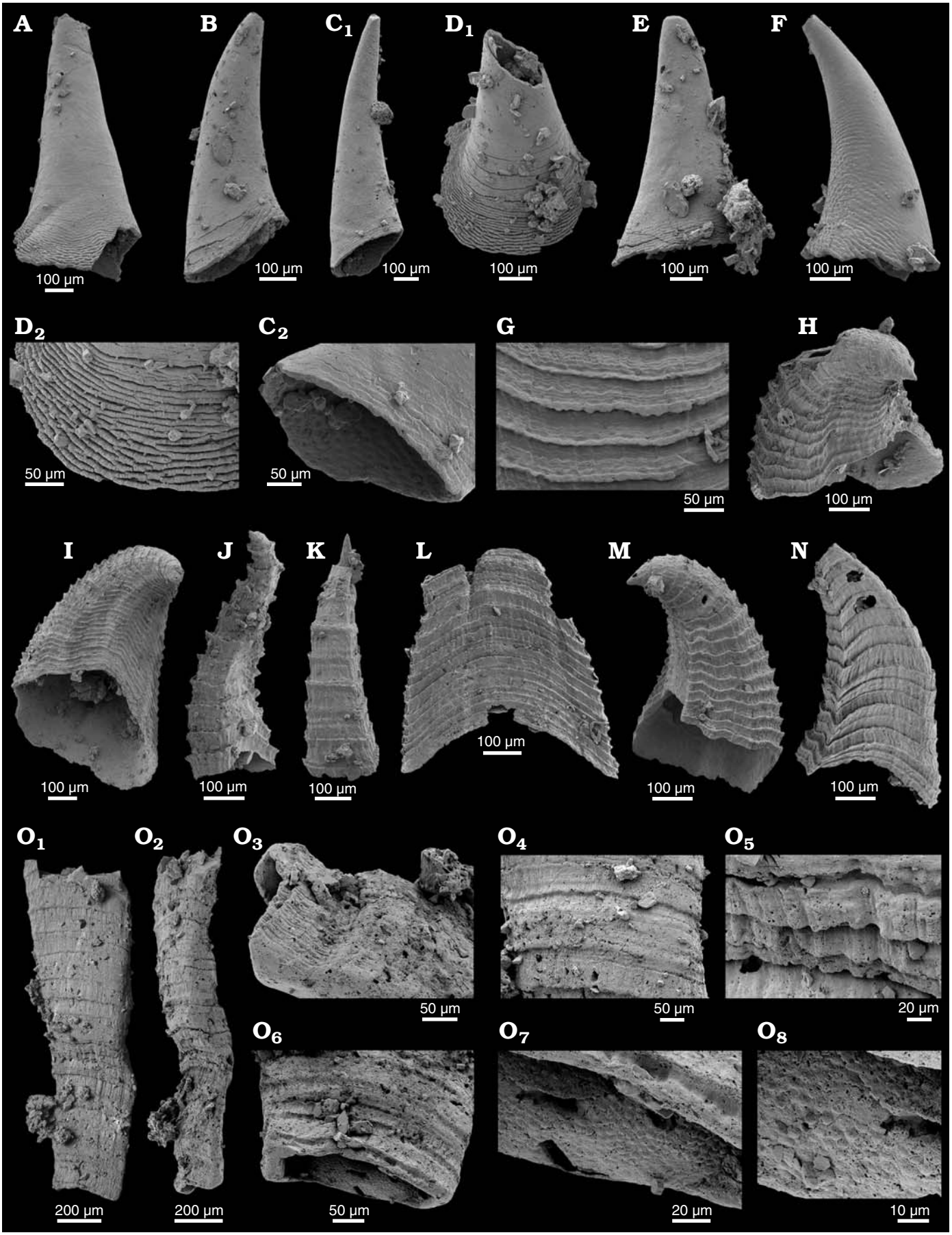
A
B
C1
D1
E
F
100 µm
100 µm
100 µm
100 µm
100 µm
100 µm
D2
C2
G
H
50 µm
50 µm
50 µm
100 µm
I
J
K
L
M
N
100 µm
100 µm
100 µm
100 µm
100 µm
100 µm
O1
O2
O3
O4
O5
200 µm
200 µm
50 µm
50 µm
20 µm
O6
O7
O8
50 µm
20 µm
10 µm

Ranges (*D. odyssei* Zone). Both bear the pustulose ridges and distinctive fasciculate microornament between co-marginal ribs, and both assemblages include spine-like forms and curved, pyramidal forms with quadrate apertures. Betts et al. (2017: fig. 21A–G, K) also figured *L. fasciculata* from the Wilkawillina Limestone and Mernmerna Formation in the Flinders Ranges that exhibit the same sub-quadrate pyramidial morphology and microornament as in the WPC specimens.

Species of *Lapworthella* were globally distributed during the early Cambrian, and have been recovered from east and west Avalonia, Baltica, Laurentia, Siberia, South China and West Gondwana (Missarzhevsky in Rozanov and Missarzhevsky 1966; Qian and Bengtson 1989; Bengtson 1980; Devaere et al. 2014a; Devaere and Skovsted 2017). *Lapworthella fasciculata* is only known from the lower Cambrian of South Australia, where it ranges from the *Micrina etheridgei* Zone to the *Dailyatia odyssei* Zone (Terreneuvian, Stage 2–Series 2, Stage 3) in the new shelly fossil biostratigraphic scheme of Betts et al. (2016, 2017b). Material assigned to *L. fasciculata* by Wrona (1989) from Antarctic glacial erratics may be a species of *Kelanella*. Both have septate sclerites with similar concentric and radial ornament (Devaere et al. 2014a; Betts et al. 2017b). The scleritome of *Kelanella* is still poorly resolved (see below), though sclerites assigned to *Kelanella* are often large (fragments up to ~5 mm in width; Betts et al. 2017b: fig. 14N–U). *Lapworthella fasciculata* sclerites are usually up to ~1 mm long (Fig. 13I–N).

A single, ~1 mm long, elongate, flattened tube-like sclerite from the WPC clasts is assigned to *Kelanella* sp. (Fig. 13O). This sclerite and *L. fasciculata* both have similar external ornament of concentric co-marginal growth sets. Growth sets consist of fine, raised ribs bordering thicker zones with longitudinal, fasciculate striae (Fig. 13G, N, O_4). The taxa can be distinguished by the presence of pustulose ridges separating growth sets in *L. fasciculata* and the presence of fine pustules on the internal surface of *Kelanella* sp. (Fig. 13O_7, O_8), which is not present in *L. fasciculata*.

A tommotiid-like "mitrosagophoran sclerite" was reported from Cambrian erratics from King George Island, West Antarctica (Wrona 1989: pl. 10: 3; Wrona and Zhuravlev 1996), which was referred to *Lapworthella fasciculata* by Topper et al. (2009). Later, Wrona (2004) reported *Lapworthella fasciculata* from the same glacial erratics. These specimens however, while septate, are more likely to be *Kelanella* based on external ornamentation, relatively large size and their overall compressed shape.

Stratigraphic and geographic range.—Lower Cambrian of South Australia: Arrowie Basin (*Micrina etheridgei–Dailyatia odyssei* zones): Andamooka Limestone, Stuart Shelf; Ajax Limestone, Mt Scott Range, northern Flinders Ranges; Winnitinny Creek Member of the Wilkawillina Limestone, Mernmerna Formation and Nepabunna Siltstone, Arrowie Syncline, northeastern Flinders Ranges; Winnitinny Creek Member of the Wilkawillina Limestone, Linns Springs and Third Plain Creek members of the Mernmerna Formation, Bunkers Range, central Flinders Ranges; Winnitinny Creek and Second Plain Creek members of the Wilkawillina Limestone, Six Mile Bore, Linns Springs and Third Plain Creek members of the Mernmerna Formation, Bunkers Graben, southern-central Flinders Ranges; Wirrapowie Limestone, Elder Range, southern Flinders Ranges and Arrowie Syncline northeastern Flinders Ranges; Mernmerna Formation, Mt. Chambers area, eastern Flinders Ranges. Stansbury Basin (*M. etheridgei–D. odyssei* zones): Kulpara Formation and Parara Limestone, Yorke Peninsula; Sellick Hill Formation, Fleurieu Peninsula; WPC clasts, Kangaroo Island.

Family incertae sedis

Genus *Kelanella* Missarzhevsky in Rozanov and Missarzhevsky, 1966

Type species: *Kelanella altaica* Missarzhevsky in Rozanov and Missarzhevsky, 1966; lower Cambrian of the Altai Mountains (Kameshkovsky horizon), Siberian Platform, Russia.

Kelanella sp.

Fig. 13O.

2017 *Kelanella* sp.; Betts et al. 2017b: fig. 14N–U.

Material.—One specimen (SAM P57235) from Clast 5. From the *Dailyatia odyssei* Zone, WPC, Kangaroo Island, South Australia.

Description.—Single, flattened, spine-like sclerite bearing concentric, fasciculate, growth-related ornamentation (Fig. 13O). Both ends of specimen with open apertures. Smaller aperture is smooth (likely intact) and larger aperture has jagged edges (Fig. 13O_1–O_3, O_6). Cross section oval with width gently increasing (from about 300–400 μm) towards wider aperture, although in the central zone, the width decreases slightly (Fig. 13O_1). In lateral view, the sclerite profile is gently undulating with a marked change in growth direction coinciding with central zone of decreasing width (Fig. 13O_2). Width of concentric growth increments variable (from about 25–100 μm), with more narrow growth increments in the central zone (Fig. 13O_4) and close to the smaller aperture (Fig. 13O_6). Internally, sclerite bears ornamentation of fine pustules (Fig. 13O_7, O_8).

← Fig. 13. Problematic, multi-element taxa *Stoibostrombus crenulatus* Conway Morris and Bengtson in Bengtson et al., 1990 (**A**–**F**), *Lapworthella fasciculata* Conway Morris and Bengtson in Bengtson et al., 1990 (**G**–**N**) and *Kelanella* sp. (**O**) from the lower Cambrian White Point Conglomerate, Kangaroo Island, South Australia. **A**. SAM P57311 in lateral view. **B**. SAM P57312 in lateral view. **C**. SAM P57313 in lateral view (C_1); C_2, detail of the aperture showing texture on the internal surface. **D**. SAM P57314 in oblique lateral view (D_1); D_2, detail of the characteristic wrinkled external microtexture. **E**. SAM P57315 in lateral view. **F**. SAM P57316 in lateral view. **G**. SAM P57317, external ornament. **H**. SAM P57318. **I**. SAM P57319. **J**. SAM P57320. **K**. SAM P57321. **L**. SAM P57322. **M**. SAM P57323. **N**. SAM P57324. **O**. SAM P57325, O_3–O_8, details of the aperture and internal and external ornament.

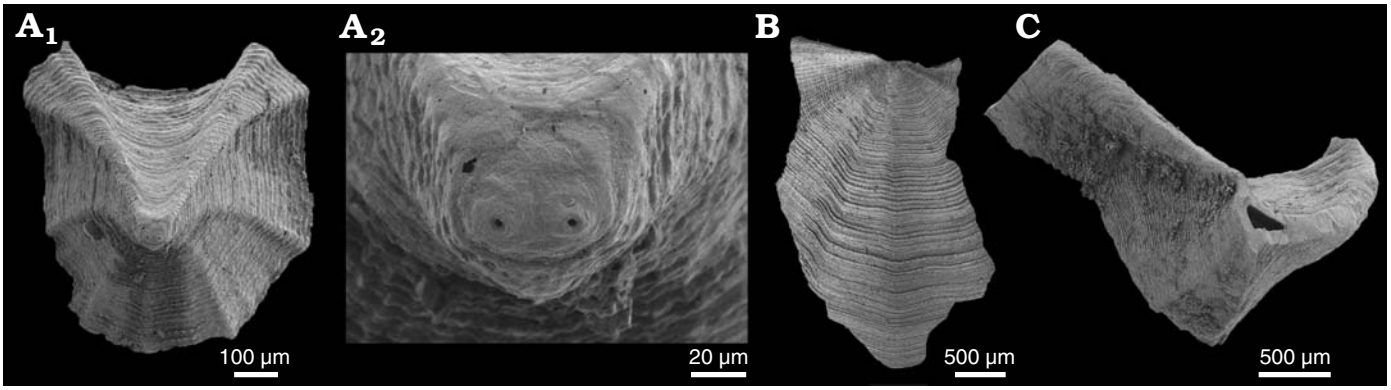

Fig. 14. The camenellan tommotiid *Dailyatia odyssei* Evans and Rowell, 1990 from the lower Cambrian White Point Conglomerate, Kangaroo Island, South Australia. **A**. SAM P57326, A2 sclerite in apical view (A_1); A_2, detail of the double perforations in the apex. **B**. SAM P57327, A2 sclerite in apical view, tilted to show deltoid. **C**. SAM P57328, C2 sclerite in dorsal view.

Remarks.—*Kelanella* is a tommotiid genus with a more or less global distribution from Cambrian Stage 3 to the Wuliuan (Devaere et al. 2014b). The sclerites of *Kelanella* are large by comparison to most other tommotiids and are characterized by multitude of internal septa and a characteristic "gridded" ornament of transverse and longitudinal ribs, often with fine longitudinal striations between ribs (Devaere et al. 2014b; Yang et al. 2015). A large number of morphologically variable sclerite morphs are known and these have often been described under different generic names (see review in Devaere et al. 2014b), but the sclerite is still poorly understood (Devaere et al. 2014b; Yang et al. 2015) and the taxonomic composition of this genus remains uncertain, pending review of larger sclerite assemblages.

In the collections from the WPC, *Kelanella* is represented by a single long, flattened, spine-shaped sclerite with the characteristic external ornament of fine longitudinal striations (Fig. $13O_1$–O_6). Apart from the broken aperture, the wall of the single sclerite is complete and internal septa could not be observed. However, similar spine-shaped and septate sclerites are often associated with the more characteristic broad sclerites of *Kelanella* in assemblages from Siberia (with specimens described under the generic name *Tesella* Missarzhevsky and Grigorieva, 1981, now considered a junior synonym of *Kelanella* by Devaere et al. 2014b) (Missarzhevsky and Grigorieva 1981: pl. 11: 15), France (Devaere et al. 2014b: fig. 9J–L), South China (Yang et al. 2015: fig. 12F–G), as well as in undescribed collections from Greenland and Siberia (CBS, personal observation 2018). This type of sclerite morphology is not known from other tommotiids.

Betts et al. (2017b) reported *Kelanella* sp. as a minor component of the fauna of the *D. odyssei* Zone of the Arrowie Basin. Although no spine-shaped sclerites were illustrated (Betts et al. 2017b: fig. 14N–U), such sclerites occur in the associated assemblages, closely matching the morphology of the specimens recovered from the WPC, suggesting these collections originate from a single, as yet undescribed species (MJB, CBS, personal observations 2018).

Family Kennardiidae Laurie, 1986

Genus *Dailyatia* Bischoff, 1976 (Skovsted et al. 2015a)

Type species: *Dailyatia ajax* Bischoff, 1976; lower Cambrian Ajax Limestone, Mt. Scott Range, northern Flinders Ranges, South Australia.

Dailyatia odyssei Evans and Rowell, 1990

Fig. 14.

1990 *Dailyatia odyssei*; Evans and Rowell 1990: 696, figs. 7.1–7.8.
2007 *Dailyatia* sp.; Skovsted and Brock in Paterson et al. 2007b: 141, fig. 4G–J.
2015 *Dailyatia odyssei*; Skovsted et al. 2015a: 58, figs. 44–50.
2017 *Dailyatia odyssei*; Betts et al. 2017b: 255, fig. 14A–I.

Material.—Two fragmentary A2 sclerites and a single fragmentary C2 sclerite (SAM P57326–57328) from Clast 5. From the *Dailyatia odyssei* Zone, WPC, Kangaroo Island, South Australia.

Description.—See Skovsted et al. (2015a: 58).

Remarks.—*Dailyatia odyssei* is the only species of the genus known from both South Australia and Antarctica. In South Australia, it has a stratigraphic range (spanning most of Series 2, Stage 3) that is mutually exclusive of most other species of *Dailyatia*, such as *D. ajax*, *D. macroptera*, *D. bacata*, and *D. helica*. Hence, *D. odyssei* is an important age-diagnostic taxon in the South Australian early Cambrian biostratigraphic scheme developed by Betts et al. (2016, 2017b), and is the eponym for the youngest biozone.

Only three *D. odyssei* sclerites have been recovered from the WPC clasts. External ornament clearly distinguishes them from the co-occurring *D. decobruta* Betts sp. nov. Ornament on both the A2 and C2 sclerites is typical of *D. odyssei*; both morphotypes exhibit low, closely set concentric ribs (Fig. $14A_1$, B, C), unlike the extravagant pustules seen in *D. decobruta* Betts sp. nov. None of the specimens display the strong pseudoplicae seen in *D. decobruta* Betts sp. nov.

The A2 sclerites from the WPC are fragmentary, but exhibit a wide, poorly defined deltoid, and a weak lateral trough between the posterolateral and the first lateral plicae, as seen in specimens of *D. odyssei* from the Flinders Ranges (Fig.

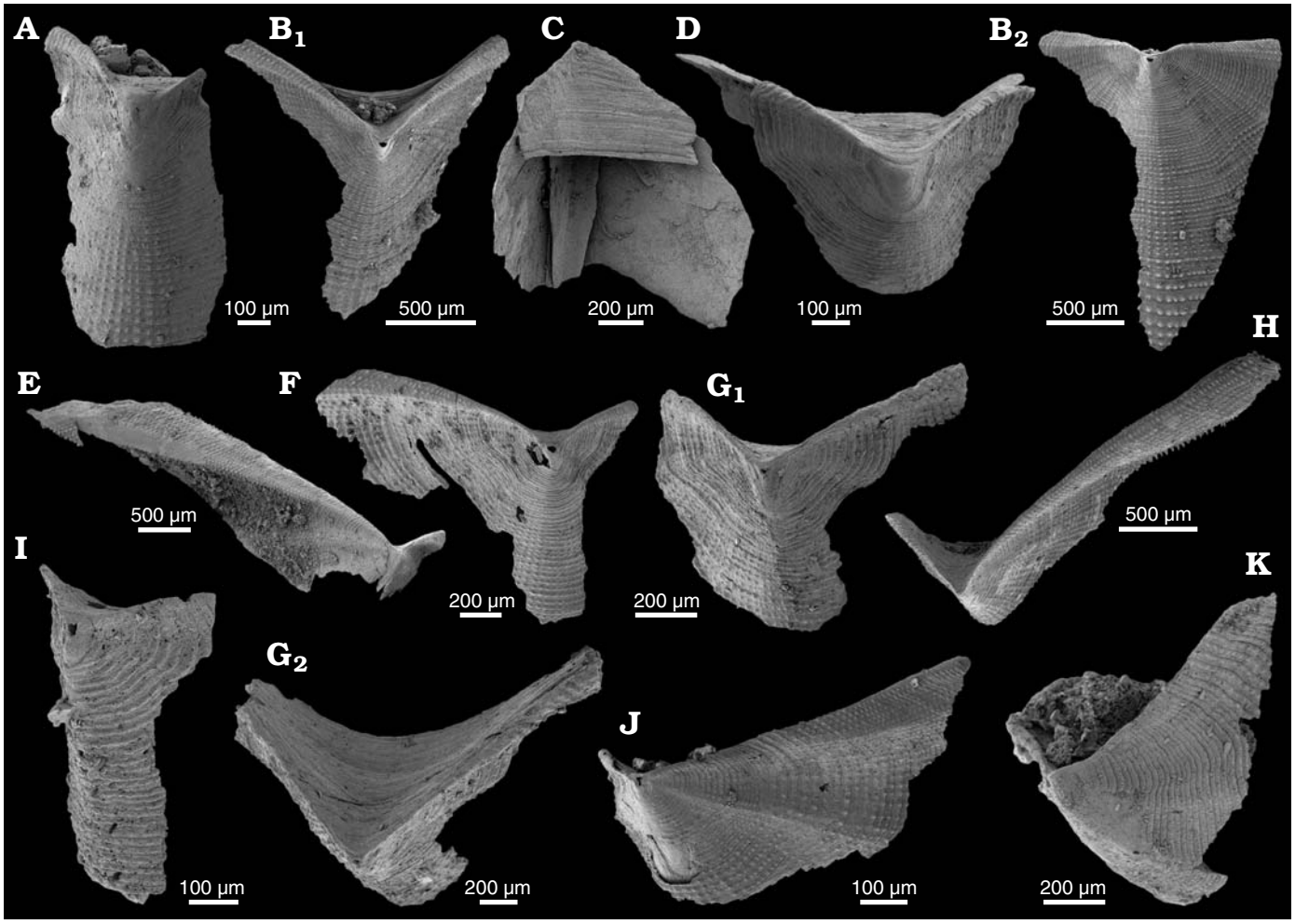

Fig. 15. The A1 sclerites of the camenellan tommotiid *Dailyatia decobruta* Betts sp. nov. from the lower Cambrian White Point Conglomerate, Kangaroo Island, South Australia. **A**. SAM P57329 in apical view. **B**. SAM P57330 in apical view (B_1); B_2 shows the broad, convex deltoid. **C**. SAM P57331 in anterior view. **D**. SAM P57332 in apical view. **E**. SAM P57333 in apical view. **F**. SAM P57334 in apical view. **G**. SAM P57335 in apical view (G_1); G_2 shows the concentric, wrinkled ornament on the anterior field. **H**. SAM P57336 in apical view. **I**. SAM P57337 in apical view. **J**. SAM P57338 in oblique lateral view. **K**. SAM P57339 in oblique lateral view.

$14A_1$, B; Skovsted et al. 2015a: fig. 46). The central plica of the C2 sclerite is well-developed, but not "wall-like", as in the Flinders Ranges specimens (Skovsted et al. 2015a: fig. 49), and the sclerite may only be weakly coiled (Fig. 14C).

Stratigraphic and geographic range.—Lower Cambrian of South Australia: Arrowie Basin (*D. odyssei* Zone); Andamooka Limestone, Stuart Shelf; Ajax Limestone, Mt Scott Range, northern Flinders Ranges; Mernmerna Formation and Nepabunna Siltstone, Arrowie Syncline, northeastern Flinders Ranges; Second Plain Creek Member of the Wilkawillina Limestone and Six Mile Bore, Linns Springs and Third Plain Creek of the Mernmerna Formation, Bunkers Graben, southern-central Flinders Ranges; Linns Springs and Third Plain Creek members of the Mernmerna Formation, central Flinders Ranges; Mernmerna Formation, Chambers Gorge area, eastern Flinders Ranges. Stansbury Basin (*D. odyssei* Zone); WPC clasts, Kangaroo Island. Antarctica: Shackleton Limestone, Churchill Range, Transantarctic Mountains.

Dailyatia decobruta Betts sp. nov.

Figs. 15–18.

2015 *Dailyatia* sp. A; Skovsted et al. 2015a: 64, fig. 51A–E.

ZooBank LSID: urn:lsid:zoobank.org:act:363F4F94-3687-4526-A0E1-347C028590D7

Etymology: From Latin *deco*, handsome or decorated, and *bruta*, beast; meaning "handsome beast".

Holotype: C2a sclerite from Clast 5 (SAM P57359; Figs. 17I and 18G).

Type locality: Cape D'Estaing, Kangaroo Island, South Australia (WGS84 coordinates: 35°34'53" S, 137°29'06" E).

Type horizon: Lower Cambrian bioclastic limestone clasts, WPC.

Material.—Six A1 sclerites from Clast 1 and seven A1 sclerites from Clast 5, 11 figured (SAM P57329–57339); 13 C1 sclerites from Clast 1 and 12 C1 sclerites from Clast 5, 13 figured (SAM P57340–57351, 57358); three C2 sclerites from Clast 1 and nine C2 sclerties from Clast 5, 6 figured (SAM P57352–57357); seven C2a sclerites from Clast 1 and three C2a sclerites from Clast 5, 9 figured (SAM P57359–57367).

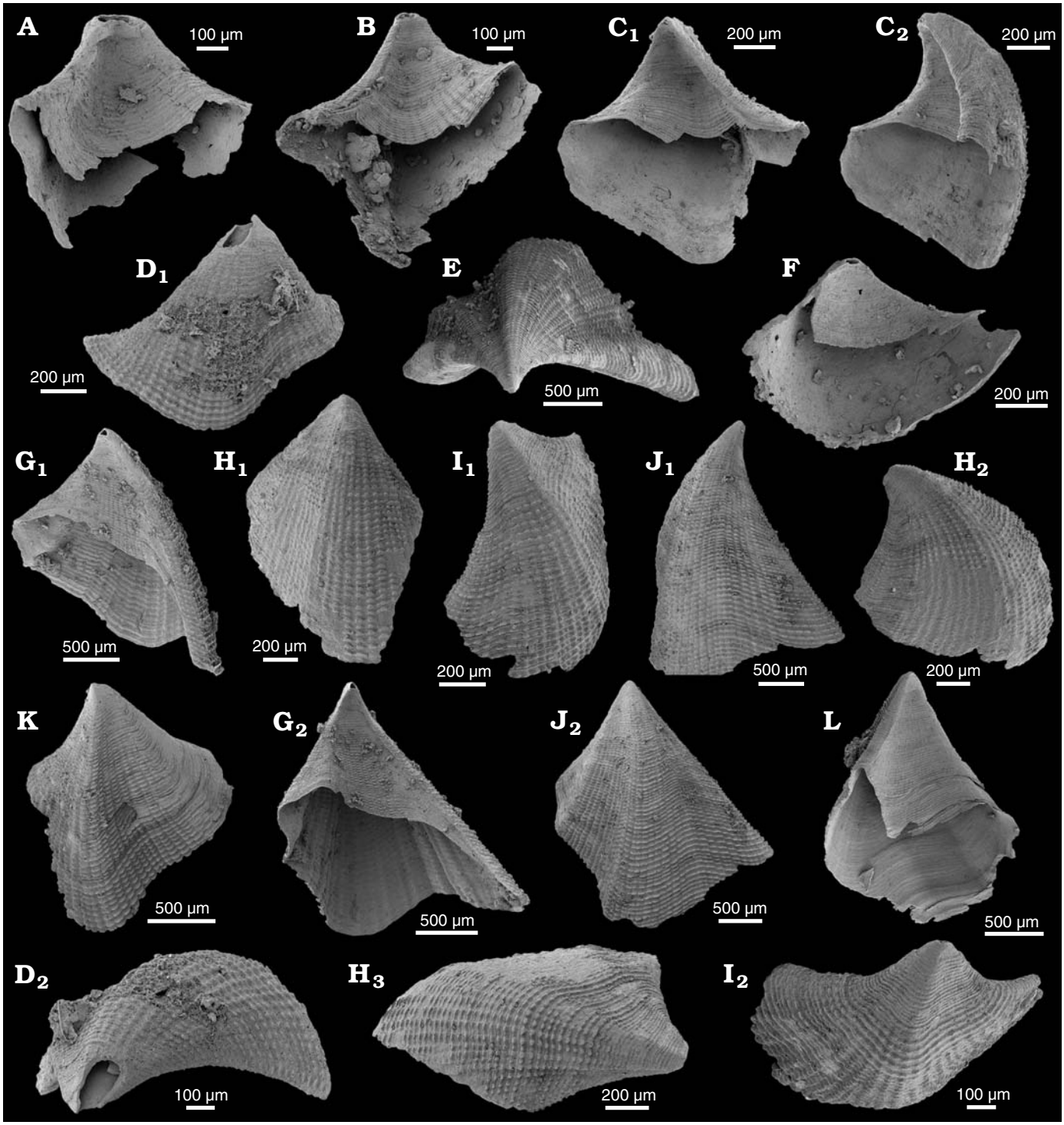

Fig. 16. C1 sclerites of the camenellan tommotiid *Dailyatia decobruta* Betts sp. nov. from the lower Cambrian White Point Conglomerate, Kangaroo Island, South Australia. **A**. SAM P57340 in ventral view. **B**. SAM P57341 in ventral view. **C**. SAM P57342 in ventral view shows shortened ventral field (C_1) and in oblique view (C_2). **D**. SAM P57343 in dorsal view (D_1); D_2, apical view oriented to show overall convexity of sclerite. **E**. SAM P57344 in apical view. **F**. SAM P57345 in apical view. **G**. SAM P57346 in oblique view showing shortened ventral field (G_1) and in ventral view (G_2). **H**. SAM P57347 in dorsal view; H_1–H_3, show convex dorsal field with very weak plication. **I**. SAM P57348 in oblique dorsal view (I_1); I_2 shows convexity. **J**. SAM P57349 in oblique dorsal view; J_1 shows curvature of sclerite in side view; J_2 shows dorsal surface. **K**. SAM P57350 in dorsal view. **L**. SAM P57351 in oblique ventral view.

Diagnosis.—Species of *Dailyatia* with strong ornament of raised pustules, often aligned to form strong pseudoplicae. A1 sclerite with strongly developed anterolateral plicae and strongly convex deltoid. Concave anterior field of A1 sclerite has closely spaced concentric wrinkles, rather than pustulose microornament. C1 and C2a sclerites are triangular, both generally with weak plication; both have strongly convex dorsal fields and strongly concave ventral fields re-

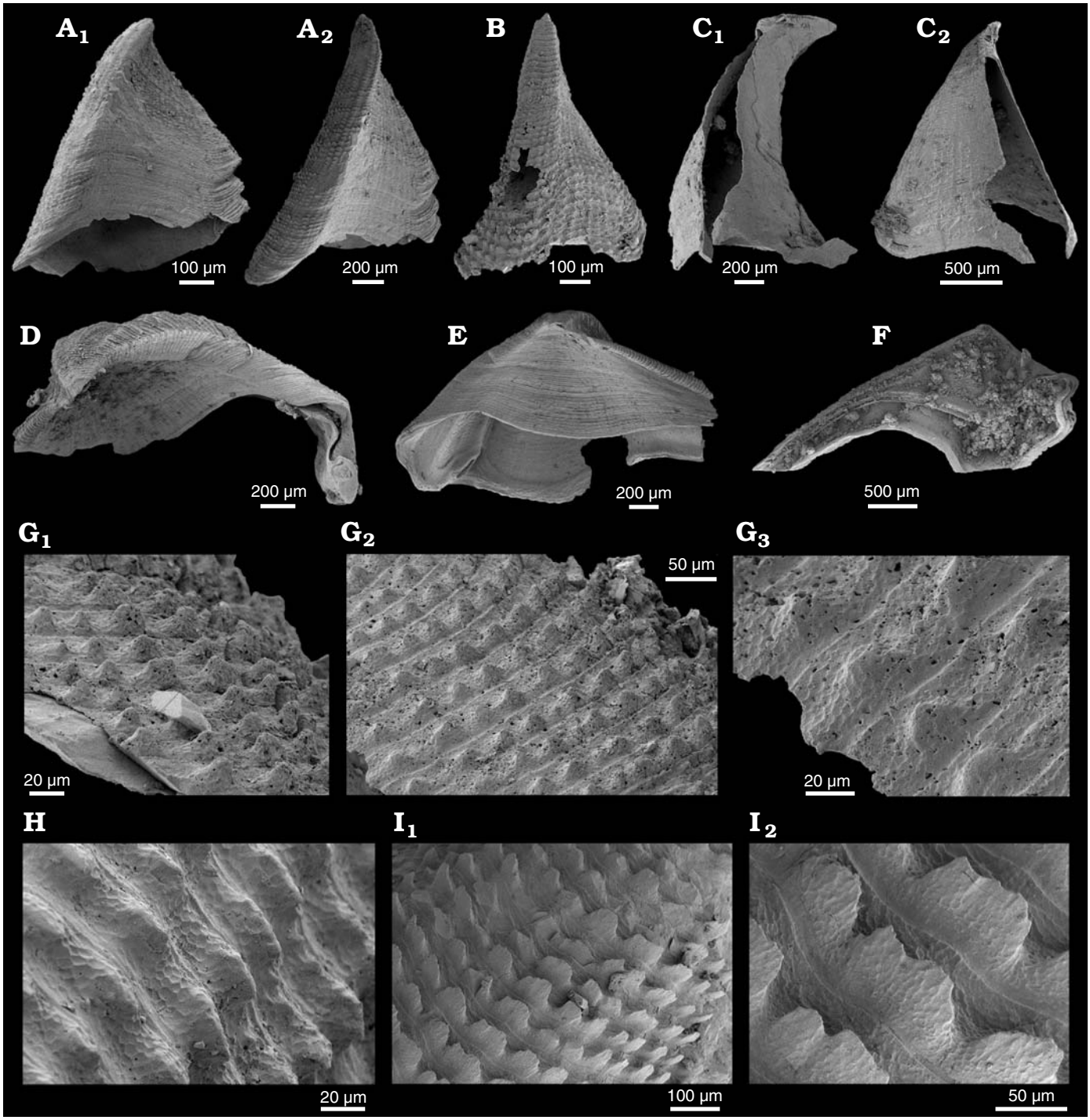

Fig. 17. C2 sclerites of the camenellan tommotiid *Dailyatia decobruta* Betts sp. nov. from the lower Cambrian White Point Conglomerate, Kangaroo Island, South Australia. **A**. SAM P57352 in lateral view; A_1, A_2 show slightly different angles to capture three dimensionality of sclerite. **B**. SAM P57353 in lateral view. **C**. SAM P57354 in dorsal view; C_1, C_2 show slightly different angles to capture three dimensionality of sclerite. **D**. SAM P57355 in ventral view. **E**. SAM P57356 in ventral view. **F**. SAM P57357 in ventral view. **G**. SAM P57358, G_1–G_3, close ups of external ornament. **H**. SAM P57348, close up of external ornament. **I**. SAM P57359, holotype; I_1, I_2, close ups of external ornament.

sulting in a reduced internal cavity. C1 sclerites have a ventral field that is shorter than the dorsal field. C2a sclerites are elongate and curved, with slight torsion. Apex may be recurved over the ventral field. C2 sclerites are triangular, but are not as compressed as C1 and C2a sclerites, and are slightly torted.

Description.—Sclerites are united by their distinctive ornament, which consists of prominent concentric ribs with regularly spaced, often high, rounded pustules. Pustules can be aligned across the ribs forming strong pseudoplicae (Fig. 17G–I). Ribs are separated by a narrow, smooth, slit-like zone between inter-rib grooves (Fig. 17G_2, G_3, H).

Delicate reticulate microornament is well-developed on ribs and pustules, and weakly on the inter-rib grooves. Ornament generally smooths toward apex. No A2 or B sclerites have been recovered.

A1 sclerites are bilaterally symmetrical, with a V-shaped apertural outline (Fig. 15). A1 sclerites have very strongly developed second anterolateral plicae that delimit a concave anterior field (Fig. 15B_1, C, D). The weak first anterolateral plicae and posterolateral plicae define narrow, elongate, triangular lateral troughs (Fig. 15J). Deltoid is strongly convex, and demarcated by weak postero-lateral creases. Field between posterolateral plication (delineating the lateral field at the posterior) and lateral crease (delineating the deltoid) slightly concave (for descriptive terminology for *Dailyatia* species see Skovsted et al. 2015a: fig. 5). Well-developed pustulose ornament and microreticulation occurs on ribs on the lateral and posterior fields, smoothing toward triangular apex. Pseudoplicae often formed by alignment of pustules. Pustules and microreticulation not developed on the anterior field, which exhibits fine, closely spaced, concentric wrinkles (Fig. 15C, G_2).

C1 sclerites are triangular in apical outline with a deeply concave ventral field and convex dorsal field, resulting in a narrow internal cavity (Fig. 16A–C). Ventral field is significantly shorter than the dorsal field resulting in a wide apertural outline (Fig. 16B, C, F, G_2, L). Weakly developed radial plication on the dorsal field demarcates convex distal and slightly concave proximal fields. Apex with a single perforation. Pustulose ornament well developed on dorsal field, and weakly developed on ventral field. Triangular C2 sclerites exhibit strong torsion, and are not as compressed as C1 sclerites, with a relatively large internal cavity (Fig. 17A–F). Apertural outline is triangular. Broad dorsal field is defined by two strong radial plicae. Ventral field is concave, and is slightly shorter than the dorsal field.

C2a sclerites are elongate (high length:width ratio), with a triangular outline. Sclerites are strongly curved and highly compressed with convex ventral fields and concave dorsal fields (Fig. 18). Sclerites are slightly torted, with the apex often twisting toward the concave ventral surface (Fig. 18C, E). Weakly developed central plication occurs on broad dorsal surface separating often slightly concave proximal field from convex distal field (Fig. 18D_1). Pseudoplication is well developed through the alignment of pustules on concentric ribs on the dorsal and ventral surfaces. Ornament on dorsal surface generally more strongly developed than on ventral surface, particularly concentric ribs (Fig. 18G, H). Ornament smooths toward apex. Apex with single perforation.

Remarks.—Only two sclerites of *D. decobruta* Betts sp. nov. have been previously described; an A1 sclerite from the Mernmerna Formation (*Pararaia janeae* Zone) in the Donkey Bore Syncline, and a C1 sclerite from the North Boundary Creek section through the Mernmerna Formation in the Mt. Chambers area, eastern Flinders Ranges (likely *P. janeae* Zone) (*Dailyatia* sp. A in Skovsted et al. 2015a: fig. 51A–E; Betts et al. 2017b: figs. 4, 10). New material from the WPC conforms to the description of *Dailyatia* sp. A by Skovsted et al. (2015a). The A1 sclerites of this taxon from both the Flinders Ranges and the WPC have very narrow lateral fields, very broad anterior and posterior fields, and a very broad deltoid. The C1 sclerite from the Chambers Gorge area has a concave ventral field that is much shorter than the concave dorsal field, similar to that in the C1 sclerites from the WPC.

Sclerites from the Arrowie Basin and the WPC are united by their distinctive external ornament (Fig. 17G–I). Sclerites generally have weakly developed radial plication and strong concentric ribs. Well developed, rounded pustules on the concentric ribs align to create strong pseudoplication on all sclerites, particularly on dorsal surfaces. Ornament on ventral surfaces is less well developed, and pustules are not as closely spaced. Pustular ornament is not developed at all on the anterior field of the A1 sclerites (Fig. 15C). Abundant new material from the WPC clearly show well developed reticulate micro-ornament on the pustules along the commarginal ribs, with slightly weaker micro-ornament on the inter-rib grooves, and a smooth, narrow, slit-like groove between growth sets (Fig. 17G_2, G_3). Material from the Arrowie Basin exhibits elevated, rounded pustules, however Skovsted et al. (2015a) did not observe any reticulate micro-ornament on the specimens from the Donkey Bore Syncline or the Mt. Chambers area, though this is likely due to abrasion and the small sample size.

Dailyatia decobruta Betts sp. nov. is readily distinguished from *D. ajax*, which is characterised by numerous strong radial plicae on all sclerite morphs. In contrast, *D. decobruta* Betts sp. nov. sclerites have few radial plicae, with aligned pustules forming pseudoplicae on broad, convex dorsal and also occasionally on concave ventral surfaces. *Dailyatia macroptera*, while bearing fewer radial plicae than *D. ajax*, is still considerably more plicate than *D. decobruta* Betts sp. nov., particularly on the anterior field. This is unlike the anterior field in *D. decobruta* Betts sp. nov., which is convex and bears fine, concentric wrinkles rather than plicae or pseudoplicae.

Like *D. decobruta* Betts sp. nov., *D. bacata* also bears a pustulose ornament with microreticulations that can align to form pseudoplicae. However, this ornament differs from that in *D. decobruta* Betts sp. nov. as the pustules in *D. bacata*, while discrete, have relatively low relief. In *D. decobruta* Betts sp. nov., the pustules can have substantial relief from the surrounding surface of the comarginal rib, often rising to form dull points. Alignment of these pustules to form strong pseudoplicae is a characteristic feature of *D. decobruta* Betts sp. nov., and is often only weakly developed in other species.

The C1 sclerite of *D. decobruta* Betts sp. nov. has a similar triangular outline and pyramidal shape to C1 sclerites of *Dailyatia odyssei*. However, C1 sclerites of *D. decobruta* Betts sp. nov. differ in that they do not exhibit the same strong central plication on the dorsal field observed in *D. odyssei* (Skovsted et al. 2015a). In addition, the micro-ornament on the external surfaces of *D. odyssei* consists of fine,

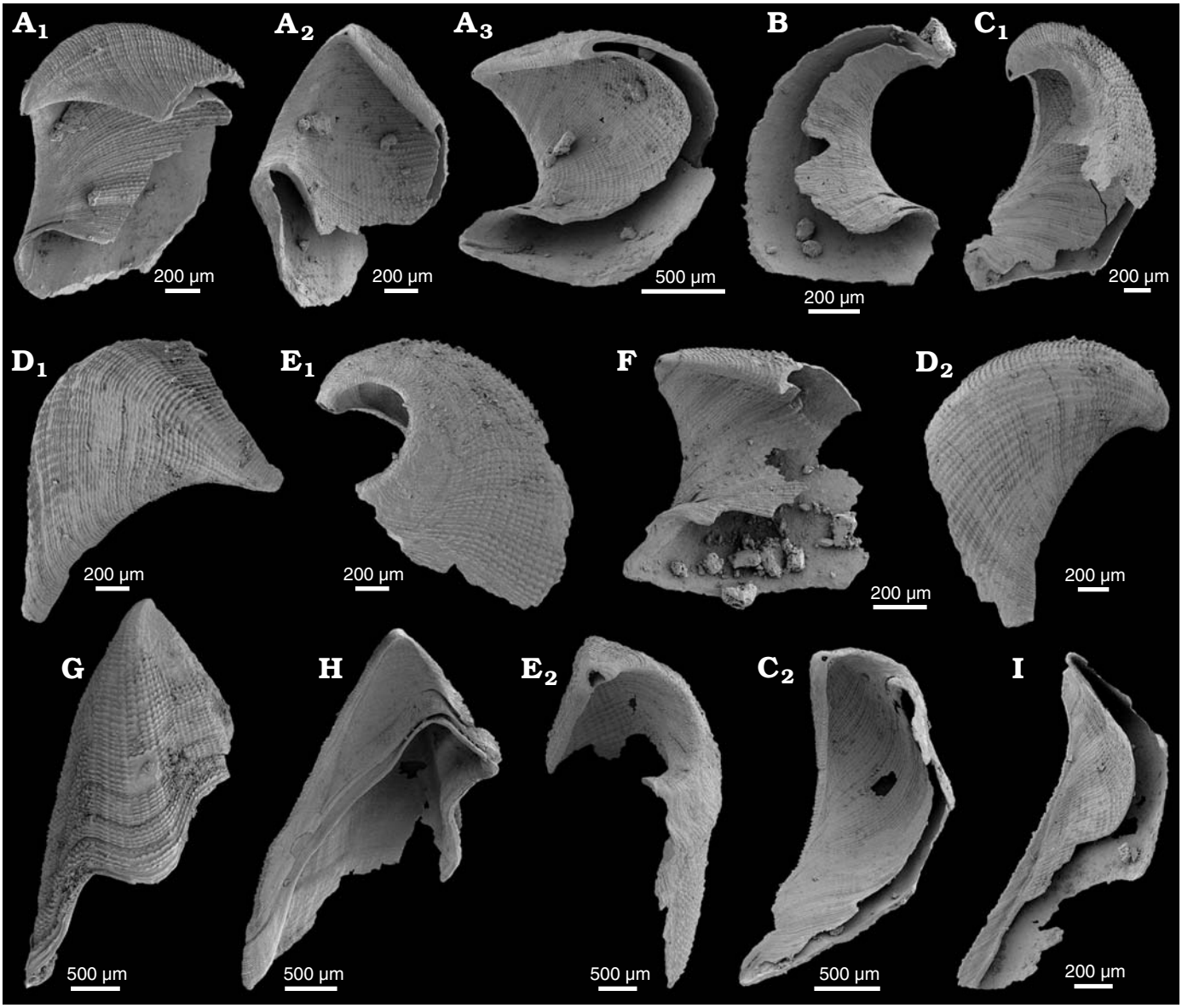

Fig. 18. C2a sclerites of the camenellan tommotiid *Dailyatia decobruta* Betts sp. nov. from the lower Cambrian White Point Conglomerate, Kangaroo Island, South Australia. **A**. SAM P57360 in ventral view; A_1–A_3, multiple views showing strong convexity and compression of sclerite. **B**. SAM P57361 in lateral view. **C**. SAM P573762 in oblique ventral view (C_1); C_2, slightly rotated view showing extreme compression of sclerite. **D**. SAM P57363 in dorsal view; D_1, D_2, different views showing strong curvature of sclerite and weak plication on dorsal surface. **E**. SAM P57364 in dorsal view, E_1, E_2, multiple views showing strong curvature (including weak torsion). **F**. SAM P57365 in ventral view. **G**. SAM P57359, holotype in dorsal view. **H**. SAM P57366 in ventral view. **I**. SAM P57367 in oblique ventral view.

flattened pustules at regular intervals along the crests of the concentric ribs. This is unlike the relatively large, raised pustules in *D. decobruta* Betts sp. nov.

Dailyatia decobruta Betts sp. nov. A1 sclerites bear some similarities to those of *Dailyatia helica* as both have concave anterior fields that lack radial plicae or pseudoplicae. In both taxa, micro-ornament is instead better developed on the deltoid. In addition, both species have C2a sclerites. In *D. helica*, C2a sclerites are very strongly compressed and recurved, with the apex coiling over the ventral field in a tight whorl (Skovsted et al. 2015a: fig. 40). The C2a sclerites of *D. decobruta* Betts sp. nov. are also compressed, with a reduced internal cavity, and while they are recurved, the apex does not coil over the ventral surfaces as in *D. helica*. Like the C1 sclerites in *D. helica*, C1 sclerites in *D. decobruta* Betts sp. nov. also appear compressed with a narrow internal cavity. However, C1 sclerites of *D. helica* have a complex pyramidial shape due to strong plication on the dorsal field, which is unlike C1 sclerites in *D. decobruta* Betts sp. nov.

Dailyatia decobruta Betts sp. nov. bears similarities to sclerites from the King George Island glacial erratics described as *Dailyata ajax* by Wrona (2004). These sclerites exhibit similar gross morphological characteristics, including compression and strong curvature, particularly in the C sclerites (Wrona 2004: figs. 8A–E, 10A–C). In the King George Island material, micro-ornament can be developed

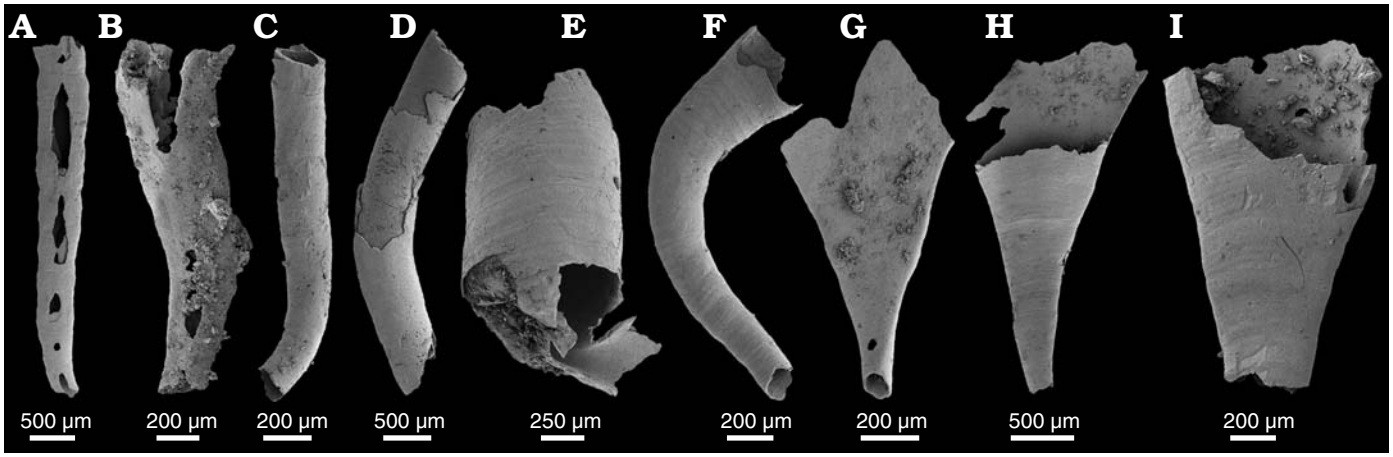

Fig. 19. The hyolithelminth tubes from the lower Cambrian White Point Conglomerate, Kangaroo Island, South Australia. *Sphenothallus*-like tubes (**A**, SAM P57368; **B**, SAM P57369). Tubes with circular cross-section (**C**, SAM P57370; **D**, SAM P57371; **E**, SAM P57372; **F**, SAM P57373). Expanding tubes (**G**, SAM P57374; **H**, SAM P57375; **I**, SAM P57376).

as blade-like projections with fine reticulations (Wrona 2004: fig. 11A_5, A_6), similar to that seen in some specimens from the WPC (Fig. 17I). However, the B sclerite illustrated by Wrona (2004: fig. 11D_6) bears a subdued, beaded micro-ornament unlike that in the WPC specimens, and the King George Island specimens do not feature the strong pseudoplication characteristic of *D. decobruta* Betts sp. nov. from the WPC. Skovsted et al. (2015a) noted the unique combination of characters in the *Dailyatia* specimens from the King George Island erratics and suggested that this assemblage may include more than one species.

B sclerites of *D. decobruta* Betts sp. nov. have not been recovered from the WPC. However, the distinctive morphologies of the A1, C1, C2, and C2a sclerites, coupled with the unique and easily identifiable external micro-ornament, is sufficient to distinguish this taxon from all previously described species of *Dailyatia*. Across most *Dailyatia* species, the A2 and B sclerites are relatively rare components of the scleritome, and it is anticipated that the as yet unknown B sclerites and perhaps A2 sclerites will be found when larger sample sizes are acquired.

Stratigraphic and geographic range.—Lower Cambrian of South Australia, Arrowie Basin (*D. odyssei* Zone): Donkey Bore Syncline, central Flinders Ranges and Mt. Chambers area eastern Flinders Ranges, Mernmerna Formation. Stansbury Basin (*D. odyssei* Zone): WPC, Kangaroo Island.

Class uncertain

Order Hyolithelminthida Fischer, 1962

Family Hyolithellidae Walcott, 1886

Hyolithelminth tubes indet.

Fig. 19.

Material.—Hundreds of specimens (all damaged or incomplete) from bioclastic Clasts 1, 4, and 5, 9 figured (SAM P57368–57376). From the *Dailyatia odyssei* Zone, WPC, Kangaroo Island, South Australia.

Remarks.—Small, phosphatic tubes are extremely common in lower Cambrian shelly fossil assemblages and constitute a large proportion of the fauna from the WPC clasts. Rare instances of hyolithelminths preserved in life position (Aftenstjernesø Formation in North Greenland) confirmed that the tubular *Hyolithellus* at least, lived buried within the substrate with the aperture emerging at the sediment-water interface, probably with a filter-feeding lifestyle (Skovsted and Peel 2011). Chang et al. (2018) described diverse early Cambrian tubular or conical fossils preserved as crack-outs with shells, and as carbonaceous compressions demonstrating that some taxa lived in gregarious communities clustered on the seafloor. Unfortunately, taxonomic identification of most early Cambrian tubes is complicated by their relatively simple morphologies and commonly fragmentary remains, particularly of those recovered via acid leaching methodologies.

The relative abundance of tubular forms in lower Cambrian shelly fossil assemblages is likely to be influenced by the suitability of available substrate. Betts (2012) noted that abundance of hyolithelminths increased in micritic and microbial limestone facies. These facies correspond with soft, muddy microbial substrates that may have been easier to penetrate in low energy conditions where smothering or accidental burial was less likely. Abundance of tubes in the limestone clasts in the WPC may be a result of hydrodynamic sorting or other biostratinomic processes concentrating these (and other) shelly fossils prior to burial.

Main morphologies of tubular fossils from the WPC include straight or very weakly curved specimens with circular cross-sections, similar to *Hyolithellus* (Fig. 19C–F). Diameter of these tubes can range from 150–1000 µm. Tubes may have thin walls or be thickened with multiple growth layers and have faint external concentric annulations, though external textures are likely to have been affected by abrasion. Others are compressed with an oval cross section, often

split along the broadest side, bifurcating into two diverging halves/thecae as in *Sphenothallus* (Fig. 19A, B; Li et al. 2004). These tubes may display a basal disc, which has been inferred as a method of substrate attachment (Bischoff 1989; Li et al. 2004). However, the holdfast or any other type of attachment structure is absent from all of the WPC specimens, which are consistently damaged or abraded, truncated at both ends, or split along the entire length of the tube.

A smaller proportion of the hyolithelminths from the WPC have distinctive, rapidly expanding, flattened tubes (Fig. 19G–I). Their cross section changes from circular at the narrow end to compressed and oval-shaped at the wider end. Similar tubes were reported by Paterson et al. (2007b: fig. 5A–C) from the KLM (Parara Limestone). Paterson et al. (2007b) noted that early Cambrian phosphatic tubes often exhibit a combination of characters belonging to a variety of taxa (Paterson et al. 2007b). They exhibit similar growth patterns, and it is possible that differences in gross morphology are due to environmental influences, rather than having taxonomic significance. Hence, the material here is left under open nomenclature.

Conclusions

The combination of new shelly fossil biostratigraphic data (Betts et al. 2016, 2017b), carbon isotope chemostratigraphic data, and radiometric dates has resulted in a reassessment of the ages and regional and global correlations of the lower Cambrian successions in South Australia (Betts et al. 2018). Correlating the predominantly siliciclastic successions on Kangaroo Island with the lower Cambrian successions on the Yorke and Fleurieu peninsulas (Stansbury Basin), and in the Flinders Ranges (Arrowie Basin) has proven difficult (Gehling et al. 2011). The WPC, in particular, lacks in situ biostratigraphic control, hence age assessment and correlation of this formation relies upon determination of the relative ages of strata that bracket the unit, as well as the fossiliferous clasts it contains. The WPC limestone clasts yield a rich shelly fauna, with many taxa being age-diagnostic, especially *Dailyatia odyssei* and *Stoibostrombus crenulatus*. These key species and other accessory taxa indicate that the WPC limestone clasts are likely to be upper *D. odyssei* Zone in age, equivalent to the Atdabanian–early Botoman in Siberia (Fig. 2; Betts et al. 2018).

Deposition of the WPC and age-equivalent strata on Fleurieu Peninsula signalled a major shift in depositional regime in the Stansbury Basin during the early Cambrian, resulting in a change from mostly carbonate-dominated to siliciclastic-dominated successions. The upper age limit of the WPC itself is constrained by biostratigraphic data from the overlying Marsden Sandstone and Emu Bay Shale, indicating that the unit cannot be younger than Cambrian Series 2, Stage 4 (*Pararaia janeae* Zone) in age. The shelly fossils from the bioclastic limestone clasts of the WPC indicate an upper *D. odyssei* Zone age, equivalent to the *Pararaia tatei* to lower *P. janeae* trilobite zones. If some of the WPC limestone clasts are indeed as young as the *P. janeae* Zone—as suggested by the presence of *Dailyatia decobruta* Betts sp. nov. and co-occuring taxa in the Donkey Bore Syncline of the Arrowie Basin (Betts et al. 2017b)—this indicates that the original limestone source was cannibalised and redeposited as a constituent of the WPC in a relatively short timeframe, most likely due to rapid uplift along a tectonic margin to the north of Kangaroo Island (Gehling et al. 2011).

Acknowledgements

The authors would like to acknowledge the Macquarie University Faculty of Science and Engineering Microscope Facility (MQFoSE MF) for access to its instrumentation and staff. Thanks also to Gerd Geyer (University of Würzburg, Würzburg, Germany) for discussions on the WPC trilobite. Thanks to Olaf Elicki (Freiberg University, Freiberg, Germany) and an anonymous referee for their constructive reviews. MJB is supported by postdoctoral funds from UNE and NWU. Additional funding was provided by an Australian Research Council Future Fellowship to JRP (FT120100770).

References

Angelin, N.P. 1854. *Palaeontologia Scandinavica. Crustacea formationis transitionis*. i–ix + 92 pp. Lund, Lipsiae.

Balthasar, U. 2009. The brachiopod *Eoobolus* from the Early Cambrian Mural Formation (Canadian Rocky Mountains). *Paläontologische Zeitschrift* 83: 407–418.

Beecher, C.E. 1891. Development of the Brachiopoda, Part 1. Introduction. *American Journal of Science*, *Series 3* 41: 343–357.

Belperio, A.P., Preiss, W.V., Fairclough, M.C., Gatehouse, C.G., Gum, J., Hough, J., and Burtt, A. 1998. Tectonic and metallogenic framework of the Cambrian Stansbury Basin—Kanmantoo Trough, South Australia. *AGSO Journal of Geology and Geophysics* 17: 183–200.

Bengtson, S. 1980. Redescription of the Lower Cambrian *Lapworthella cornu*. *GFF* 102: 53–55.

Bengtson, S., Conway Morris, S., Cooper, B.J., Jell, P.A., and Runnegar, B.N. 1990. Early Cambrian fossils from South Australia. *Memoirs of the Association of Australasian Palaeontologists* 9: 1–364.

Betts, M.J. 2012. *Small Shelly Fossils and Archaeocyath Bioherms from Lower Cambrian Hawker Group Carbonates at Moro Gorge, Central Flinders Ranges*. 193 pp. Honours thesis, Macquarie University, Sydney.

Betts, M.J., Paterson, J.R., Andrew, A.S., Hall, P.A., Jago, J.B., Jagodzinski, E.A., Preiss, W.V., Crowley, J.L., Brougham, T., Mathewson, C.P., García-Bellido, D., Topper, T.P., Jacquet, S.M., Skovsted, C.B., and Brock, G.A. 2018. Early Cambrian chronostratigraphy and geochronology of South Australia. *Earth-Science Reviews* 185: 498–543.

Betts, M.J., Paterson, J.R., Jago, J.B., Jacquet, S.M., Skovsted, C.B., Topper, T.P., and Brock, G.A. 2016. A new lower Cambrian shelly fossil biostratigraphy for South Australia. *Gondwana Research* 36: 176–208.

Betts, M.J., Paterson, J.R., Jago, J.B., Jacquet, S.M., Skovsted, C.B., Topper, T.P., Brock, G.A. 2017a. A new lower Cambrian shelly fossil biostratigraphy for South Australia: Reply. *Gondwana Research* 44: 262–264.

Betts, M.J., Paterson, J.R., Jago, J.B., Jacquet, S.M., Skovsted, C.B., Topper, T.P., and Brock, G.A. 2017b. Global correlation of the early Cambrian of South Australia: Shelly fauna of the *Dailyatia odyssei* Zone. *Gondwana Research* 46: 240–279.

Bischoff, G.C.O. 1976. *Dailyatia*, a new genus of the Tommotiidae from Cambrian strata of SE Australia (Crustacea, Cirripedia). *Senkenbergiana Lethaea* 57: 1–33.

Bischoff, G.C.O. 1989. Byroniida new order from early Palaeozoic strata of eastern Australia (Cnidaria, thecate scyphopolyps). *Senckenbergiana lethaea* 59: 275–327.

Brasier, M.D. 1986. The succession of small shelly fossils (especially conoidal microfossils) from English Precambrian–Cambrian boundary beds. *Geological Magazine* 123: 237–256.

Brock, G.A. and Cooper, B.J. 1993. Shelly fossils from the Early Cambrian (Toyonian) Wirrealpa, Arrona Creek, and Ramsay limestones of South Australia. *Journal of Paleontology* 67: 758–787.

Brock, G.A. and Percival, I.G. 2006. Cambrian stratigraphy and faunas at Mount Arrowsmith, north-western New South Wales, Australia. *Memoirs of the Association of Australasian Palaeontologists* 32: 75–101.

Brock, G.A., Engelbretsen, M., Jago, J., Kruse, P., Laurie, J., Shergold, J., Shi, G., and Sorauf, J. 2000. Palaeobiogeographic affinities of Australian Cambrian faunas. *Memoirs of the Association of Australasian Palaeontologists* 23: 1–62.

Caron, J.B., Smith, M.R., and Harvey, T.H.P. 2013. Beyond the Burgess Shale: Cambrian microfossils track the rise and fall of hallucigeniid lobopodians. *Proceedings of the Royal Society B* 280: 20131613.

Chang, W.T. 1963. A classification of the Lower and Middle Cambrian trilobites from north and northeastern China, with description of new families and new genera. *Acta Palaeontologica Sinica* 11: 447–487.

Chang, S., Clausen, S., Zhang, L., Feng, Q.-L., Steiner, M., Bottjer, D.J., Zhang, Y., and Shi, M. 2018. New probable cnidarian fossils from the lower Cambrian of the Three Gorges area, South China, and their ecological implications. *Palaeogeography, Palaeoclimatology, Palaeoecology* 505: 150–166.

Cobbold, E.S. 1921. The Cambrian horizons of Comley (Shropshire) and their Brachiopoda, Pteropoda, Gasteropoda, etc. *Quarterly Journal of the Geological Society, London* 76: 325–386.

Daily, B. 1990. Cambrian stratigraphy of Yorke Peninsula. *In*: J.B. Jago and P.S. Moore (eds.), The Evolution of a Late Precambrian–Early Palaeozoic Rift Complex: The Adelaide Geosyncline. *Geological Society of Australia, Special Publication* 16: 215–229.

Daily, B. and Forbes, B.G. 1969. Notes on the Proterozoic and Cambrian, southern and central Flinders Ranges, South Australia. *In*: B. Daily (ed.), *Geological Excursions Handbook*, 23–30. Australian and New Zealand Association for the Advancement of Science (ANZAAS), 41st Congress, Section 3, Adelaide.

Daily, B., Moore, P.S., and Rust, B.R. 1980. Terrestrial-marine transition in the Cambrian rocks of Kangaroo Island, South Australia. *Sedimentology* 27: 379–399.

Debrenne, F. and Gravestock, D.I. 1990. Archaeocyatha from the Sellick Hill Formation and Fork Tree Limestone on Fleurieu Peninsula, South Australia. *Geological Society of Australia Special Publication* 16: 290–309.

Demidenko, Y.E. 2004. New data on the sclerite morphology of the tommotiid species *Lapworthella fasciculata*. *Paleontological Journal* 38: 134–140.

Devaere, L. and Skovsted, C.B. 2017. New early Cambrian sclerites of *Lapworthella schodakensis* from NE Greenland: advancements in knowledge of lapworthellid taxonomy, sclerite growth and scleritome organization. *Geological Magazine* 154: 1061–1072.

Devaere, L., Clausen, S., Monceret, E., Tormo, N., Cohen, H., and Vachard, D. 2014a. Lapworthellids and other skeletonized microfossils from the Cambrian Stage 3 of the northern Montagne Noire, southern France. *Annales de Paléontologie* 100: 175–191.

Devaere, L., Clausen, S., Monceret, E., Vizcaïno, D., Vachard, D., and Genge, M.C. 2014b. The tommotiid *Kelanella* and associated fauna from the Early Cambrian of southern Montagne Noire (France): Implications for camenellan phylogeny. *Palaeontology* 57: 979–1002.

Devaere, L., Clausen, S., Steiner, M., Álvaro, J.J., Vachard, D. 2013. Chronostratigraphic and palaeogeographic significance of an early Cambrian microfauna from the Heraultia Limestone, northern Montagne Noire, France. *Palaeontologia Electronica* 16: 1–91.

Duméril, A.M.C. 1806. *Zoologie analytique, ou Méthode naturelle de classification des animaux: rendue plus facile à l'aide de tableaux synoptiques*. 344 pp. Allais, Paris.

Dzik, J. 2003. Early Cambrian lobopodian sclerites and associated fossils from Kazakhstan. *Palaeontology* 46: 93–112.

Endo, R. 1937. Addenda to Parts 1 and 2. *In*: R. Endo and C.E. Resser (eds.), The Sinian and Cambrian Formations and Fossils of Southern Manchoukuo. *Manchurian Science Museum, Bulletin* 1: 302–369.

Esakova, N.V. and Zhegallo, E.A. [Žegallo, E.A.] 1996. Biostratigraphy and fauna of the lower Cambrian of Mongolia [in Russian]. *Trudy Sovmestnoj Rossijsko-Mongol'skoj paleontologičeskoj ekspedicii* 46: 1–216.

Evans, K.R. and Rowell, A.J. 1990. Small shelly fossils from Antarctica: An early Cambrian faunal connection with Australia. *Journal of Paleontology* 64: 692–700.

Fisher, D.W. 1962. Small conoidal shells of uncertain affinities. *In*: R.C. Moore (ed.), *Treatise on Invertebrate Paleontology, Part W, Miscellanea*, 98–143. Geological Society of America, New York and University of Kansas, Lawrence.

Gehling, J.G., Jago, J.B., Paterson, J.R., García-Bellido, D., and Edgecombe, G.D. 2011. The geological context of the lower Cambrian (Series 2) Emu Bay Shale Lagerstätte and adjacent stratigraphic units, Kangaroo Island, South Australia. *Australian Journal of Earth Sciences* 58: 243–257.

Gorjansky, W.J. and Popov, L.Y. 1986. On the origin and systematic position of the calcareous-shelled inarticulate brachiopods. *Lethaia* 19: 233–240.

Gravestock, D.I. 1995. Early and Middle Palaeozoic. *In*: J.F. Drexel and W.V. Preiss (ed.), The Geology of South Australia, Vol. 2, The Phanerozoic. *South Australia Geological Survey, Bulletin* 54: 3–61.

Gravestock, D.I., Alexander, E.M., Demidenko, Y.E., Esakova, N.B., Holmer, L.E., Jago, J.B., Lin, T.-R., Melnikova, N., Parkhaev, P.Y., Rozanov, A.Y., Ushatinskaya, G.T., Sang, W.-L., Zhegallo, E.A., and Zhuravlev, A.Y. 2001. The Cambrian biostratigraphy of the Stansbury Basin, South Australia. *Transactions of the Palaeontological Institute of the Russian Academy of Sciences* 282: 1–341.

Guo, J.-F., Li, Y., and L, G.-X. 2014. Small shelly fossils from the early Cambrian Yanjiahe Formation, Yichang, Hubei, China. *Gondwana Research* 25: 999–1007.

Holl, H.B. 1865. On the geological structure of the Malvern Hills and adjacent districts. *Geological Society of London, Quarterly Journal* 21: 72–102.

Holmer, L.E. 1993. The Lower Ordovician brachiopod genus *Lamanskaya* and the family Elkaniidae. *Transactions of the Royal Soceity of Edinburgh: Earth Sciences* 84: 151–160.

Holmer, L.E. and Popov, L.E. 2007. Organophosphatic bivalved stem-group brachiopods. *In*: P.A. Selden (ed.), *Treatise on Invertebrate Paleontology, Part H, Brachiopoda, Revised, Vol. 6*, 2580–2590. The Geological Society of America, Boulder and the University of Kansas, Lawrence.

Holmer, L.E., Popov, L.E., and Wrona, R. 1996. Early Cambrian lingulate brachiopods from glacial erratics of King George Island (South Shetland Islands), Antarctica. *In*: A. Gaździcki (ed.), Palaeontological Results of the Polish Antarctic Expeditions. Part II. *Palaeontologica Polonica* 55: 37–50.

Holmer, L.E., Popov, L.E., Koneva, S.P., and Bassett, M.G. 2001. Cambrian-early Ordovician brachiopods from Malyi Karatau, the western Balkash region, and Tien Shan, Central Asia. *Special Papers in Palaeontology* 65: 1–180.

Jacquet, S.M., Betts, M.J., Selly, T., Schiffbauer, J.D., and Brock, G.A. 2018. Shell ultrastructure of the organophosphatic brachiopod *Eodicellomus* from the lower Cambrian of South Australia. *International Conference on Ediacaran and Cambrian Sciences*, *Abstracts with Programs*, 119. Xi'an.

Jago, J.B., Gehling, J.G., Betts, M.J., Brock, G.A., Dalgarno, C.R., Garcia-Bellido, D.C., Haslett, P.G., Jacquet, S.M., Kruse, P.D., Langsford, N.R., Mount, T.J., and Paterson, J.R. 2018. The Cambrian System in the Arrowie Basin, Flinders Ranges, South Australia. *Australian Journal of Earth Sciences* [published online https://doi.org/10.1080/08120099.2018.1525431].

Jago, J.B., Zang, W.-L., Sun, X., Brock, G.A., Paterson, J.R., and Skovsted, C.B. 2006. A review of the Cambrian biostratigraphy of South Australia. *Palaeoworld* 15: 406–423.

Jell, P.A. and Adrain, J.M. 2003. Available generic names for trilobites. *Memoirs of the Queensland Museum* 48: 331–553.

King, W. 1846. Remarks on certain genera belonging to the class Palliobranchiata. *Annals and Magazine of Natural History* 18: 26–24, 83–94.

Koneva, S.P. 1979. *Stenotekoidy i bezzamkovye brahiopody nižnego i nižov srednego kembriâ Central'nogo Kazahstana*. 124 pp. Nauka, Alma Ata.

Koneva, S.P. 1986. A new family of Cambrian inarticulate brachiopods [in Russian]. *Paleontologičeskij žurnal* 1986 (1): 49–55.

Kruse, P.D. 1990. Cambrian paleontology of the Daly Basin. *Northern Territory Geological Survey Report* 7: 1–58.

Kruse, P.D. 1991. Cambrian fauna of the Top Springs Limestone, Georgina Basin. *The Beagle, Records of the Northern Territory Museum of Arts and Sciences* 8: 169–188.

Kruse, P.D. and Moreno-Eiris, E. 2013. Archaeocyaths of the White Point Conglomerate, Kangaroo Island, South Australia. *Alcheringa* 38: 1–64.

Kuhn, O. 1949. *Lehrbuch der Paläozoologie*. 326 pp. E. Schweizerbart'sche Verlagsbuchhandlung, Stuttgart.

Landing, E. 1984. Skeleton of lapworthellids and the suprageneric classification of tommotiids (Early and Middle Cambrian phosphatic problematica). *Journal of Paleontology* 58: 1380–1398.

Landing, E. 1988. Lower Cambrian of eastern Massachusetts: Stratigraphy and small shelly fossils. *Journal of Paleontology* 62: 661–695.

Landing, E., Geyer, G., and Bartowski, K.E. 2002. Latest Early Cambrian small shelly fossils, trilobites, and Hatch Hill dysaerobic interval on the Québec continental slope. *Journal of Paleontology* 76: 287–305.

Lankester, E.R. 1904. The structure and classification of Arthropoda. *Quarterly Journal of Microscopical Science* 47: 523–582.

Laurie, J.R. 1986. Phosphatic fauna of the Early Cambrian Todd River Dolomite, Amadeus Basin, central Australia. *Alcheringa* 10: 431–454.

Laurie, J.R. 2000. Paterinata. *In*: A. Williams, C.H.C. Brunton, and S.J. Carlson (eds.), *Treatise on Invertebrate Paleontology: Part H. Brachiopoda, Vol. 2 (revised)*, 147–157. Geological Society of America, Boulder and University of Kansas Press, Lawrence.

Li, G.-X. and Holmer, L.E. 2004. Early Cambrian lingulate brachiopods from the Shaanxi Province, China. *GFF* 126: 193–211.

Li, G.-X., Steiner, M., Zhu, M.Y., and Zhao, X. 2012. Early Cambrian eodiscoid trilobite *Hupeidiscus orientalis* from South China: ontogeny and implications for affinities of *Mongolitubulus*-like sclerites. *Bulletin of Geosciences* 87: 159–169.

Li, G.-X., Zhu, M.Y., van Iten, H., and Li, C.-W. 2004. Occurrence of the earliest known *Sphenothallus* Hall in the Lower Cambrian of southern Shaanxi Province, China. *Geobios* 37: 229–237.

Lokier, S.W. and Al Junaibi, M. 2016. The petrographic description of carbonate facies: are we all speaking the same language? *Sedimentology* 63: 1843–1885.

Matthew, G.F. 1902. Notes on Cambrian faunas. *Royal Society of Canada, Transactions* (Series 2, Section 4) 18: 93–112.

Menke,C.T. 1828. *Synopsis methodica molluscorum generum omnium et specierum earum quae in Museo Menkeano adservantur*. 91 pp. Georgi Uslar, Pyrmont.

Meshkova, N.P. [Meškova, N.P.] 1985. New tubular problematics of theMiddle Cambrian of Siberia and Middle Asia [in Russian]. *In*: B.S. Skolov and I.T. Žuravleva (eds.), Problematiki pozdnego dokembriâ i paleozoâ. *Trudy Instituta geologii i geofiziki SO AN SSSR* 632: 127–133.

Missarzhevsky, V.V. [Missarževskij, V.V.] 1970. New generic name *Tommotia* nom. nov. [in Russian]. *Paleontologičeskij žurnal* 1970 (2): 100.

Missarzhevsky, V.V. [Missarževskij, V.V.] 1977. Conodonts (?) and phosphatic problematica from the Cambrian of Mongolia and Siberia [in Russian]. *In*: L.P. Tatarinov (ed.), *Bespozvonočnye paleozoâ Mongolii*, 10–19. Nauka, Moskva.

Missarzhevsky, V.V. [Missarževskij, V.V.] 1989. The oldest skeletal fossils and stratigraphy of the Precambrian-Cambrian boundary beds [in Russian]. *Trudy Geologičeskogo Instituta Akademii Nauk SSSR* 443: 1–237.

Missarzhevsky, V.V and Grigorieva, N.V. 1981. New representatives of the order Tommotiida. *Palaeontological Journal* 15: 96–103.

Missarzhevsky, V.V. [Missarževskij, V.V.] and Mambetov, A.M. 1981. Stratigraphy and fauna of the Cambrian and Precambrian boundary beds of the Lesser Karatau Range [in Russian]. *Trudy Geologičeskogo Instituta AN SSSR* 326: 1–92.

Moberg, J.C. and Segerberg, C.O. 1906. Bidrag till kännedomen of ceratopygeregionen med särskild hänsyn till dess utveckling i Fogelsångstrakten. *Acta Universitatis Lundensis* 2: 1–116.

Ortega-Hernández, J. 2016. Making sense of "lower" and "upper" stem-group Euarthropoda, with comments on the strict use of the name Arthropoda von Siebold, 1848. *Biological Reviews* 91: 255–273.

Paterson, J.R. 2014. Trilobites in early Cambrian tidal flats and the landward expansion of the Cambrian explosion: Comment. *Geology* 42: e341.

Paterson, J.R. and Brock, G.A. 2007. Early Cambrian trilobites from Angorichina, Flinders Ranges, South Australia, with a new assemblage from the *Pararaia bunyerooensis* Zone. *Journal of Paleontology* 81: 116–142.

Paterson, J.R. and Edgecombe, G.D. 2006. The Early Cambrian trilobite family Emuellidae Pocock, 1970: systematic position and revision of Australian species. *Journal of Paleontology* 80: 496–513.

Paterson, J.R., García-Bellido, D.C., Jago, J.B., Gehling, J.G., Lee, M.S.Y., and Edgecombe, G.D. 2016. The Emu Bay Shale Konservat-Lagerstätte: a view of Cambrian life from East Gondwana. *Journal of the Geological Society* 173: 1–11.

Paterson, J.R., Jago, J.B., Brock, G.A., and Gehling, J.G. 2007a. Taphonomy and palaeoecology of the emuellid trilobite *Balcoracania dailyi* (early Cambrian, South Australia). *Palaeogeography, Palaeoclimatology, Palaeoecology* 249: 302–321.

Paterson, J.R., Jago, J.B., Gehling, J.G., García-Bellido, D., Edgecombe, G.D., and Lee, M.S.Y. 2008. Early Cambrian arthropods from the Emu Bay Shale lagerstätte, South Australia. *In*: I. Rábano, R. Gozalo, and D. García-Bellido (eds.), *Advances in Trilobite Research*, 319–325. Instituto Geológico y Minero de España, Madrid.

Paterson, J.R., Skovsted, C.B., Brock., G.A., and Jago, J.B. 2007b. An early Cambrian faunule from the Koolywurtie Limestone Member (Parara Limestone), Yorke Peninsula, South Australia and its biostratigraphic significance. *Memoirs of the Association of Australasian Palaeontologists* 34: 131–146.

Peel, J.S. and Blaker, M.R. 1988. The small shelly fossil *Mongolitubulus* from the Lower Cambrian of North Greenland. *Rapport Grønlands geologiske Undersøgelse* 137: 55–60.

Pelman, Y.L. [Pelman, Û.L.] 1977. Early and Middle Cambrian inarticulate brachiopods of the Siberian Platform fossils [in Russian]. *Trudy Instituta Geologii i Geofiziki AN SSSR, Sibirskoe Otdelenie* 316: 1–168.

Pelman, Y.L. [Pelman, Û.L.] 1983. Middle Cambrian brachiopods of the Muna River (lower reaches of the Lena River) [in Russian]. *Trudy lnstituta Geologii i Geofiziki SO AN SSSR* 541: 115-128.

Pelman, Y.L. [Pelman, Û.L.], Aksarina, N.A., Koneva, S.P., and Popov, L.E. 1992. The earliest brachiopods of northern Eurasia [in Russian]. *In*: L.N Repina and A.Û. Rozanov (eds.), Drevneišie brahiopody territorii Severnoj Evrasii. *Trudy lnstituta Geologii i Geofiziki NO AN SSSR* 788: 83–85.

Peng, S.-C., Babcock, L., and Cooper, R. 2012. The Cambrian Period. *In*: F.M. Gradstein, J.G. Ogg, M. Schmitz, and G. Ogg (eds.), *The Geologic Time Scale, Volume 2*, 437–488. Elsevier, Amsterdam.

Percival, I.G. and Kruse, P.D. 2014. Middle Cambrian brachiopods from the southern Georgina Basin of central Australia. *Memoirs of the Association of Australasian Palaeontologists* 45: 349–402.

Pocock, K.J. 1970. The Emuellidae, a new family of trilobites from the lower Cambrian of South Australia. *Palaeontology* 13: 522–562.

Popov, L.E and Holmer, L.E. 1994. Cambrian-Ordovician lingulate brachiopods from Scandinavia, Kazakhstan, and South Ural Mountains. *Fossils and Strata* 35: 1–156.

Popov, L.E, Holmer, L.E, Hughes, N.C, Ghobadi Pour, M., and Myrow, P.M. 2015. Himalayan Cambrian brachiopods. *Papers in Palaeontology* 1: 345–399.

Poulsen, C. 1932. The Lower Cambrian faunas of East Greenland. *Meddelelser om Grønland* 87: 1–66.

Qian, Y. and Bengtson, S. 1989. Palaeontology and biostratigraphy of the Early Cambrian Meishucunian Stage in Yunnan Province, South China. *Fossils and Strata* 24: 1–156.

Raymond, P.E. 1935. *Leanchoilia* and other mid-Cambrian Arthropoda. *Bulletin of the Museum of Comparative Zoology* 76: 205–230.

Rowell, A.J. 1965. Inarticulata. *In*: R.C. Moore (ed.), *Treatise on Inverte-*

brate Paleontology, Part H, 260–296. Geological Society of America, Boulder and University of Kansas Press, Lawrence.

Rowell, A.J., Evans, K.R., and Rees, M.N. 1988. Fauna of the Shackleton Limestone. *Antarctic Journal* 20: 13–14.

Rozanov, A.Y., Missarzhevsky, V.V., Volkova, N.A., Voronova, L.C., Krylov, I.N., Keller, B.M., Korolyuk, I.K., Lendzion, K., Michniak, R., Pykhova, N.G., and Sidorov, A.D. 1969. The Tommotian Stage and the Cambrian lower boundary problem [in Russian]. *Trudy Geologičeskogo Instituta AN SSSR* 206: 1–380.

Rozanov, A.Y. 1986. Problematica of the early Cambrian. *In*: A. Hoffman and M.H. Nitecki (eds.), *Problematic Fossil Taxa*, 87–96. Oxford University Press, New York.

Rozanov, A.Y. and Missarzhevsky, V.V. 1966. Biostratigraphy and fauna of the lower Horizons of the Cambrian [in Russian]. *Biostratigrafiâ i fauna nižnih gorizontov kembriâ* 148: 1–118.

Schindewolf, O.H. 1955. Über einige kambrische Gattungen inartikulater Brachiopoden. *Neues Jahrbuch für Mineralogie, Geologie und Palaeontologie, Monatshefte* 12: 538–557.

Schuchert, C. 1893. A classification of the Brachiopoda. *American Geologist* 11: 141–167.

Skovsted, C.B. and Holmer, L.E. 2005. Early Cambrian brachiopods from north-east Greenland. *Palaeontology* 48: 325–345.

Skovsted, C.B. and Holmer, L.E. 2006. The Lower Cambrian brachiopod *Kyrshabaktella* and associated shelly fossils from the Harkless Formation, southern Nevada. *GFF* 128: 327–337.

Skovsted, C.B. and Peel, J.S. 2001. The problematic fossil *Mongolitubulus* from the Lower Cambrian of Greenland. *Bulletin of the Geological Society of Denmark* 48: 135–147.

Skovsted, C.B. and Peel, J.S. 2011. *Hyolithellus* in life position from the Lower Cambrian of North Greenland. *Journal of Paleontology* 85: 37–47.

Skovsted, C.B., Betts, M.J., Topper, T.P., and Brock, G.A. 2015a. The early Cambrian tommotiid genus *Dailyatia* from South Australia. *Memoirs of the Association of Australasian Palaeontologists* 48: 1–117.

Skovsted, C.B., Brock, G.A., and Paterson, J.R. 2006. Bivalved arthropods from the Lower Cambrian Mernmerna Formation, Arrowie Basin, South Australia and their implications for identification of Cambrian "small shelly fossils". *Memoirs of the Association of Australasian Palaeontologists* 32: 7–41.

Skovsted, C.B., Brock, G.A., and Topper, T.P. 2011. Sclerite fusion in the problematic early Cambrian spine-like fossil *Stoibostrombus* from South Australia. *Bulletin of Geosciences* 86: 651–658.

Skovsted, C.B., Knight, I., Balthasar, U., and Boyce, W.D. 2017. Depth related brachiopod faunas from the lower Cambrian Forteau Formation of southern Labrador and western Newfoundland, Canada. *Palaeontologica Electronica* 20.3.54A: 1–52.

Skovsted, C.B., Ushatinskaya, G., Holmer, L.E., Popov, L.E., and Kouchinsky, A. 2015b. Taxonomy, morphology, shell structure and early ontogeny of *Pelmanotreta* nom. nov. from the lower Cambrian of Siberia. *GFF* 137: 1–8.

Smith, M. 2006. *The palaeobiology of* Lapworthella fasciculata *from the Lower Cambrian of South Australia*. 99 pp. Honours thesis, Macquarie University, Sydney.

Steiner, M., Li, G.-X., Qian, Y., and Zhu, M. 2004. Lower Cambrian small shelly fossils of northern Sichuan and southern Shaanxi (China), and their biostratigraphic importance. *Geobios* 37: 259–275.

Steiner, M., Li, G.-X., Qian, Y., Zhu, M.-Y., and Erdtmann, B.-D. 2007. Neoproterozoic to Early Cambrian small shelly fossil assemblages and a revised biostratigraphic correlation of the Yangtze Platform (China). *Palaeogeography, Palaeoclimatology, Palaeoecology* 254: 67–99.

Streng, M., Holmer, L.E., Popov, L.E., and Budd, G.E. 2008. Columnar shell structures in early linguloid brachiopods—new data from the Middle Cambrian of Sweden. *Earth and Environmental Science Transactions of the Royal Society of Edinburgh* 98: 221–232.

Tate, R. 1892. The Cambrian fossils of South Australia. *Transactions of the Royal Society of South Australia* 15: 183–189.

Topper, T.P. and Skovsted, C.B. 2014. A new name for a classic Cambrian Swedish brachiopod, *Tallatella undosa* (Moberg). *GFF* 136: 429–435.

Topper, T.P., Brock, G.A., Skovsted, C.B, and Paterson, J.R. 2009. Shelly fossils from the lower Cambrian *Pararaia bunyerooensis* Zone, Flinders Ranges, South Australia. *Memoirs of the Association of Australasian Palaeontologists* 37: 199–246.

Topper, T.P., Skovsted, C.B., Brock, G.A., and Paterson, J.R. 2007. New bradoriids from the lower Cambrian Mernmerna Formation, South Australia: Systematics, biostratigraphy and biogeography. *Memoirs of the Association of Australasian Palaeontologists* 33: 67–100.

Topper, T.P., Skovsted, C.B., Brock, G.A., and Paterson, J.R. 2011. The oldest bivalved arthropods from the early Cambrian of East Gondwana: Systematics, biostratigraphy and biogeography. *Gondwana Research* 19: 310–326.

Topper, T.P., Skovsted, C.B., Harper, D.A.T., and Ahlberg, P. 2013. A bradoriid and brachiopod dominated shelly fauna from the Furongian (Cambrian) of Västergotland, Sweden. *Journal of Paleontology* 87: 69–83.

Ushatinskaya, G.T. 1987. Unusual inarticulate brachiopods from the lower Cambrian of Mongolia [in Russian]. *Paleontologičeskij žurnal* 1987 (2): 62–68.

Ushatinskaya, G.T. 1993. Early and Middle Cambrian lingulids of the Siberian Platform [in Russian]. *Paleontologičeskij žurnal* 1993 (2): 133–136.

Ushatinskaya, G.T. and Korovnikov, I.V. 2014. Revision of the Early–Middle Cambrian Lingulida (Brachiopoda) from the Siberian Platform. *Paleontological Journal* 48: 26–40.

Waagen, W.H. 1885. Salt-range fossils, Pt. 4 (2), Brachiopoda. *Memoirs of the Geological Survey of India, Series 13* 1 (5): 729–770.

Walch, J.E.I. 1771. *Die naturgeschichte der versteinerungen zur erläuterung der knorrischen Sammlung von merkwürdigkeiten der Natur*. 235 pp. Paul Jonathan Feltstecker. Nürnberg.

Walcott, C.D. 1886. Second contribution to the studies on the Cambrian faunas of North America. *US Geological Survey, Bulletin* 30: 1–369.

Walcott, C.D. 1908. Cambrian geology and paleontology. No. 3, Cambrian Brachiopoda, descriptions of new genera and species. *Smithsonian Miscellaneous Collections* 53: 53–137.

Williams, A., Carlson, S.J., Brunton, C.H.C., Holmer, L.E., and Popov, L.E. 1996. A supra-ordinal classification of the Brachiopoda. *Philosophical Transactions of the Royal Society of London, Series B* 351: 1171–1193.

Williams, A., Popov, L.E., Holmer, L.E., and Cusack, M. 1998. The diversity and phylogeny of the paterinate brachiopods. *Palaeontology* 41: 221–262.

Wrona, R. 1989. Cambrian limestone erratics in the Tertiary glacio-marine sediments of King George Island, West Antarctica. *Polish Polar Research* 10: 533–553.

Wrona, R. 2004. Cambrian microfossils from glacial erratics of King George Island, Antarctica. *Acta Palaeontologica Polonica* 49: 13–56.

Wrona, R. 2009. Early Cambrian bradoriide and phosphatocopide arthropods from King George Island, West Antarctica: Biogeographic implications. *Polish Polar Research* 30: 347–377.

Wrona, R. and Zhuravlev, A.Y. 1996. Early Cambrian archaeocyaths from glacial erratics of King George Island (South Shetland Islands), Antarctica. *In*: A. Gaździcki (ed.), Palaeontological Results of the Polish Antarctic Expeditions. Part II. *Palaeontologica Polonica* 55: 9–36.

Yang, B., Steiner, M., and Keupp, H. 2015. Early Cambrian palaeobiogeography of the Zhenba-Fangxian Block (South China): Independent terrane or part of the Yangtze Platform? *Gondwana Research* 28: 1543–1565.

Yuan, J.-L., Li, Y., Mu, X.-N., Lin, J.-P., and Zhu, X.-J. 2012. Trilobite fauna of the Changhia Formation (Cambrian Series 3) from Shandong and adjacent area, North China. *Palaeontologica Sinica, New Series B* 35: 1–758.

Zhang, W. and Jell, P.A. 1987. *Cambrian Trilobites of North China—Chinese Cambrian Trilobites Housed in the Smithsonian Institution*. 459 pp. Science Press, Beijing.

Zhang, Z.-I., Zhang, Z.-F., Holmer, L.E., and Chen, F. 2018. Post-metamorphic allometry in the earliest acrotretoid brachiopods from the lower Cambrian (Series 2) of South China, and its implications. *Palaeontology* 61: 183–207.

Zhuravlev, A.Y. and Gravestock, D.I. 1994. Archaeocyaths from Yorke Peninsula, South Australia and archaeocyathan Early Cambrian zonation. *Alcheringa* 18: 1–54.